

**THE IMPACTS OF DYNAMIC SOLAR SCREENS ON ENERGY
PERFORMANCE AND NATURAL VENTILATION EFFECTIVENESS IN
OFFICE BUILDINGS VIA CFD SIMULATION UNDER DIFFERENT
CLIMATIC CONDITION**

by

ZIA MOHAJERZADEH

A THESIS

Presented to the Department of Architecture
and the Division of Graduate Studies of the University of Oregon
in partial fulfillment of the requirements
for the degree of
Master of Science

June 2022

THESIS APPROVAL PAGE

Student: Zia Mohajerzadeh

Title: The Impacts of Dynamic Solar Screens on Energy Performance and Natural Ventilation Effectiveness in Office Buildings via CFD simulation under Different Climatic Conditions

This thesis has been accepted and approved in partial fulfillment of the requirements for the Master of Science degree in the Department of Architecture by:

Ihab M. K. Elzeyadi	Chair of Committee
Thomas Hahn	Member
Alexandra Rempel	Member

and

Krista Chronister	Vice Provost for Graduate Studies
-------------------	-----------------------------------

Original approval signatures are on file with the University of Oregon Division Of Graduate Studies.

Degree awarded June 2022

© 2022 Zia Mohajerzadeh

THESIS ABSTRACT

Zia Mohajerzadeh

Master of Science

Department of Architecture

June 2022

Title: The Impacts of Dynamic Solar Screens on Energy Performance and Natural Ventilation Effectiveness in Office Buildings via CFD simulation under Different Climatic Conditions

Architects and designers are increasingly interested in employing dynamic façades in contemporary office buildings. One of the dynamic facade types, which is widely used is a solar screen and they affect the indoor environment. This study evaluates the effect of a solar screen across a range of perforation ratios and its distance to the building on energy utilization, natural ventilation, indoor air temperature, and CO₂ concentration in contemporary office buildings. Results demonstrate that dynamic solar screens have a promising positive impact on reducing energy consumption while improving indoor air quality. When these screens are in a closed state, they can reduce indoor air temperature up to 1°C and reduce energy consumption up to 60% in their most optimized state. Furthermore, the study's results show that the dynamic solar screens impact airflow inside the office space based on their different states (open, semi-open, or closed).

CURRICULUM VITAE

NAME OF AUTHOR: Zia Mohajerzadeh

GRADUATE AND UNDERGRADUATE SCHOOLS ATTENDED:

University of Oregon, Eugene
Iran University of Science and Technology
University of Tehran

DEGREES AWARDED:

Master of Science in Architecture, 2022, University of Oregon
Master of Architecture, 2020, Iran University of Science and Technology
Bachelor of Architecture, 2016, University of Tehran, Iran

AREAS OF SPECIAL INTEREST:

High Performance Building
Dynamic Facades
Environmental Friendly Design
IES-VE Software

ACKNOWLEDGMENTS

I would like to express my most profound appreciation to my committee chair, Professor Ihab Elzeyadi; this thesis would not have been possible without his guidance and persistent mentorship. I would like to thank my committee members, Professor Alexandra Rempel and Professor Tom Hahn, whose support and supervision helped me focus throughout this thesis. I thank the School of Architecture faculty at the University of Oregon for being available and opening up new avenues of research for me.

With the utmost respect, I acknowledge and thank my family in Iran for their prayers and encouragement; my parents, and Hadi Ghiassi, a friend of mine, for being incredibly patient and understanding in the difficult times.

TABLE OF CONTENTS

Chapter	Page
CHAPTER I: INTRODUCTION.....	1
1.1. Problem Statement.....	1
1.2- Research Questions.....	2
1.2.1- Main Question	2
1.2.2-Sub Questions	2
1.3- Research Objectives	2
1.4- Research Significance.....	3
1.5- Research Scope.....	3
1.6- Conceptual Framework.....	4
CHAPTER II: PARAMETERS AFFECTING THE STUDY	6
2.1-Dynamic Façade	6
2.2- Natural Ventilation	9
2.3- Indoor Air Quality	12
CHAPTER III: METHODOLOGY	18
3.1- Experimental Design	18
3.2- IES-VE Simulation Software.....	18
3.2.1- Suncast.....	19

3.2.2- MacroFlo	19
3.2.3- ApacheSim.....	20
3.2.4- MicroFlo (CFD).....	20
3.3- Building Characteristics	21
3.4- Apache HVAC system.....	26
3.5- Phoenix Arizona (ASHRAE climate zone 2)	28
3.6- Boston Massachusetts (ASHRAE climate zone 5).....	30
3.7- Physical Properties of Solar Screen.....	32
3.8- Dynamism.....	32
3.9- Simulation Scenarios	32
3.9.1- The building without solar screen (base case).....	33
3.9.2- 30% perforation ratio (closed state).....	33
3.9.3- 50% perforation ratio (semi-open state)	34
3.9.4- 70% perforation ratio (open state)	34
CHAPTER IV: DATA ANALYSIS AND FINDINGS.....	37
4.1- Simulation results for Phoenix Arizona, ASHRAE climate zone 2	37
4.1.1- SunCast.....	37
4.1.2- Energy Performance	39
4.1.3. Total Energy Consumption.....	40
4.1.4- MacroFlo	43

4.1.4.1- MacroFlo with opening profile.....	43
4.1.4.2- MacroFlo without opening profile.....	45
4.1.5- Room Air Temperature.....	48
4.1.6- Room CO2 Concentration	50
4.1.7- CFD Analysis for Phoenix.....	52
4.1.7.1- CFD Analysis for a screen with 30% perforation ratio	53
4.1.7.2- CFD Analysis for a screen with 50% perforation ratio	54
4.1.7.3- CFD Analysis for a screen with 70% perforation ratio	56
4.2- Boston Massachusetts, ASHRAE climate zone 5	57
4.2.1- SunCast.....	57
4.2.2- Energy Performance	59
4.2.3- Whole Building Energy	60
4.2.4- MacroFlo	63
4.2.4.1- MacroFlo with opening profile.....	63
4.2.4.2- MacroFlo without opening profile.....	65
4.2.5- Room Air Temperature.....	68
4.2.6- Room CO2 Concentration	70
4.2.7- CFD Analysis for Boston	72
4.2.7.1- CFD Analysis for a screen with 30% perforation ratio	73
4.2.7.2- CFD Analysis for a screen with 50% perforation ratio	74

4.2.7.3- CFD Analysis for a screen with 70% perforation ratio	75
CHAPTER V: CONCLUSION.....	77
5.1- Energy Performance and natural ventilation	77
5.2- Room CO2 Concentration	78
5.3- Room air temperature	78
5.4- Room Airflow.....	79
5.5- Limitation and Future Research	80
APPENDIX A.....	81
SENSITIVITY STUDY RESULTS FOR DIFFERENT SCREEN THICKNESS AND MATERIAL	81
APPENDIX B	84
ADDITIONAL SIMULATION RESULTS	84
REFERENCES CITED.....	96

LIST OF FIGURES

Figure	Page
Figure 1: Research conceptual framework	5
Figure 2: The dynamic solar screen on Al Bahar towers.....	7
Figure 3: Solar Screen types, impacts and variables.....	8
Figure 4: Ventilation types.....	11
Figure 5: Pollution sources and how it penetrates	13
Figure 6: Effects of low indoor air quality.....	13
Figure 7: Controlling indoor air quality.....	14
Figure 8: Schematic shape of the building.....	22
Figure 9: The actual model (1) and the prepared model in IES-VE (2)	23
Figure 10: Air temperature condition for windows to get open (left picture) operability period (9:00 AM- 9:00 PM) during the day (right picture)	26
Figure 11: different opening types in the model.....	26
Figure 12: HVAC system temperature profile.....	27
Figure 13: Location of Phoenix and Boston in the U.S map	28
Figure 14: Annual Climate Zones in Arizona.....	29
Figure 15: Cooling and heating degree days for Phoenix Arizona (ASHRAE 2)	30
Figure 16: Annual Climate Zones in Boston	31
Figure 17: Cooling and heating degree days for Boston Massachusetts (ASHRAE 5)....	31
Figure 18: Simulation scenarios based on the different perforation ratios	35
Figure 19: SunCast analysis for the city of Phoenix during the cooling season months ..	38
Figure 20: Baseline EUI for an office building in the city of Phoenix	39

Figure 21: The bar chart diagram for energy consumption in Phoenix for cooling season months.....	41
Figure 22: The outdoor air temperature for the city of Phoenix is based on the weather data.....	42
Figure 23: The impact of different solar screen configurations on energy consumption in a week of July in Phoenix.....	43
Figure 24: Airflow volume bar chart for cooling season months in Phoenix (with opening profile).....	45
Figure 25: Airflow volume bar chart for cooling season months in Phoenix (without opening profile).....	46
Figure 26: Airflow volume for a week of July in Phoenix without opening profile	47
Figure 27: Airflow volume for a day of July in Phoenix without opening profile	48
Figure 28: The room air temperature for a week of April as a result of various configurations in Phoenix.	49
Figure 29: Room air temperature and outdoor air temperature for a week of August in Phoenix	49
Figure 30: The room air temperature for a day of April as a result of various configurations in Phoenix.	50
Figure 31: The room CO2 concentration for a week of July in Phoenix.....	51
Figure 32: The room CO2 concentration and airflow volume for a day of July in Phoenix	52
Figure 33: Air velocity pattern for the screen with 30% perforation ratio	54
Figure 34: Air velocity pattern for the screen with 50% perforation ratio	55

Figure 35; Air velocity for the screen with 70% perforation ratio	57
Figure 36: SunCast analysis for the city of Boston during the cooling season months....	58
Figure 37: Baseline EUI for an office building in the city of Boston.....	59
Figure 38: The impact of different solar screen configurations on energy consumption for the cooling season months in Boston.....	61
Figure 39 Boston outdoor air temperature	62
Figure 40: The impact of different solar screen configurations on energy consumption in a week of July in Boston.	63
Figure 41: Airflow volume bar chart for cooling season months in Boston (with opening profile).....	65
Figure 42: Airflow volume bar chart for cooling season months in Boston (without opening profile).....	66
Figure 43: MacroFlo external vent without opening profile for a week of August in Boston	67
Figure 44: MacroFlo external vent without opening profile for a day of August in Boston	68
Figure 45: The room air temperature for a week of August as a result of various configurations in Boston.	69
Figure 46: Room air temperature and outdoor air temperature for a week of August in Boston.	69
Figure 47: The room air temperature for a day of August as a result of various configurations in Boston.	70
Figure 48: The room CO2 concentration for a week of August in Boston.....	71

Figure 49: The room CO2 concentration and airflow volume for a day of August in Boston	72
Figure 50: Air velocity pattern for the screen with 30% perforation ratio	74
Figure 51: Air velocity pattern for the screen with 50% perforation ratio	75
Figure 52: Air velocity pattern for the screen with 70% perforation ratio	76
Figure 53: Air velocity pattern based on the different perforation ratios in Phoenix.	79
Figure 54: Air velocity pattern based on the different perforation ratios in Boston.	80
Figure 55: Total energy consumption for a solar screen with a 50 % perforation ratio and two different thickness in Boston	81
Figure 56: Airflow volume for a solar screen with a 50 % perforation ratio and two different thickness in Boston	82
Figure 57: Total energy consumption for a solar screen with a 50 % perforation ratio and two different materials in Boston.....	83
Figure 58: Airflow volume for a solar screen with a 50 % perforation ratio and two different materials in Boston.....	83
Figure 59: Air temperature for the screen with 30% perforation ratio in Phoenix	84
Figure 60: Air velocity vector for the screen with 30% perforation ratio in Phoenix	85
Figure 61: Air temperature pattern for the screen with 50% perforation ratio in Phoenix	86
Figure 62: Air velocity vector for the screen with 50% perforation ratio in Phoenix	87
Figure 63: Air temperature pattern for the screen with 70% perforation ratio in Phoenix	88
Figure 64: Air velocity vector for the screen with 70% perforation ratio in Phoenix	89
Figure 65: Air temperature pattern for the screen with 30% perforation ratio in Boston.	90
Figure 66: Air velocity vector for the screen with 30% perforation ratio in Boston	91

Figure 67: Air temperature pattern for the screen with 50% perforation ratio in Boston. 92

Figure 68: Air velocity vector for the screen with 50% perforation ratio in Boston 93

Figure 69: Air temperature pattern for the screen with 70% perforation ratio in Boston. 94

Figure 70: Air velocity vector for the screen with 70% perforation ratio in Boston 95

LIST OF TABLES

Table	Page
Table 1: Dynamic facade types and their performance	7
Table 2: Literature review.....	15
Table 3: Envelope properties	23
Table 4: Ground Floor properties	24
Table 5: Internal Floor properties	24
Table 6: External wall properties.....	24
Table 7: Windows properties	25
Table 8: Roof properties	25
Table 9: Local shade properties	33

CHAPTER I: INTRODUCTION

1.1. Problem Statement

In the last decade, designers and architects have shown great interest in designing buildings with dynamic facades (Elzeyadi, [2017](#)). In general, dynamic facades are the type of façades that are made of elements that could be modified in response to outdoor weather conditions, which could be either changing elements' geometry or installing movable elements. In other words, dynamic facades have the potential to interact with the outdoor condition (Luther, [2000](#)). The result of this interaction is providing favorable conditions for occupants, such as appropriate natural ventilation, acceptable indoor air quality, and improved daylighting for occupants with glare management. (Al-Masrani, [2019](#); Al-Obaidi, [2019](#); Elzeyadi, [2017](#)). Numerous studies have assessed the impacts of dynamic facades on parameters such as daylight and energy consumption in different buildings (Shia, Tabladab, Wanga, [2020](#)); however, there is a lack of enough studies to evaluate dynamic facades' effectiveness in improved natural ventilation in buildings.

One of the barriers that inhibit designers from evaluating the impact of dynamic facades on natural ventilation is the complexity of working with simulation tools such as computational fluid dynamics (CFD) (Stoakes, Passe, Battaglia, [2011](#)). Another issue is thermodynamics complexity, the interaction of natural ventilation flow with thermal heat transfer properties in solid materials is intensive and thus not well integrated into architectural simulation and design modeling tools yet (Passe, Battaglia, [2015](#)). In order to have a holistic evaluation of dynamic facades performance, this study sees it essential to deal with these challenges and fill this gap (Elzeyadi, [2017](#)).

1.2- Research Questions

The questions for this study could be broken into two parts:

1.2.1- Main Question

How does a dynamic solar screen façade impact energy consumption related to natural ventilation in office buildings in cold and hot climates against the base case? (ASHRAE climate number two and five) and how similar or different they would perform in cooling and heating climate zones.

1.2.2-Sub Questions

- 1- How does a dynamic solar screen façade contribute to natural ventilation effectiveness in office buildings?
- 2- How does a dynamic screen façade control the amount of room CO₂ concentration?
- 3- How does a dynamic screen façade affect room air temperature?
- 4- In which ASHRAE climate zones (heating vs. cooling dominated) do dynamic solar screen façades have a better performance for improving natural ventilation and under what design parameters?

1.3- Research Objectives

The objectives of this research are categorized into three parts:

- 1- To evaluate the performance of a dynamic solar screen façade in energy consumption and natural ventilation in two different ASHRAE climate zones (2B and 5A).
- 2- To figure out the most optimum state of dynamic screen façade (degree of opening and perforation ratio) for saving energy and regulating the indoor air temperature, and CO₂ level.
- 3- To provide a guideline for further research and applications on solar screens usage in other climates.

1.4- Research Significance

Commercial buildings are responsible for consuming significant amounts of energy, which leads to increased air pollution Green House Gas emissions (GHG). Statistics show that the building sector accounts for 23-47% of total primary energy consumption worldwide, and this energy is used for ventilation, lighting, cooling, and heating (Lombard, Ortiz, Pout, [2008](#)). During the summer, most of this energy is used by air conditioners for cooling and air ventilation for commercial buildings; thereby, utilizing passive strategies like taking advantage of natural ventilation for buildings would be beneficial to consume less energy. In most cases, not only does it help to reduce energy consumption, but it can lead to better indoor air quality and occupant comfort (Elzeyadi, [2017](#)). Improved indoor air quality is essential as it directly relates to occupants' health and performance. In the contemporary era, people spend a considerable amount of their time indoors; therefore, they need to spend their time in a place with acceptable indoor air quality (Ren, Liu, Cao, Hou, [2017](#)). Besides the stated reasons, due to the COVID-19 pandemic, the significance of appropriate ventilation and acceptable indoor air quality for indoor spaces is crystal clear for everyone. In general, this research aims to evaluate natural ventilation by taking advantage of a dynamic façade to reduce energy consumption and improve indoor air quality in office buildings.

1.5- Research Scope

This study explores the performance of solar screen façades in terms of both energy consumption and natural ventilation performance.

In the context of this research, the research is limited by:

- 1. Location:** A three story office building in which is modeled based on ASHRAE standards is documented for its environmental performance. This building is used as a base case and for further analysis of the impact of solar screen façades.
- 2. Orientation:** Shading devices, perform more efficiently on the southern and western sides of the buildings (Sherif et al. [2012](#)). Thus, solar screens could be added in the

simulation as external perforated shading for south and west sides of the building. However, in this study the main focus is on only south side of the building.

3. Parameters: Based on previous studies, dynamic solar screens have shown superior performance in terms of energy-saving (Elzeyadi, [2017](#)). Based on their characteristics, solar screens directly impact building performance. It is shown that solar screens with perforation ratios between 30% and 50% are more optimum than other perforation ratios for energy-saving performance. Similarly, it is discovered that the 1:1 depth to width ratio has a better energy performance (Elzeyadi, Batool, [2017](#)). Thus, the impact of the solar screen with 30% and 50% perforation ratio on building performance is simulated. In addition, to these perforation ratios, 70% perforation ratio will be tested in order to have a more comprehensive results.

4. Simulation period: This building is simulated by IES-VE software for the cooling season months.

1.6- Conceptual Framework

For this study, an ASHRAE prototypical three-story building has been selected as a representative of the office building typology. This building will be simulated by IES-VE software for the cooling season months for two climate zones (ASHRAE 2 and 5). Based on the previous studies, solar screens have shown superior performance in terms of energy consumption in ASHRAE climate zone number four (Elzeyadi, [2017](#)). Based on their characteristics, solar screens directly impact building performance, and it is shown that solar screens with perforation ratios between 30% and 50% are more optimum than other perforation ratios for energy-saving performance. Similarly, it has been discovered that the 1:1 depth to width ratio has a better energy performance (Elzeyadi, Batool, [2017](#)). Therefore, based on these studies, a solar screen is selected for further analysis in these two climate zones, and the building is simulated with a dynamic solar screen under three different states; open, semi-open, and closed. These screens could be installed in the east, west, and south orientation; however, the southern side has the highest efficiency for energy consumption, so in this study, the solar screen is simulated for the southern side. In

order to clearly explore the impact of these screens on energy-saving, the building first is simulated without any solar screen, and the results of this step could be used as a baseline. The outcomes of this study are evaluating the impact of the solar screen on energy consumption and natural ventilation performance. The results of ventilation performance could be broken into air velocity, indoor air temperature, and room CO₂ concentration. Based on the ASHRAE standard, 55 acceptable indoor air velocity is between 0.2 m/s and 0.8 m/s. In addition, indoor air temperature is better to be within the range of 75 F - 80.5 F during the cooling season months. In terms of indoor CO₂ concentration, ASHRAE recommends that for the office building, it is better to be less than 800 ppm. Figure 1 shows the entire map of this study which will be discussed in more detail in the next chapters (De Dear, Brager, 2002).

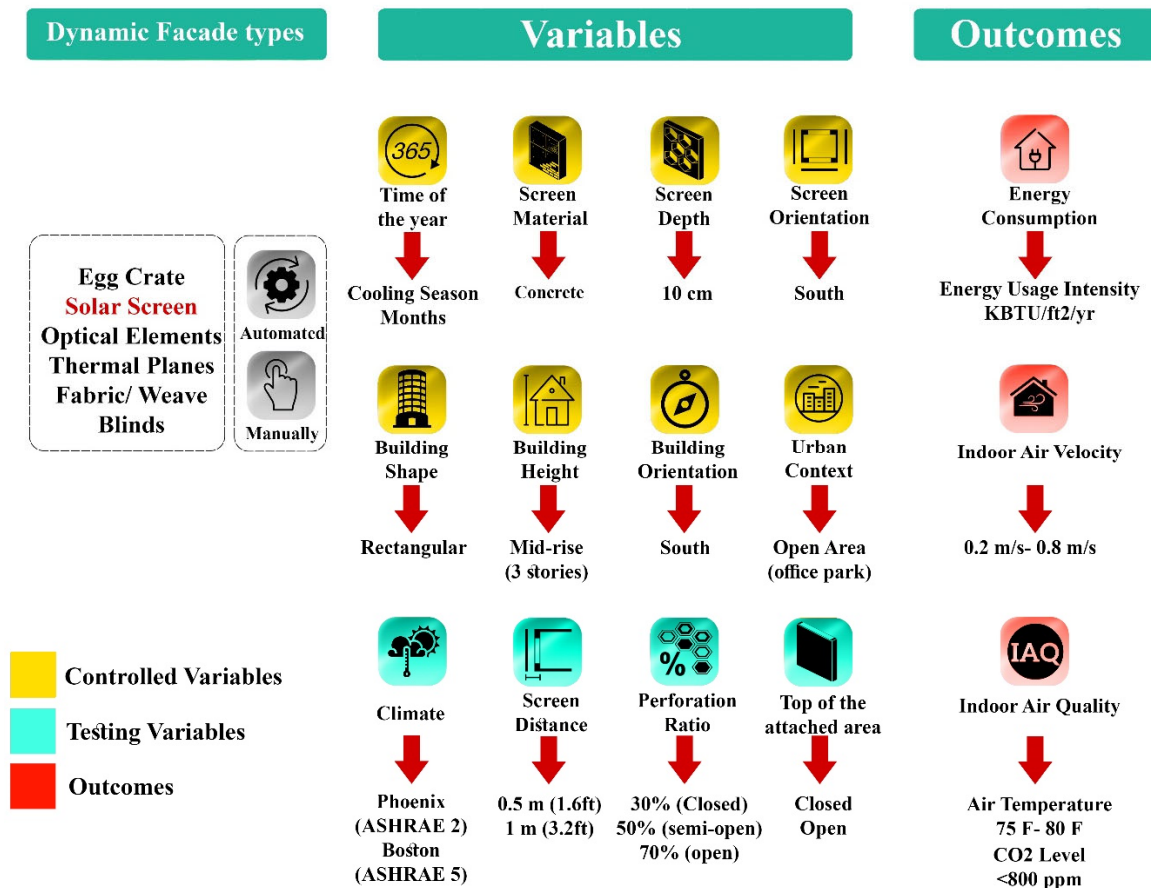


Figure 1: Research conceptual framework

CHAPTER II: PARAMETERS AFFECTING THE STUDY

2.1-Dynamic Façade

Due to technological development, the construction of buildings with dynamic facades has increased in the last decades. Dynamic facades are made of elements that could be modified in response to outdoor weather conditions and, as a result, provide favorable conditions for occupants. This modification could be either changing elements' geometry or installing movable elements. In other words, dynamic facades have the potential to interact with the outdoor condition and improve the indoor environment for occupants (Luther, [2000](#)). Dynamic façades can also be installed to refurbish the existing buildings and improve the buildings' performance (Cao, Ouyang, Zhu, Huang, Hub, Deng, [2012](#)). There is a direct correlation between dynamic façade energy consumption, ventilation, daylight, and building cost. However, it should be stated that finding a balance between different metrics and parameters is necessary to have a high-performance building (Srisamranrungruang, Hiyama, [2020](#)). Table 1 shows the dynamic façade types and based on their typologies could be divided into six main categories; 1- Dynamic Egg-Crates 2- Automated Movable Screens 3- Optical Elements Panels 4- Stretched Fabrics/ Weaved Panels 5-Automated Exterior Blinds 6- Thermal Change Planes. Each one of these typologies has its own benefits, which can positively impact buildings' performance; thereby, it is crucial for designers to know these typologies' pros and cons in order to use them in the right climate and situation. Previous studies have shown that among all of these six categories, dynamic solar screens have a better performance for energy saving in most climate zones as well as egg crates. Table 1 shows the summary of previous studies which has been carried out to assess different dynamic façade typologies in terms of energy consumption and thermal performance (Elzeyadi, [2017](#)).







Dynamic façade types		Energy consumption performance	Thermal Performance
Egg Crate		✓✓✓✓	✓✓
Solar Screen		✓✓✓✓	✓✓✓
Optical Elements		✓✓	✓
Fabric/ Weave		✓✓	✓✓
Blinds		✓✓	✓✓✓✓
Thermal Planes		✓✓✓	✓✓✓✓

Table 1: Dynamic facade types and their performance

Based on the superior performance of solar screen, this dynamic façade has been selected for this study. Dynamic solar screens are the type of dynamic façades which consist of shading systems with perforations that are designed using parametric processes. Solar screen performance depends on various variables like screen material, perforation ratio, depth, geometry, and the place where it is used. Furthermore, utilizing vernacular elements for screens could be beneficial for occupants' thermal comfort in hot climates (Elzeyadi, Batool, [2018](#)). Figure 2 shows a dynamic solar screen with different perforation ratio on Al Bahar towers in Abu Dhabi.



Figure 2: The dynamic solar screen on Al Bahar towers

Statistics show that screens with a 30-50% perforation ratio provide a more optimized design that balances energy savings in cooling and lighting loads and leads to better occupant's thermal and visual comfort in hot climates (Elzeyadi, Batool, [2017](#)). Installation of external deep perforated solar screens in the West and South orientations could effectively achieve energy savings up to 30% of the total energy consumption (Sherif, El-Zafarany, Arafa, [2012](#)). The dynamic exterior shading provides the highest indoor environmental quality, including continuous daylight and views for occupants, with the lowest possible energy consumption, rarely requiring greater than the minimum building ventilation rates (Meek, Breshears, [2010](#)). Some studies have explored the influence of external dynamic louvers on the energy consumption of office buildings in hot and humid cities. The results show that the dynamic louvers system can save 34.02%, 28.57%, and 30.31% for the south, east and west orientations, respectively (Hosseini, Mohammadi, Rosemann, Schröder, Lichtenberg, [2019](#)). However, it has been explored that rotating the screen slats had an insignificant effect on energy performance for a screen with squared perforation and the optimal depth ratio of 1. While, rotation of the screen slats up to 30° downwards enhanced the screen energy performance (Sherif, El Zafarany, Arafa, [2012](#)). Figure 3 is a diagram of all different solar screen variables, types, and their impact on the indoor environment.

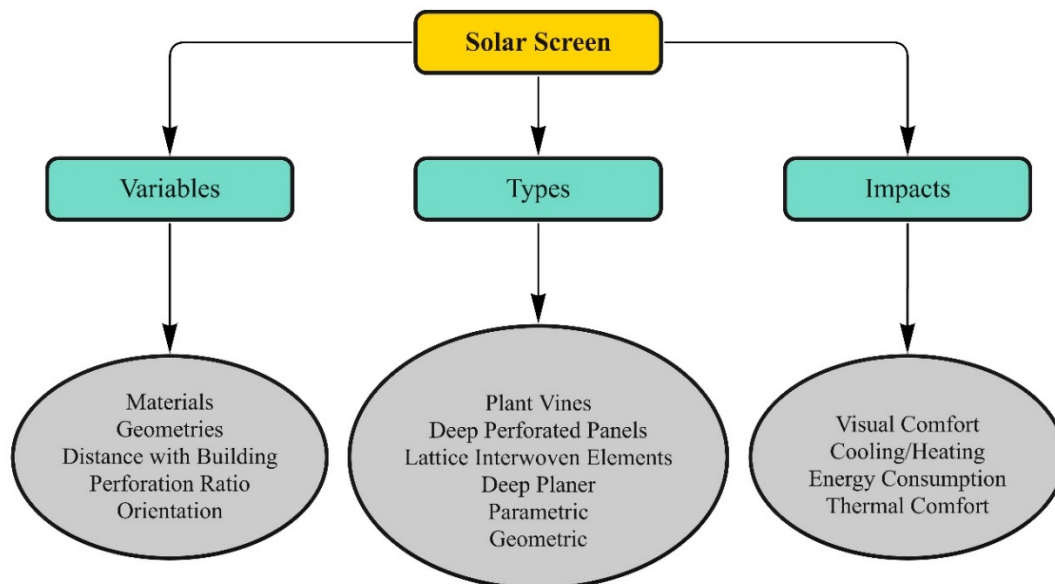


Figure 3: Solar Screen types, impacts and variables

The use of external perforated solar screens in reducing energy consumption and achieving thermal comfort is documented in the literature (Harris 2006). However, articles that quantitatively address the issue of passive cooling through solar screens are difficult to find. In the research on solar screens, there is evidence that external fixed deep perforated solar screens could effectively achieve energy savings up to 30% of the total energy consumption in the West and South orientations. Optimum range of depths and perforation percentages were recommended: 80–90% perforation rate and 1:1 depth/opening width ratio (Sherif et al. [2012](#)). These lighter and deeper solar screen configurations were found to be more efficient in energy consumption in comparison with the traditional ones. Screen depth is cited as an important factor that affects energy savings

In a related study, using EnergyPlus simulation, researchers find that thermal loads quickly dropped when screens with high ratios (85%) of perforation are used (Sherif et al. [2012](#)). Screens with perforations below this rate do not significantly reduce thermal load, according to the study reduction of cooling energy was attributed to the substantial reduction of solar energy and the energy transmitted heat gain window. Sherif also explores the impact of external perforated solar screens on thermal performance in desert climates (Sherif et al. [2012](#)) and finds that the use of perforated screens have a significant effect on reducing the cooling energy, especially in south, west and east orientations, with screens with a perforation range between 80% and 90% having the highest saving rate. Further studies by the same authors reveal that the most significant saving was achieved when using screens with depth to perforation ratio 0.75/0.75.

2.2- Natural Ventilation

Natural ventilation occurs due to pressure difference between two areas, and the air starts flowing from higher pressure to lower pressure. Natural Ventilation has multiple advantages, and it is vital for human health and comfort. If it works properly, it could consume less energy in comparison with mechanical ventilation. Energy consumption has significantly increased in the last decades due to the population growth and increasing demand for thermal comfort (Santamouris, Papanikolaou, Livada, Koronakis, Georgakis, Argiriou, Assimakopoulos, [2016](#)). The statistics show that the building sector accounts for

23-47% of total primary energy consumption in developed and developing countries worldwide. Furthermore, air conditioning represents greater than 50% of the annual energy consumption in standard buildings (Lombard, Ortiz, Pout, [2008](#)). Removal heat through air flowing while providing fresh air by decreasing humidity and diluting particles is another advantage of natural ventilation. Moreover, natural ventilation cools down the building envelope during the night by removing heat from thermal mass and providing additional energy storage capacity for the daytime. (Passe, Battaglia, [2015](#)).

Some places have a better potential for natural ventilation due to the extensive diurnal temperature range. Subtropical highland, Mediterranean, and arid climates like the Middle Eastern countries are the most favorable climates for natural ventilation (Chen, Tong, Malkawi, [2017](#)).

Several studies have investigated the effective parameters for improving natural ventilation. Building orientation, height, and configuration have the most significant impact (Aflaki, Mahyuddin, Baharum, [2016](#)). In addition, there is a direct correlation between weather conditions, outdoor airspeed, and occupants' behavior on natural ventilation performance (Chenari, Carrilho, daSilva, [2016](#)). Another study discovered the impact of utilizing vernacular elements, window-to-wall ratio, and shape of the louver on building natural ventilation (Aflaki, Mahyuddin, Mahmoud, Baharum, [2015](#)). It is also proved that creating a wind path into the internal zone, and constructing two windows rather than one, could optimize natural ventilation (Zhou, Wang, Chen, Pei, [2014](#)). A study by Pasquay indicates that double façade configurations are reasonable for enhancing natural ventilation and saving energy in high-rise buildings (Pasquay, [2004](#)). Priyadarsini, Cheong, and Wong have investigated the application of passive and active stack systems for improving natural ventilation in tropical areas (Priyadarsini, Cheong, Wong, [2004](#)). Computer simulations showed that natural ventilation in a building with double-skin facades was available from the cavity to the indoor space at appropriate air temperatures when the sky was partly cloudy and clear (Kim, Lee, [2011](#)). By designing a suitable building facade, indoor air temperature can be reduced by 2-3°C in comparison with outdoor temperature (Liping, Hien, [2007](#)).

However, urban contexts adversely affect natural ventilation performance like strip apartments in rows, high-rise buildings with large podium bulk, and enclosed city blocks

(Guo, Zhu, Wang, Duan, Jin, [2017](#)). In this case, mixed-mode ventilation has been proven as a practical and reliable solution for constrained buildings due to their types and urban context. Placing buildings farther away from one another substantially promoted the ventilation rate, and the airflow rates could be doubled with an appropriate shift (Cheung, Liu, [2011](#)). Another strategy could be using solar shading and wind shielding, especially for night natural ventilation. This is more pronounced in high-density urban buildings such as offices in central parts of metropolitan cities (Ramponi, Gaetani, Angelotti, [2014](#)). Figure 4 shows the different types of ventilation; natural ventilation, stack ventilation, mechanical ventilation, and mixed-mode ventilation. Furthermore, natural ventilation is divided into two subcategories; single-sided ventilation and cross ventilation. Compared to single-sided ventilation, cross ventilation operation leads to more comfort zones for indoor thermal conditions (Omrani, Garcia-Hansen, R. Capra, Drogemuller, [2017](#)). Most people prefer natural ventilation and manageable windows, and the thermal tolerance in such rooms with the user-controlled opening is an exemplary configuration for them (da Graça, Linden, [2016](#)). It may be valuable to create a comfortable and healthy internal microclimate inside a building, and it offers the possibility to save energy by reducing mechanical ventilation systems usage (Baxevanou, Fidaros, Tsangrassoulis, [2017](#)).

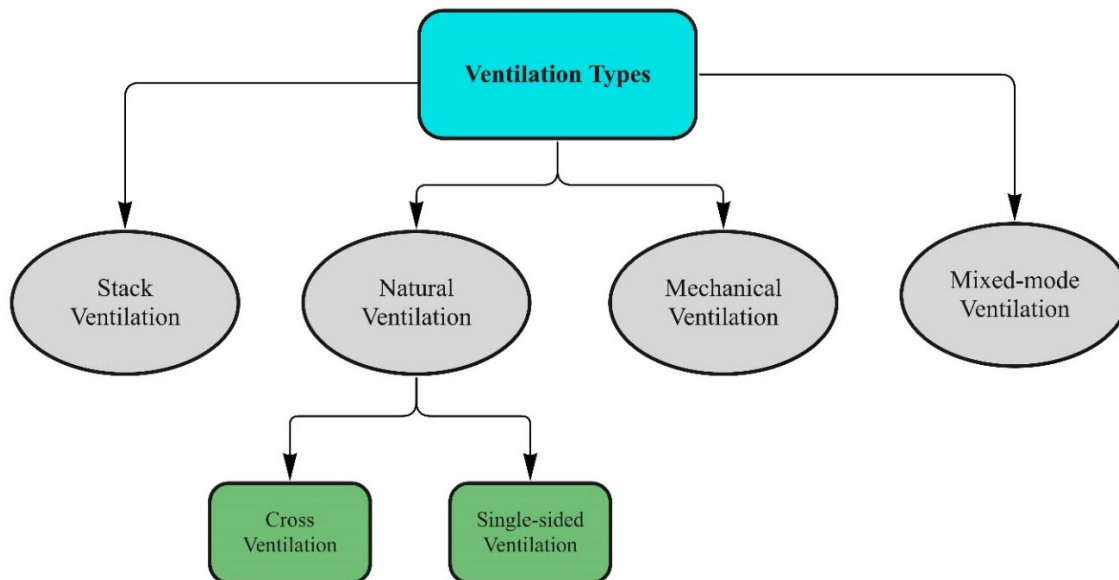


Figure 4: Ventilation types

It is recommended to take into account some parameters to have better cross-ventilation. In general, narrower buildings have a better potential for cross ventilation due to the difficulty of fresh air distribution in all portions of wider buildings. Moreover, orienting the buildings with prevailing summer winds provides the most natural ventilation, while orienting perpendicular to prevailing winds provides the least ventilation. Internal spaces and structural elements can channel air through the building in different directions. However, cross ventilation usage is not applicable in some places like the urban area due to the lots of noise and air pollution. Furthermore, it would be better to utilize ventilation systems to ensure that ventilation continues when the wind is unavailable or outdoor air quality is not in good condition. The utilization of natural ventilation through mixed-mode ventilation systems is critical for reducing energy consumption in buildings and maintaining a healthy indoor environment (Tong, Chen, Malkawi, [2017](#)).

2.3- Indoor Air Quality

Another outcome of dynamic solar screen could be improving indoor air quality, which directly impacts occupants' health and performance. Since people spend a considerable amount of time in office buildings; hence, they need to be in a place with acceptable indoor air quality (Ren, Liu, Cao, Hou, [2017](#)). Poor indoor air quality, as shown in figure 5, results from elevated exposure to air pollutants derived from building materials, furnishings, consumer products, and pollutants emissions. These sources can be entered through the doors, windows, apertures, and cracks. Current health concerns related to indoor environmental quality in residential, public, and commercial buildings include asthma and cancer risks potentially caused by VOCs, radon, odors and chemicals, allergies, ozone irritation, and other respiratory symptoms. Indoor humidity is considered a widespread cause of diseases because high humidity in indoor air promotes mold growth. Therefore, moisture removal can reduce health risks; on the other hand, if too much moisture is removed, the dry air may cause other detrimental effects such as respiratory issues. (Carrer, Wolkoff, [2018](#)). Modeling and predicting the prevalence of indoor air pollutants while buildings are being designed is one of the best ways to increase their energy efficiency.

However, due to the complicated nature of these models, it is challenging for designers to simulate them (Okochi, Yao, [2016](#)).

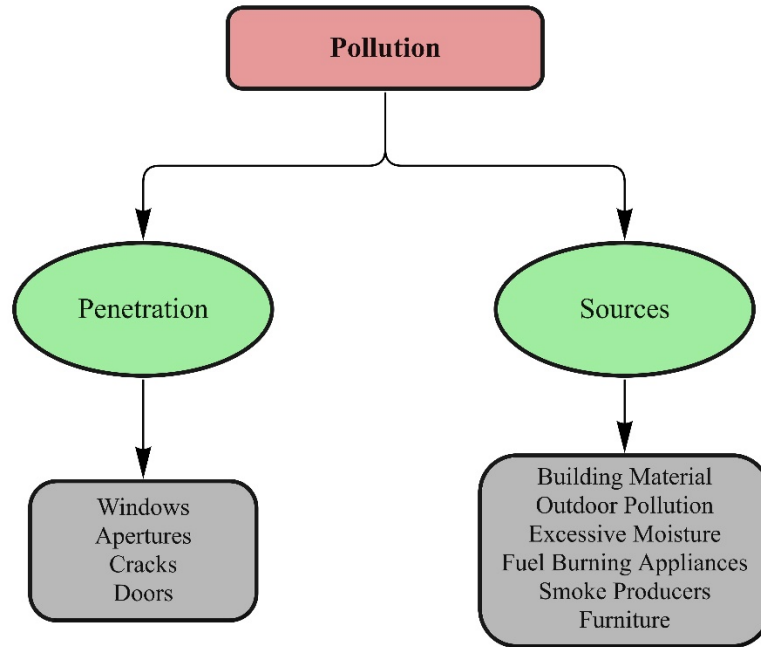


Figure 5: Pollution sources and how it penetrates

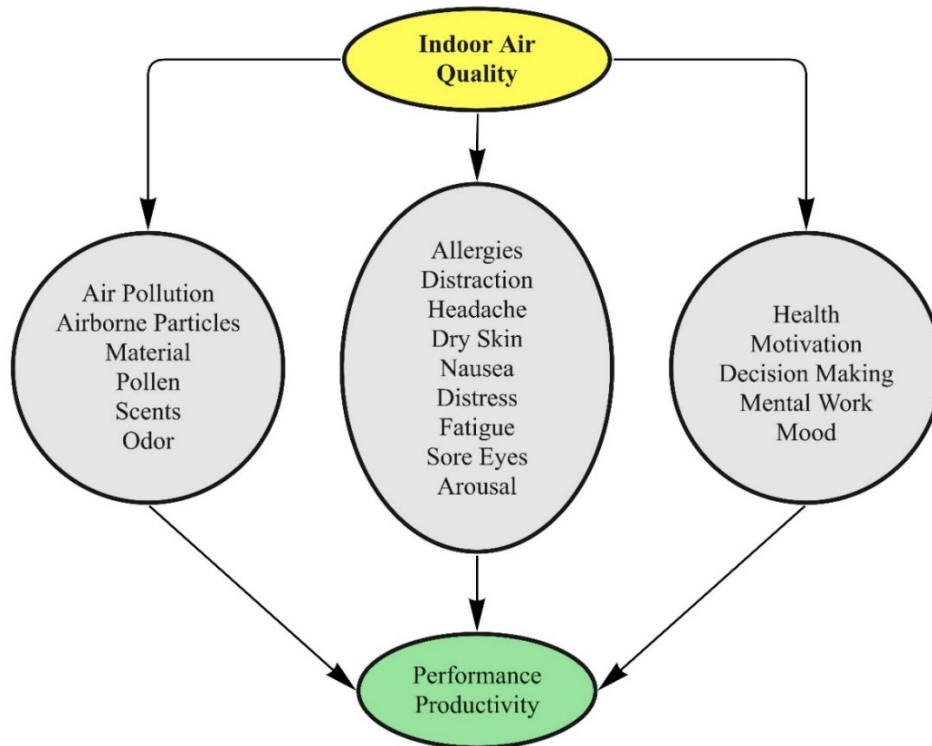


Figure 6: Effects of low indoor air quality

Indoor air quality as shown in figure 7 can be controlled by monitoring the pollution sources and blocking the way of their penetration into the buildings. The most apparent approach is removing or reducing the pollutant source or increasing the ventilation rate to dilute and dispose of particles and keep their concentration below a proven acceptable range. Natural ventilation helps provide a favorable indoor air quality without electricity demand for moving the air and improves occupants' thermal comfort in the summer by increasing air velocity during the day and high night ventilation rate (Schulze, Eicker, 2013). It is shown that using automated windows can potentially reduce the risk of overheating in office buildings by 64% and improve indoor air quality in highly occupied environments by 90% (Khatami, Hashemi, 2017). However, improperly controlled ventilation systems cause increased health risks and more energy consumption (Ma, Aviv, Guo, Braham, 2021).

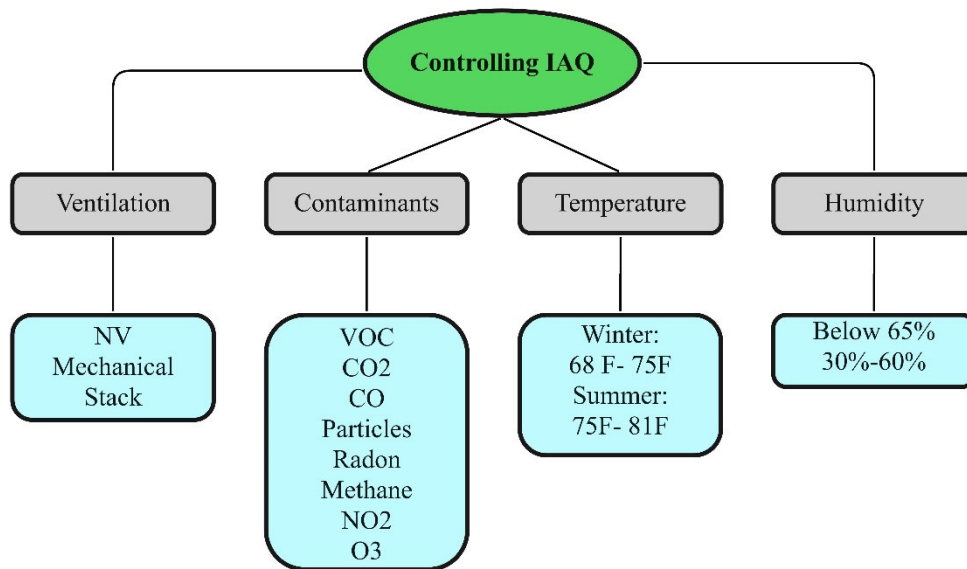


Figure 7: Controlling indoor air quality

Table 2 summarizes all the papers and information that have been explained in the chapter one and two.

Table 2: Literature review

Source	Parameters	Impact
Zheming Tong , Yujiao Chen, Ali Malkawi 2017	Climate Regional Condition	Natural Ventilation Energy Saving Building Cost
Zheming Tong , Yujiao Chen , Ali Malkawi 2017	Climate	Natural Ventilation Natural Ventilation hour
Ardalan Aflaki, Norhayati Mahyuddin, Mohamad Rizal Baharum 2016	Climate Building Height	Natural Ventilation Thermal Condition Occupant's Comfort
Ardalan Aflaki, Norhayati Mahyuddin, Zakaria Al-Cheikh Mahmoud, Mohamad Rizal Baharum 2015	Climate Building Orientation Window-to-Wall Ratio	Natural Ventilation Energy Saving
Chaobin Zhou, Zhiqiang Wang, Qingyan Chen, Yi Jiang, Jingjing Pei 2014	Building Orientation Creating a wind- path into the internal zone	Natural Ventilation Ventilation Performance
Wei You Jialei Shen Wowo Ding 2017	Climate Building Location Building Configuration	Ventilation Efficiency
Kun Lai , Wen Wanga, Harry Giles 2017	Climate Solar Shading	Solar Heat Gain Daylight Thermal Comfort
Pimolsiri Prajongsan, Steve Sharples 2012	Ventilation Shaft	Ventilation Efficiency Thermal Comfort Energy Consumption

Table 2: Literature review

Source	Parameters	Impact
Sara Omrani, Veronica Garcia-Hansen, Bianca R. Capra, Robin Drogemuller 2017	Outdoor Air Velocity Crossed ventilation	Ventilation Efficiency Residents Comfort Internal Air Flow
James O.P. Cheung, Chun-Ho Liu 2011	Building Height Building Orientation	Ventilation Efficiency Indoor Air Velocity
Guilherme Carrilho da Graça, Paul Linden 2016	Windows Operability	Ventilation Efficiency Thermal Comfort
Elisabeth Gratia, André De Herde 2003	Double Facade Orientation Climate	Natural Ventilation Performance
Till Pasquay 2004	Double Façade Mechanical Equipment	Energy Consumption Indoor Air Quality
Rubina Ramponi Isabella Gaetani Adriana Angelotti 2014	Surrounding Buildings Solar Shading	Ventilation Efficiency Energy Consumption
Behrang Chenari , João Dias Carrilho, Manuel Gameiro da Silva 2016	Users' behavior Building Characteristics	Indoor Air Quality Energy Consumption Occupant's satisfaction
Ihab Elzeyadi 2017	Dynamic Facade States	Energy Consumption Daylight Indoor Air Quality
Christopher Meek, John Breshears 2010	Solar Shading	Energy Efficiency Occupants' Comfort

Table 2: Literature review

Source	Parameters	Impact
Fawwaz Hammad, Bassam Abu-Hijleh 2010	Dynamic Facade External Louvers	Energy Consumption Lighting Intensity
Ihab Elzeyadi, Ayesha Batool 2018	Climate Solar Screen Shading Type	Cooling Load Daylight Visual Comfort Energy Consumption Thermal Comfort
Yu-Min Kim, Ji-Hyun Lee, Sang-Min Kim, Sooyoung Kim 2010	Double Façade Climate	Heating Load Natural Ventilation Energy Consumption Air flow
G. S. Brager, R. De Dear 2000	Wind Speed Building Location Building Configuration Outdoor Air Quality	Ventilation Efficiency Air Flow Indoor Air Quality
Ahmed Sherif, Abbas El Zafarany, and Rasha Arafa 2012	Screen's Shape Screen's Angle	Cooling Energy Load Daylight Energy Efficiency
MSantamouris, N Papanikolaou, I Livada, I Koronakis, C Georgakis, A Argiriou, D.N Assimakopoulos 2001	Double Facade Climate	Heating Load Natural Ventilation Energy Consumption Air flow

CHAPTER III: METHODOLOGY

3.1- Experimental Design

This study uses an experimental research design using a computational simulation as the primary research method. Simulation techniques offer a more controlled environment in which each parameter can be tested, analyzed, and optimized. Integrated Environmental Solutions Virtual Environment (IES-VE) has been selected as the simulation software for this study. This is due to the reliability of IES-VE to provide a better factor of reality between simulation outcomes and on-site fieldwork performance (Elzeyadi, Batool, [2017](#)). Furthermore, the software can perform yearly dynamic simulations across multiple platforms, including energy, ventilation, solar, thermal, and lighting in one interconnected package, as well as displaying the results in graphical output forms that are appropriate to spatial comfort and occupant's performance (Elzeyadi, Batool, [2017](#)).

3.2- IES-VE Simulation Software

IES-VE program is an integrated collection of applications linked by a standard user interface and a single integrated data model (Kim et al., 2012). It consists of different modules, each of them performing specific calculations, such as, "SunCast" which is used for solar shading analysis, "Apache" for thermal simulation, MacroFlo for defining opening types and characteristics, VistaPro for analyzing Apache simulation results, and finally MicroFlo for CFD simulation. The package modules that are used to carry out this study are ModelIT, SunCast, Apache, MacroFlo, VistaPro, and MicroFlo (CFD). In the next few sections each one of these items will be discussed in more details.

3.2.1- Suncast

One of the early stages of running simulation in IES-VE is running SunCast, which could be used at any step of the design process to analyze shading and solar insolation studies. SunCast could be used to investigate external obstruction and self-shading of a building, the impacts of changing the orientation of the building, and solar mapping through windows and openings. Furthermore, it generates shadows and internal solar insolation from any sun position defined by date, time, orientation, site latitude, and longitude.

3.2.2- MacroFlo

MacroFlo is one of the fundamental parts of the simulation process in IES-VE, and it has a direct impact on the simulation results. The MacroFlo is positioned within the Virtual Environment's Thermal category, which provides facilities to prepare input data for the MacroFlo bulk airflow simulation program. However, it is worth mentioning that MacroFlo is just used for defining the opening types for further simulations like ApacheSim. Basically, MacroFlo is a program for analyzing natural ventilation and infiltration in buildings that uses a zonal airflow model to calculate bulk air movement in and through the building, driven by wind and buoyancy-induced pressures.

An opening type is a building element in the context of MacroFlo, which consists of a specification of the element's airflow characteristics and the way they vary with time. In MacroFlo, openings could be defined based on various categories, ranging from exposure to the outside environment, operable area, and, more importantly, degree of opening. Defining the opening types is a worthwhile action for specifying the airflow characteristics of windows and doors to analyze natural ventilation and infiltration in MacroFlo. The exposure to the outside environment is used to show if the building is located in an open space or is surrounded by city blocks. Defining the operable area helps to show the area of the pivoting element of the window/door.

As it is mentioned earlier, the degree of opening is among the most critical characteristics of openings because, in this section, each opening has its own profile, which could be set

based on various parameters such as indoor air temperature, outdoor air temperature, wind direction, etc.

3.2.3- ApacheSim

ApacheSim is among the most critical parts of this study which acts as a foundation for further analysis of this software. ApacheSim is a dynamic thermal simulation program based on first-principles mathematical modeling of the heat transfer processes occurring within and around a building. This tool could be linked to MacroFlo and sunCast. The result of the simulation covers every issue related to the building performance, ranging from weather data to building parameters like room air temperature, relative humidity, carbon concentration, energy consumption, etc. In the Apache view each room has a set of attributes that describe conditions in the room. This condition, could be either room construction data or room thermal data such as internal gains and HVAC system.

Once the simulation is done, the results are automatically open in the VistaPro section, which provides so many different options for comparing and analyzing. In addition, the thermal information of each boundary could be exported to MicroFlo to do further analysis like CFD.

3.2.4- MicroFlo (CFD)

Computational Fluid Dynamics (CFD) is a powerful tool for modeling air flows and climate patterns. The impact of envelope characteristics, wind direction, and location of the mechanical ventilation devices on different microclimatic parameters like air temperature and humidity, ventilation flow rate, and incident solar radiation could be investigated by using CFD.

As it is mentioned in the previous section, the results of ApacheSim could be exported to MicroFlo to do further analysis. MicroFlo basically is the CFD analysis tool within the IES Virtual Environment which provides some of the features as follows.

In general, CFD is based on the ‘Finite Volume Method’ of discretization of the partial differential equations that describe the fluid flow. The formulation uses a steady-state three-dimensional convection-condition heat transfer and flow model. In addition, the ‘SIMPLE’ algorithm is used to achieve the coupling between pressure and velocity fields. MicroFlo uses wall functions to calculate near-wall properties of turbulence as well as the flux of heat and momentum. Since there is no direct radiation model within MicroFlo, the effects of radiation could be modeled when boundary conditions are imported from VistaPro.

It is important to mention that MicroFlo is an ad-hoc CFD tool which means that it cannot read data directly from the systems profiles, templates, and constructions that have been set up. Therefore, the only way it can read the data related to gains is when the boundary conditions are exported from VistaPro and imported into MicroFlo. Boundary conditions can be added to the model at the surface level of decompositions. The boundary conditions define the property of the surfaces included in the MicroFlo model. These are applicable for internal simulations only.

3.3- Building Characteristics

For this study, an ASHRAE standardized model of a mid-sized office building (IES-VE software) has been selected and analyzed in two different climate zones. One is Phoenix, Arizona, which is in ASHRAE climate zone 2B, and the other is Boston which is in ASHRAE climate zone 5A (iaqsource.com). This building is used as a base case to test further analyses like the impact of dynamic solar screen façades on natural ventilation, energy consumption, and controlling indoor air quality. Figure 8 shows the schematic picture of the building. As shown, it is a three-story rectangular building with dimensions of 50m (156 feet) by 33m (108.2 feet). The height of each floor is 4m (13.1 feet) and could be broken into two spaces, the lower part is the office space 2.8m (9.18 feet) and the upper

part is air plenum which is 1.2m (3.93 feet). In addition to this building, another area has been attached in front of the building which is marked as blue and its dimensions are 12m (39.3 feet) height, 50m width (156 feet) and 1m (3.2 feet) depth. The reason why this area has been attached is due to running CFD simulations which can only be applied to indoor spaces. Thus, an exterior bounded space need to be modeled with open windows to be able to run the simulation properly.

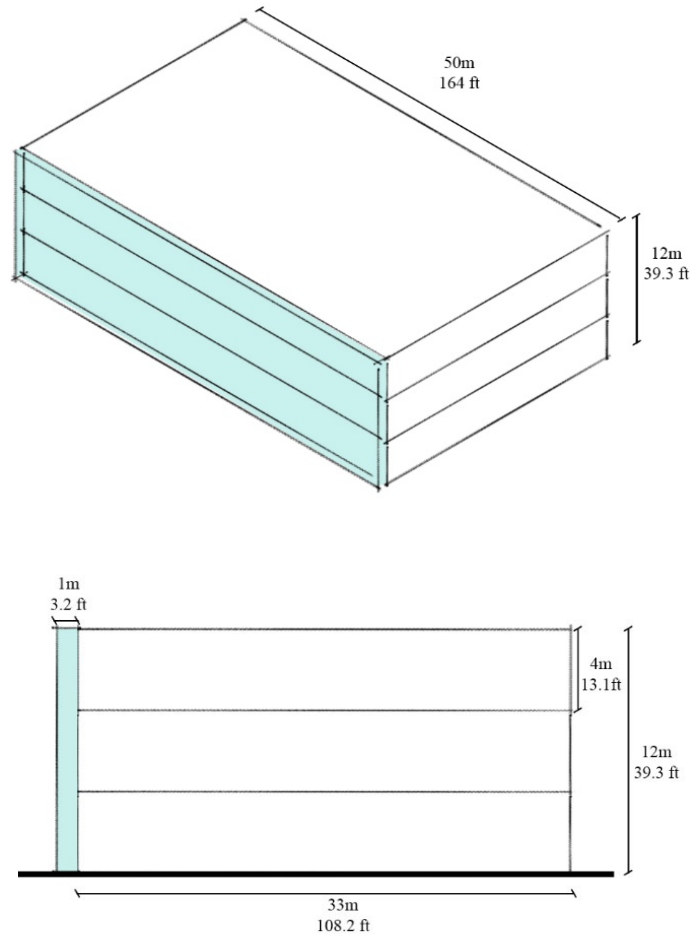


Figure 8: Schematic shape of the building

Another issue about this attached area that needs to be mentioned is its properties. This bounded area is set as additional room with external planes as 100% open windows at all times to simulate the external conditions. This is the zone where the screen configuration is modeled and tested. This solution allows the top of the screen to be modeled as closed and open to control for the draft velocity of the air between the screen and the building

envelope. Figure 9 shows the regular solar screen (1) and prepared version for running in IES-VE (2).

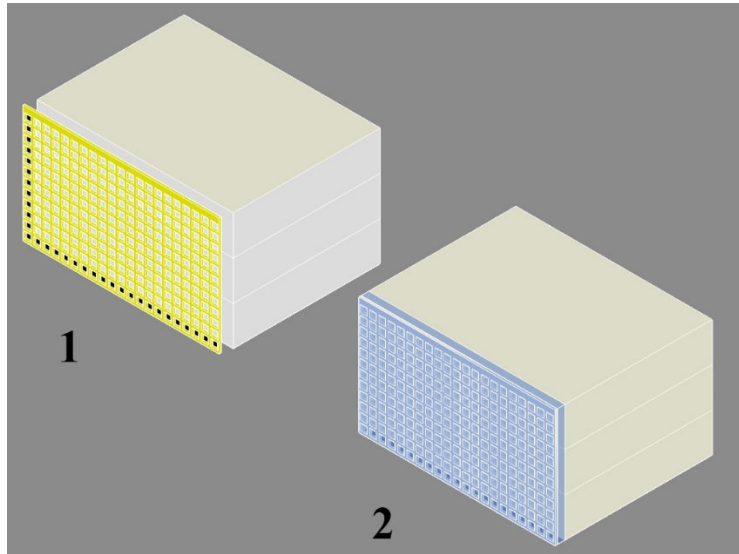


Figure 9: The actual model (1) and the prepared model in IES-VE (2)

Since this is an office building, it has been set to be used during the weekdays from 9 AM to 5 PM. Based on this assumption, all the profiles in MacroFlo and Apache have been set for weekdays from 9 AM to 5 PM. The main internal gain sources for this office are people, computers, and lighting. The maximum sensible gain for people is set as 90 W/person and 60 W/person for maximum latent gain. This amount for computers is set as 10 W/ m². In addition, these amounts for fluorescent lighting have been set as 9 W/ m².

In general, this building, in terms of walls, could be broken into four categories: External walls, roof, external windows, and internal ceiling/floor. Table 3 shows the envelope properties like thickness, and their U values.

Category	U value (W/m ² K)	Thickness mm
Internal Ceiling/Floor	1.0866	282.5
External Window	1.6	24
Roof	0.18	317
External Wall	0.26	208.9

Table 3: Envelope properties

Tables 4 to 8 show the properties of the material for each specific category such as ground floor, internal floor, external walls, windows and roof.

Material	Thickness mm	Conductivity (W/mK)	Density kg/m³
Insulation	98.2	0.025	700
Reinforced concrete	100	2.30	2300
Cavity	50	-	-
Chipboard Flooring	20	0.13	500

Table 4: Ground Floor properties

Material	Thickness mm	Conductivity (W/mK)	Density kg/m³
Chipboard Flooring	20	0.13	500
Cavity	50	-	-
SCREED	50	1.15	1800
Reinforced Concrete	100	2.3	1000
Cavity	50	-	-
Plasterboard	12.5	0.21	700

Table 5: Internal Floor properties

Material	Thickness mm	Conductivity (W/mK)	Density kg/m³
Rain screen	3	50	7800
Cavity	50	-	-
Insulation	81.4	0.02	20
Cement bonded particle board	12	0.23	1100
Cavity	50	-	-
Plasterboard	12.5	0.21	700

Table 6: External wall properties

Material	Thickness mm	Conductivity (W/mK)	Convection Coefficient W/m²k
Outer Pane	6	1.06	-
Cavity	12	-	1.4
Inner Pane	6	1.06	-

Table 7: Windows properties

Material	Thickness mm	Conductivity (W/mK)	Density kg/m³
Insulation	154.4	0.03	40
Membrane	0.1	1	1100
Concrete deck	100	2	2400
Cavity	50	-	-
Plasterboard	12.5	0.21	700

Table 8: Roof properties

After setting the internal gains sources and building construction properties, opening types need to be set in MacroFlo. This section is among the most important parts of the simulation because directly impacts all the results related to various parameters like room air temperature, energy consumption, relative humidity, room CO₂ concentration, etc. In general, the opening types of this office could be divide into four types.

- 1- Fixed windows
- 2- Side hung windows for the longer walls
- 3- Side hung windows for the shorter walls
- 4- The opening for the attached area

Each individual window has been marked as a different color based on its type. Blue window panes are fixed, the green and red are operable windows. These windows have been defined as side-hung windows with 80% operability which have their specific profile, and defines the condition to get opened. Besides their operability which is from 9:00 AM to 5:00 PM another condition has been which is based on indoor and outdoor temperatures. In this study, windows will not get open if the indoor air temperature is less than 21° C

(70° F) and the outside temperature is higher than 27° C (80° F). Figure 10 shows the window's profile for controlling the air temperature as well as the time of the day.

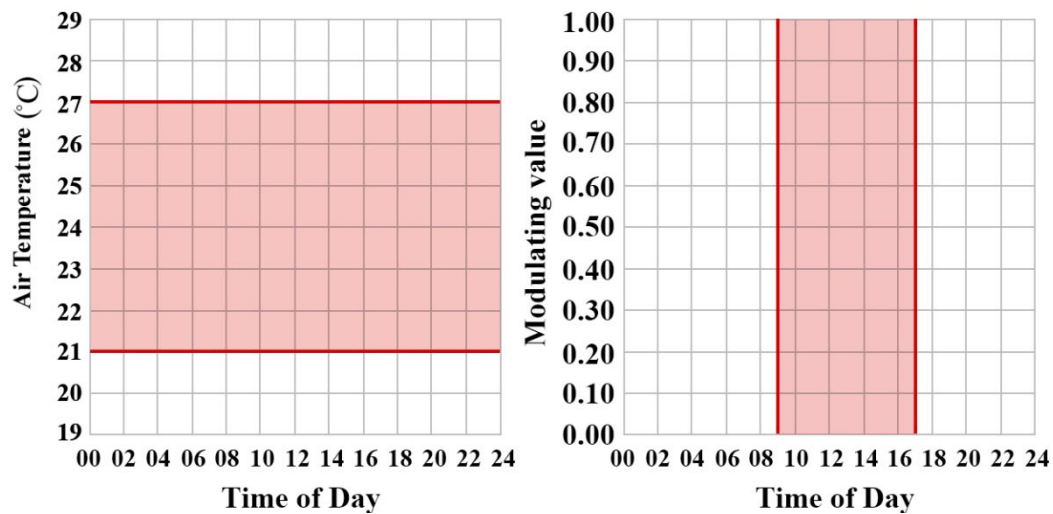


Figure 10: Air temperature condition for windows to get open (left picture) operability period (9:00 AM- 9:00 PM) during the day (right picture)

In addition to the windows, a yellow area has been attached in front of the building, and as explained earlier is because of helping the boundary condition get extended for CFD simulation. Figure 11 depicts all four different windows types for this study.

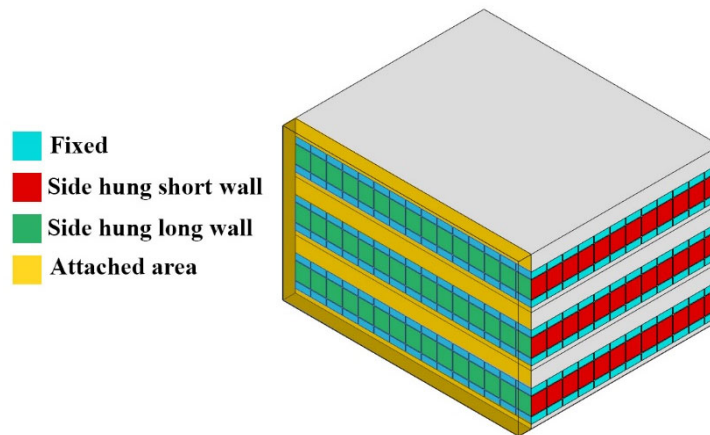


Figure 11: different opening types in the model

3.4- Apache HVAC system

ApacheHVAC is used for modeling heating, ventilating, and air-conditioning (HVAC) systems, and falls within the Virtual Environment's Thermal application category. In general, IES-VE has two major HVAC methodology: Apache system and Apache HVAC.

For this study Apache system is used as a methodology which is a simplified HVAC modeling. In addition, it is fully integrated with the thermal, solar, and bulk-airflow modeling at every simulation time step. Based on this methodology, the cooling and heating set points are 24° C and 19° C respectively which are plotted in figure 12. In other words, the cooling system will get active if the temperature rises above 24° C as well as heating system if the temperature goes under 19° C. Furthermore, air conditioner has been set for cooling and ventilation for this office building and electricity is the fuel for that. Based on this system, natural gas is the fuel for heating.

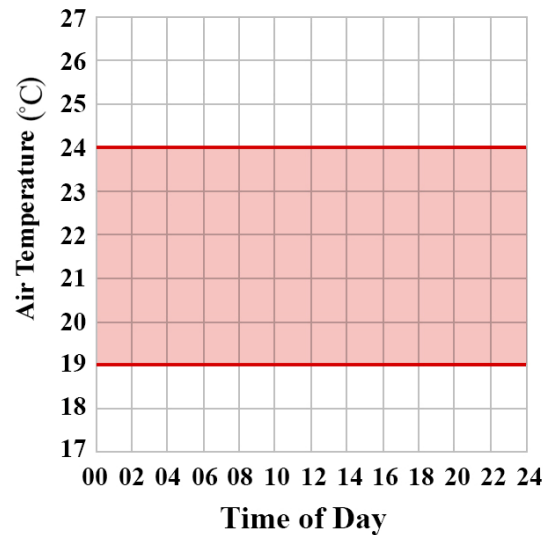


Figure 12: HVAC system temperature profile

The primary goal of this research is to assess the impact of dynamic solar screens on buildings under different parameters during the cooling season months. As it is stated earlier, this study aims to test the performance of dynamic solar screens in two different ASHRAE climate zones against their base case, one in Phoenix (ASHRAE climate zone 2) and the other in Boston (ASHRAE climate zone 5). These two climate zones are chosen as representatives of cooling-dominated and heating-dominated climate zones, respectively. Therefore, it is important to find the cooling season months at first in order to set the simulations during these months.



Figure 13: Location of Phoenix and Boston in the U.S map

3.5- Phoenix Arizona (ASHRAE climate zone 2)

Phoenix, Arizona which is marked in figure 14, is located in the southwest part of the United States of America, a nearly flat plain. The climate type is considered as desert with low annual rainfall and low relative humidity. Daytime temperatures are high, specifically throughout the summer months, and the winters are pretty mild. The afternoon temperatures are usually warm, and the nighttime temperatures frequently drop below freezing during the three coldest months. The temperature typically ranges from 7° C (45° F) to 42° C (107° F) and the predominant wind direction in Phoenix is from the west for six months.

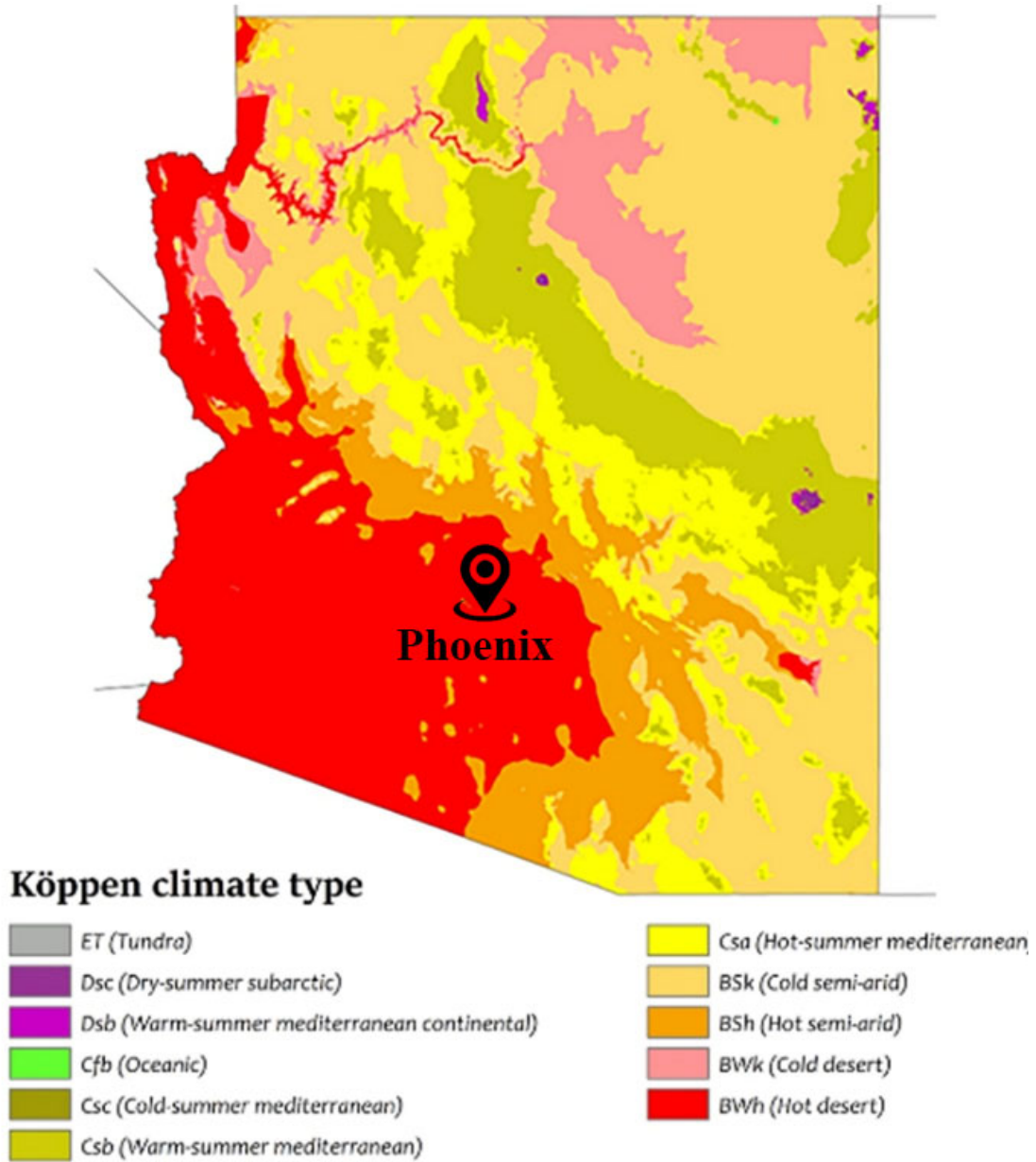


Figure 14: Annual Climate Zones in Arizona

Figure 15 which is generated in Clima tool (CBE Clima Tool) shows the number of cooling and heating degree days for the city of Phoenix. This table has been set based on 18° C (65° F) for cooling degree days and 10° C (50° F) for heating degree days. Based on this picture, Phoenix has 2768 and 72 cooling and heating degree days respectively.

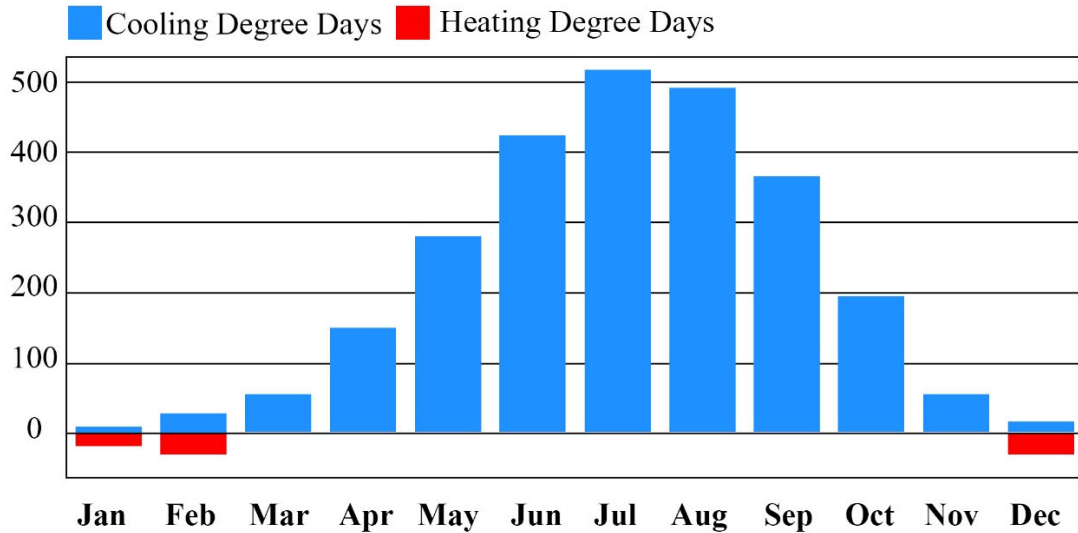
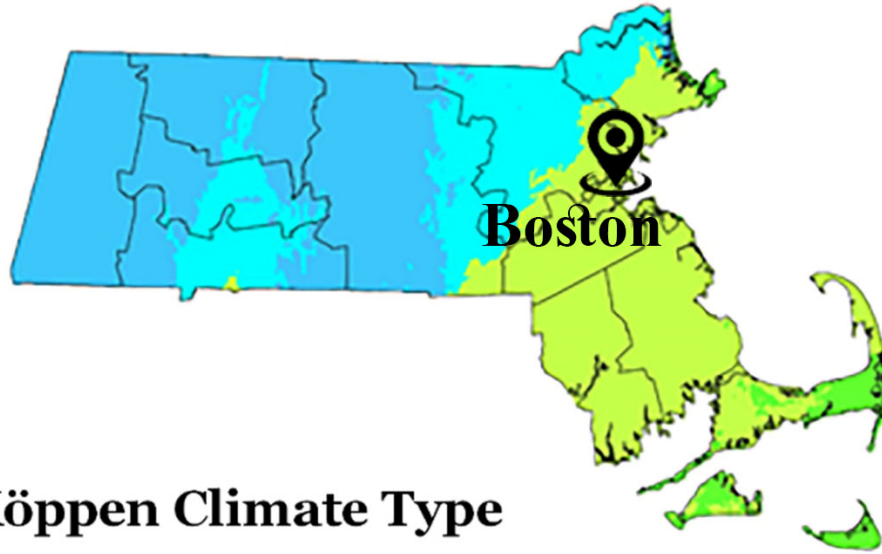


Figure 15: Cooling and heating degree days for Phoenix Arizona (ASHRAE 2)

3.6- Boston Massachusetts (ASHRAE climate zone 5)

Boston, Massachusetts which is marked in figure 16, is located in the northeast part of the United States of America. The climate type is considered a humid continental climate with hot and humid summers. In addition, Boston has cold and snowy winters and gets lots of precipitation during the year. Boston has 5711 heating degree days and 747 cooling degree days. The temperature typically ranges from -17°C (0°F) to 38°C (100°F). The predominant wind direction in Boston is from the west throughout the year. Figure 17 which is generated in Clima tool (CBE Clima Tool) shows the number of cooling and heating degree days for the city of Boston. Similar to Phoenix, this table has been set based on 18°C (65°F) for cooling degree days and 10°C (50°F) for heating degree days. Based on this picture, Phoenix has 423 and 1449 cooling and heating degree days respectively.



Köppen Climate Type



Figure 16: Annual Climate Zones in Boston

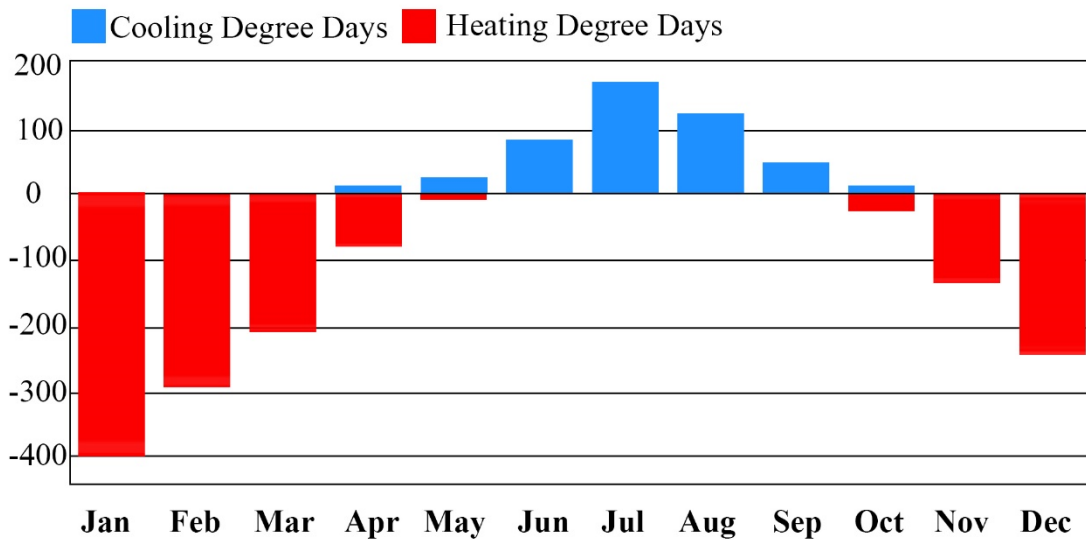


Figure 17: Cooling and heating degree days for Boston Massachusetts (ASHRAE 5)

Based on the cooling and heating degree days for these two cities, June to September has been set for Boston and March to September has been set for Phoenix in order to run simulations.

3.7- Physical Properties of Solar Screen

The physical properties of solar screens could be divided into two categories; solar screen geometry and solar screen materiality. Geometry itself could be divided into three subcategories: Perforation ratio, which is the proportion of the opening area to the whole area of the screen, depth ratio, which is the ratio between the width and depth of each perforation opening, and screen pattern.

Another screen property is its material which is basically related to the thermal mass of the material. In other words, the conductivity of heat through the solar screen depends on the screen material.

3.8- Dynamism

This study aims to evaluate the impact of a dynamic solar screen on different parameters, so in order to show dynamism in IES-VE, different scenarios could be defined based on the dynamic solar screen behavior. In addition, these scenarios help to have a more simplified model in IES-VE, which is highly recommended. As mentioned earlier, dynamic façades are programmed to respond in real-time to changes in indoor and outdoor conditions in order to improve occupant comfort and satisfaction with the indoor environment (Luther, [2000](#)). The effectiveness of façade automated controls depends on occupant interaction and satisfaction with these controls (Cao, Ouyang, Zhu, Huang, Hub, Deng, [2012](#)). Based on this issue, in order to show dynamism in this study, different solar screen perforation ratios and positions can be defined which will be discussed below. It is worth mentioning that during the simulation for each one of these scenarios, the screen does not close and open.

3.9- Simulation Scenarios

In this study, three perforation ratios have been defined to show the different dynamic façade states. The solar screen with 30% represents a closed state, 50% represents semi-open, and 70% represents an open state. It is worth mentioning that these screens have been

modeled as local shade in the software, which are shading objects, and the properties of the solar screen are shown in table 9.

Material	Thickness mm	Conductivity w/(m.k)	Density Kg/m ³	Specific Heat capacity J/(kg.k)
Cast Concrete	100	1.4	2100	840

Table 9: Local shade properties

3.9.1- The building without solar screen (base case)

The performance of these buildings will be assessed under two conditions. In the first stage, they will be tested without any solar screen to figure out the baseline condition, and the results of this part could be compared with the further simulations. After that, the performance of these buildings will be evaluated with a solar screen façade. The performance of geometric screens is evaluated in terms of energy consumption, natural ventilation, indoor air velocity, as well as indoor air quality, in particular room CO₂ concentration, and air temperature.

3.9.2- 30% perforation ratio (closed state)

The 30% perforation ratio solar screen represents the closed state for this dynamic façade. In order to model it in IES-VE, the whole area of the wall is calculated first, which is 600 m² (6458.35 sq. feet). Since the opening area is supposed to be 30%, the whole area is multiplied by 30% to find the void area, which is equal to 180 m² (1937 sq. feet). In other words, the sum of all these squares needs to be around 180 m² (1937 sq. foot). For this building, the dimension of each square is 50 cm (1.6 feet) by 50 cm, and the distance between each square is 40 cm (1.3 feet). This building has 13 rows in which has 55 squares, and overall has 715 squares.

3.9.3- 50% perforation ratio (semi-open state)

The 50% perforation ratio solar screen represents the semi-open state for this dynamic façade. In order to model it in IES-VE, the whole area of the wall is calculated first, which is 600 m² (6458.35 sq. feet). Since the opening area is supposed to be 50%, the whole area is multiplied by 50% to find the void area, which is equal to 300 m² (3229 sq. feet). In other words, the sum of all these squares needs to be around 300 m² (3229 sq. foot). For this building, the dimension of each square is 70 cm (2.3 feet) by 70 cm, and the distance between each square is 25 cm (0.8 feet). This building has 12 rows in which has 52 squares, and overall has 624 squares.

3.9.4- 70% perforation ratio (open state)

The 70% perforation ratio solar screen represents the open state for this dynamic façade. In order to model it in IES-VE, the whole area of the wall is calculated first, which is 600 m² (6458.35 sq. feet). Since the opening area is supposed to be 70%, the whole area is multiplied by 70% to find the void area, which is equal to 420 m² (4520 sq. feet). In other words, the sum of all these squares needs to be around 420 m² (3229 sq. foot). For this building, the dimension of each square is 100 cm (3.2 feet) by 100 cm, and the distance between each square is 20 cm (0.65 feet). This building has 10 rows in which has 41 squares, and overall has 410 squares. Figure 18 shows all the different scenarios and the base case.

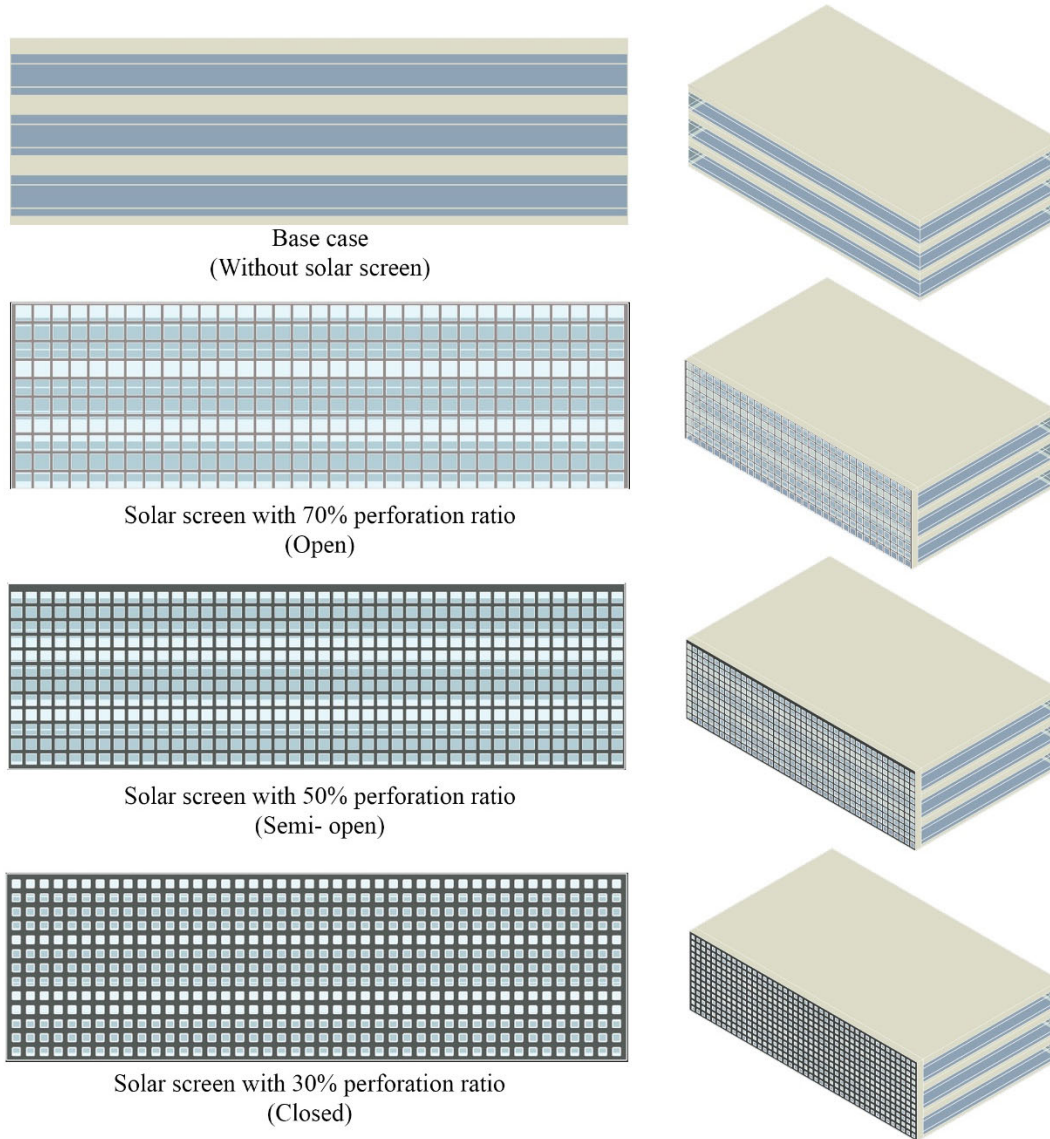


Figure 18: Simulation scenarios based on the different perforation ratios

In this study, the variables that will be tested are listed below.

- 1- Climate zones (ASHRAE 2 and ASHRAE 5)
- 2- Screen perforation ratio (30%, 50% and 70%)
- 3- The distance between the building and the solar screen. (1 m gap and 0.5 m gap).
- 4- State of top of the attached area (Open and closed)
- 5- Screen Materials (Concrete and wood)
- 6- The screen depth (10 cm and 20 cm).

However, the sensitivity study results showed that the software is not sensitive to different depths and materials; therefore, the testing variables for this study is limited to climate zones, screen perforation ratio, the distance between the building and solar screen, and top of the attached area. The results of sensitivity have been attached in appendix A.

CHAPTER IV: DATA ANALYSIS AND FINDINGS

This chapter covers the findings and results of the experimental study for two different climate zones (Phoenix ASHRAE climate 2 and Boston ASHRAE climate 5). The analysis of findings will be organized based on the conceptual framework in Chapter 2 to compare the total energy consumption, MacroFlo external Vent (Natural ventilation), air velocity pattern, and indoor air quality (Indoor air temperature and room CO₂ concentration).

4.1- Simulation results for Phoenix Arizona, ASHRAE climate zone 2

4.1.1- SunCast

As discussed earlier, the early stage of running simulation in IES-VE is running SunCast, which could be used at any step of the design process to analyze shading and solar insolation studies. SunCast is used to investigate external obstruction and self-shading of a building, the impacts of changing the orientation of the building, and solar mapping through windows and openings. Figure 19 shows the result of running SunCast for the city of Phoenix based on the six different solar screen types. This tool could generate shadow and internal solar insolation from any sun position defined by date, time, building's orientation, site latitude, and longitude. These results are based on the impact of the solar screen on the building's façade, and since, in this study, the solar screen is located on the southern side of the building, the results are just for the southern side of the building. As it is plotted on the buildings' façade, even changing the distance between the building and the solar screen has an impact on the solar heat gain (kWh/m²); the closer the screen to the building, the lower the solar energy could be absorbed. Moreover, the results show that increasing the perforation ratio corresponds to increasing the amount of absorbed energy because the solar screen has a more open area, and solar energy could pass through the openings and be absorbed by the building façade.

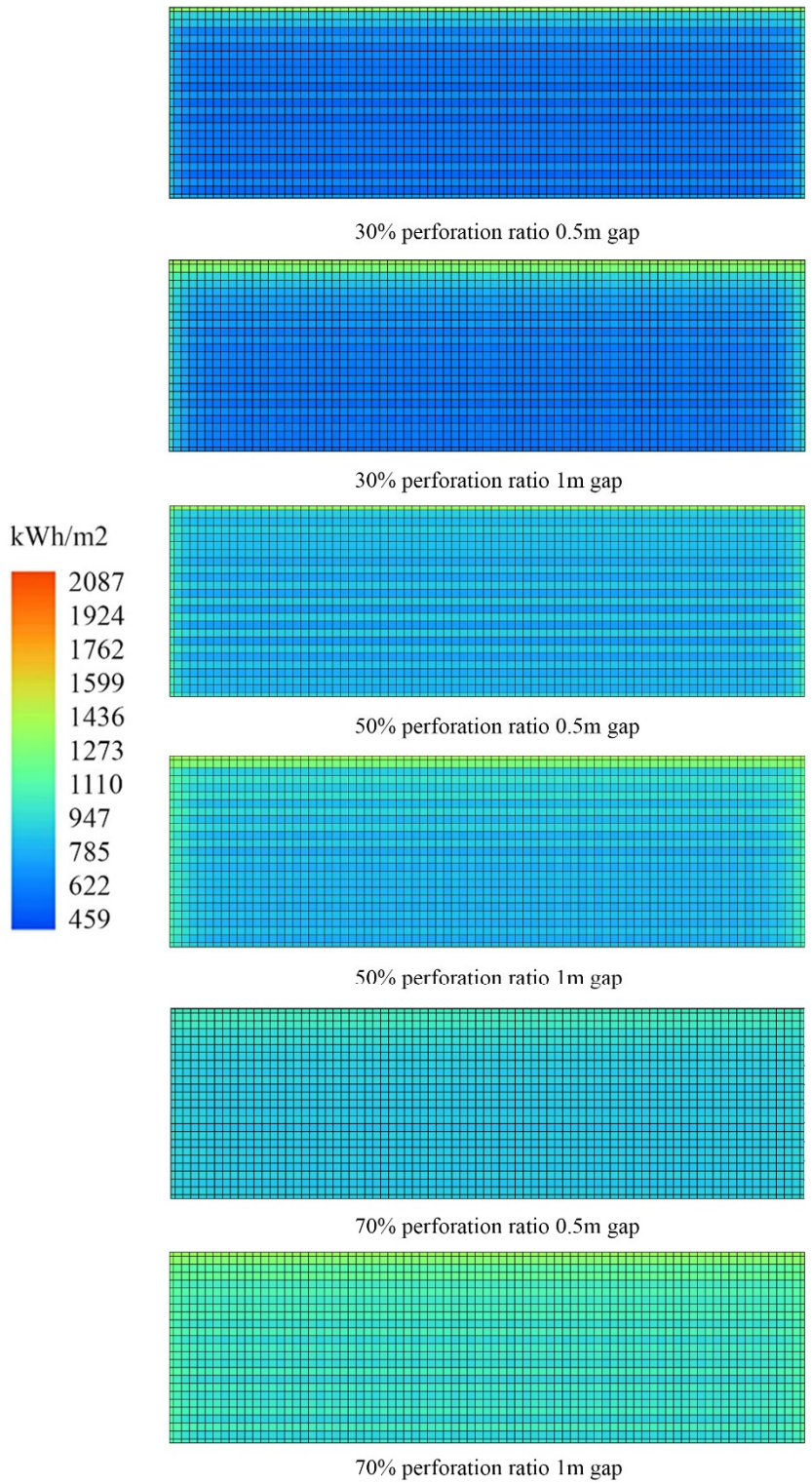
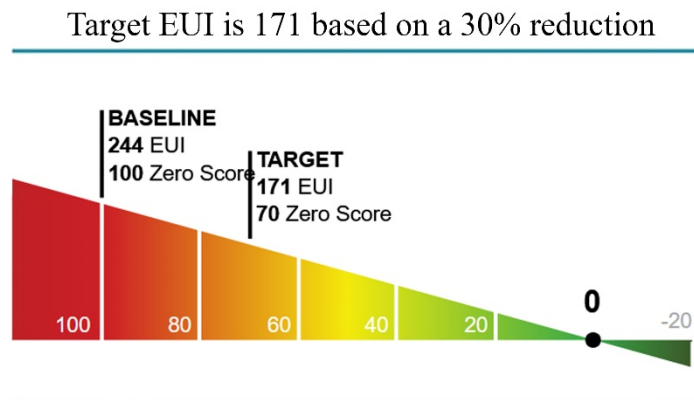


Figure 19: SunCast analysis for the city of Phoenix during the cooling season months

4.1.2- Energy Performance

Energy Utilization Index (EUI) was used in various studies to show the energy benchmarking of building and design strategies. The mean EUI of commercial buildings in the US was calculated from the Zero Tool website and used to compare the base case with the building with different solar screen configurations. Based on the result of the Zero tool website as shown in figure 20, the energy usage intensity for an office building with a dimension of 50m (164 ft) by 33m (108 ft) is 244 (kWh/m²/yr) for Phoenix, and the target EUI based on 30% reduction is 171 (kWh/m²/yr).



Building Summary

Location	Phoenix,AZ	85003
Uses	Office	1,650 sq.m

Results	Baseline	Target
EUI reduction % from baseline	0%	30%
Zero Score	100	70
Site EUI (kWh/m ² /yr)	244	171
Source EUI (kWh/m ² /yr)	613	429

Figure 20: Baseline EUI for an office building in the city of Phoenix

4.1.3. Total Energy Consumption

This chapter investigates the impact of different solar screen configurations on energy consumption during the cooling season months of the year for Phoenix. Based on its climate, the period between June and August has the highest energy consumption in this city because the outdoor air temperature is very high, and most of this energy is used for cooling. Figure 21 shows the total energy consumption for this city during the cooling season months, as stated before. For this study, 14 different variations have been defined to delineate the effect of important designs and constructions, including solar screens with different levels of perforation. This seems to be an essential parameter that directly affects the energy consumption while keeping the indoor environment like air velocity, air temperature, and relative humidity at an acceptable level. The results show that among all of these configurations, the building which has a solar screen with a 30% perforation ratio has the best performance in terms of energy consumption. Since each of these perforation ratios represent of different state of the dynamic façade, it can be concluded that once the dynamic façade is in a closed state, it has the best performance in terms of energy consumption. As is plotted in the bar chart, the performance of this screen is different based on its position on the building and the state of the attached area's top. Figure 21 shows that the best performance happens when the top of the attached area is closed. Furthermore, when the solar screen is closer to the building, its performance can increase. This bar chart shows the solar screen does not have the same performance in these six months. As it is plotted, the highest reduction can be seen in June, July, and August, which is more than a 60% reduction in some cases. Since this period has the highest outdoor air temperature, the solar screen with a low perforation ratio blocks the majority of solar energy.

Once the state of the dynamic façade is changed from closed (30% perforation ratio) to semi-open (50% perforation ratio), the performance of the screen in terms of energy-saving is decreased. However, in some cases, the screen with a 50% perforation ratio is able to reduce energy consumption up to 40%. Similar to the screen with a 30% perforation ratio, once the top of the attached area is closed, the screen has a better performance for energy consumption. In addition, the graph shows that if the screen is located closer to the building, its performance will increase. Once the state of the dynamic façade changes from semi-

open (50% perforation ratio) to open (70% perforation ratio), as is shown in the bar chart, the performance of the screen is at its lowest. In other words, increasing the perforation ratio corresponds to the reduction of performance for energy consumption. However, this screen with a 70% perforation ratio is still effective in reducing energy consumption and, in some case, is able to reduce the energy consumption up to 25%. As discussed earlier, the impact of these screens on energy consumption is not the same during the cooling season months. The bar chart shows that in April, the performance of the screen with a 70% perforation ratio is very low, and in some cases, it does not have an impact on energy consumption.

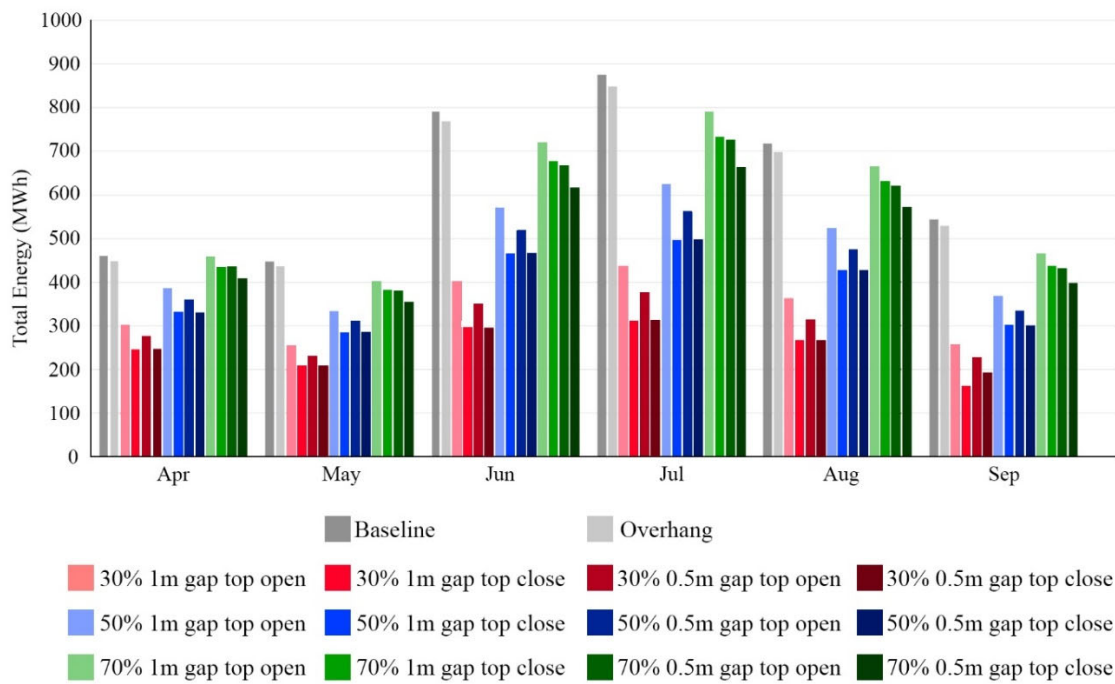


Figure 21: The bar chart diagram for energy consumption in Phoenix for cooling season months

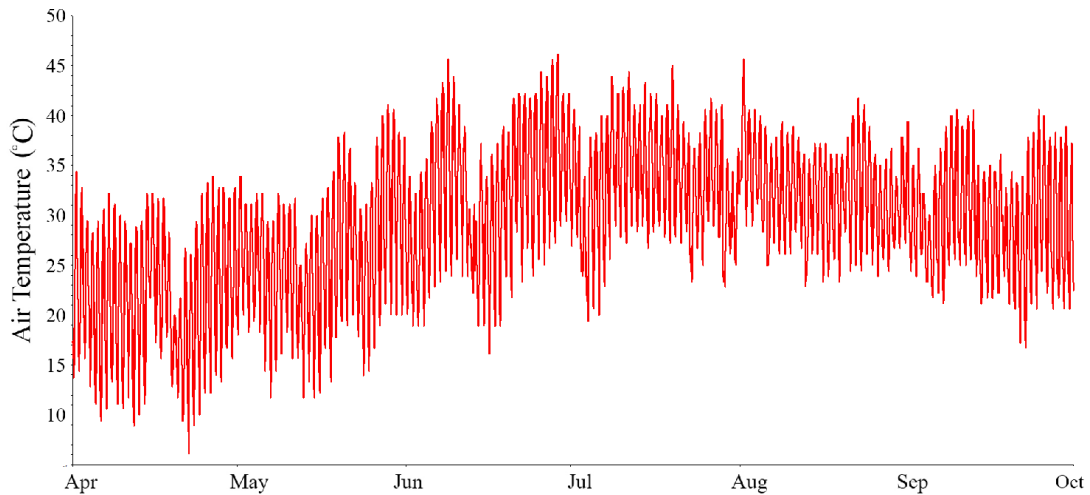


Figure 22: The outdoor air temperature for the city of Phoenix is based on the weather data

To better observe the superior effect of solar screens on the energy consumption of buildings, a more detailed graph has been provided in the Figure 23. In this graph, the energy consumption for a shorter period of one week in the month of July has been plotted and demonstrates the amount of energy consumption for this given week in Phoenix. In addition, the outdoor air temperature has been plotted, which shows that by increasing the outdoor air temperature during the day, the energy consumption increases, and during the cooler days, the energy consumption is lower. It should be borne in mind that the data presented in this graph belong to an office where the cooling devices are mainly used during office hours, i.e., between 9 am and 5 pm. By referring to this Figure, one can see how the solar screening is efficient in reducing the energy from a high value of 3800 KW to less than 1100 KW, an almost fourfold reduction in energy consumption. It is worth mentioning that the total system energy contains various energy constituents such as boilers energy, air-conditioning, lighting, and ventilation. Since this simulation has been carried out for the cooling season, the major impact of solar screens has been to reduce the cooling energy consumption. This graph clearly shows that even a small change in the position of the screen could change the energy consumption of the whole building effectively.

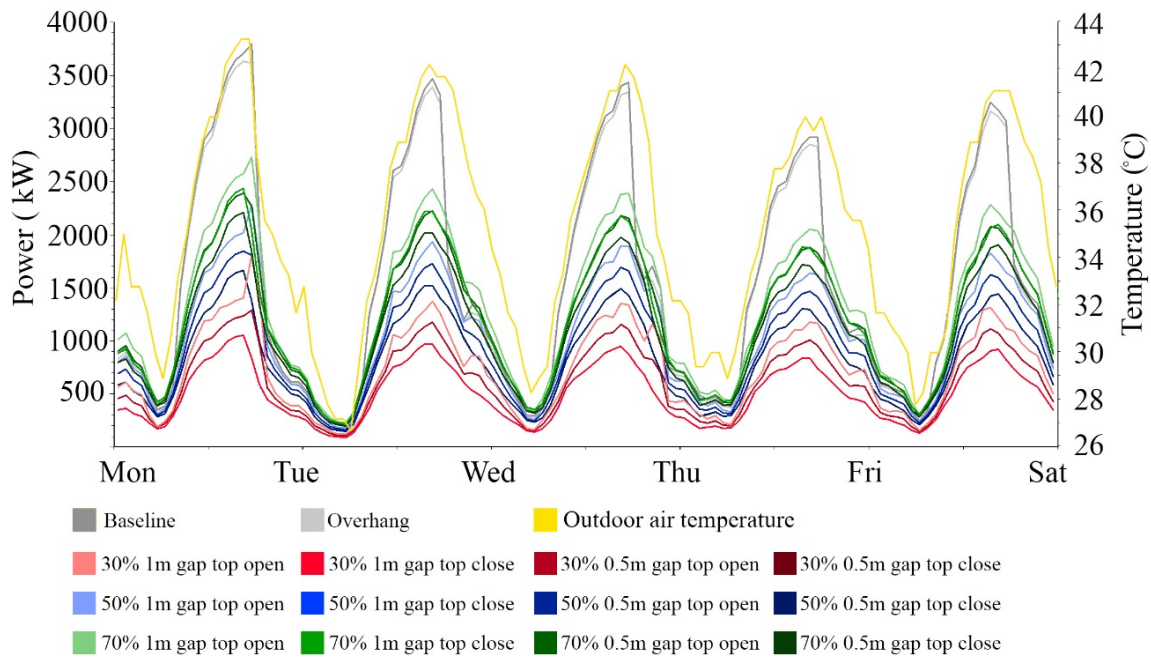


Figure 23: The impact of different solar screen configurations on energy consumption in a week of July in Phoenix

4.1.4- MacroFlo

4.1.4.1- MacroFlo with opening profile

Figure 24 collects the MacroFlo external vent (airflow volume) for the third floor of this office building during the cooling season months (April to September). As previously discussed in the methodology, the result of this section is directly related to the opening profiles and their opening degree. For this study, it has been assumed that windows will not open unless the indoor air temperature goes upper than 21 °C, and at the same time, the outdoor temperature is lower than 27 °C. In addition, since this is an office building, the windows are closed during the weekends or night hours. All different configurations would lead to similar venting values, a rather surprising result which does not show any direct impact of solar-screening on the ventilation of the building. Based on this profile, the openings are almost closed in July and August, and it is because of the very high outdoor

temperate in Phoenix. On the other hand, the period between April and June has a better potential to take advantage of natural ventilation due to the cooler outdoor temperatures. The bar chart below demonstrates that the building without any solar screen has better potential for taking advantage of the outdoor wind. Furthermore, a solar screen with 70% perforation ratios shows good potential for natural ventilation and taking advantage of the outdoor wind. On the other hand, a solar screen with a 30% perforation ratio has the lowest potential for natural ventilation, and it is due to the minimum opening area. Although air ventilation is more effective for the baseline or solar screens with high perforation ratios (higher openings), the difference is not quite significant for all different configurations. For instance, by looking at the graph, one can observe that for April (first chart in this figure), the MacroFlo External Vent has a value of 2.05 million cubic meters (2050 times 1000 m³) for a baseline configuration. By digging up the data for the screen with a 30% perforation ratio in this figure and for the very same month, one can realize that the level of MacroFlo External Vent is around 1.75 million cubic meters (1750 times 1000m³), which is about 14% lower in terms of ventilation potential. Although ventilation is more powerful for the baseline or overhang structures, the amount of energy saving is about two times for configurations with solar screening with proper perforation. Furthermore, based on this chart, the room has a higher MacroFlo external vent once the top of the attached area is closed. In terms of the position of the screen, it is depicted that the distance of the screen does not have an impact on MacroFlo external vent once the top of the attached area is closed. Conversely, once the top gets opened, the amount of MacroFlo external vent is changed in different positions, and it shows the closer screen is able to improve MacroFlo external vent. It is worth mentioning that this chart is the total amount of entered air for the third floor and does not show the exact behavior of the air inside the room. In order to have a better picture of the impact of these screens on natural ventilation and airflow, it is essential to run a CFD simulation.

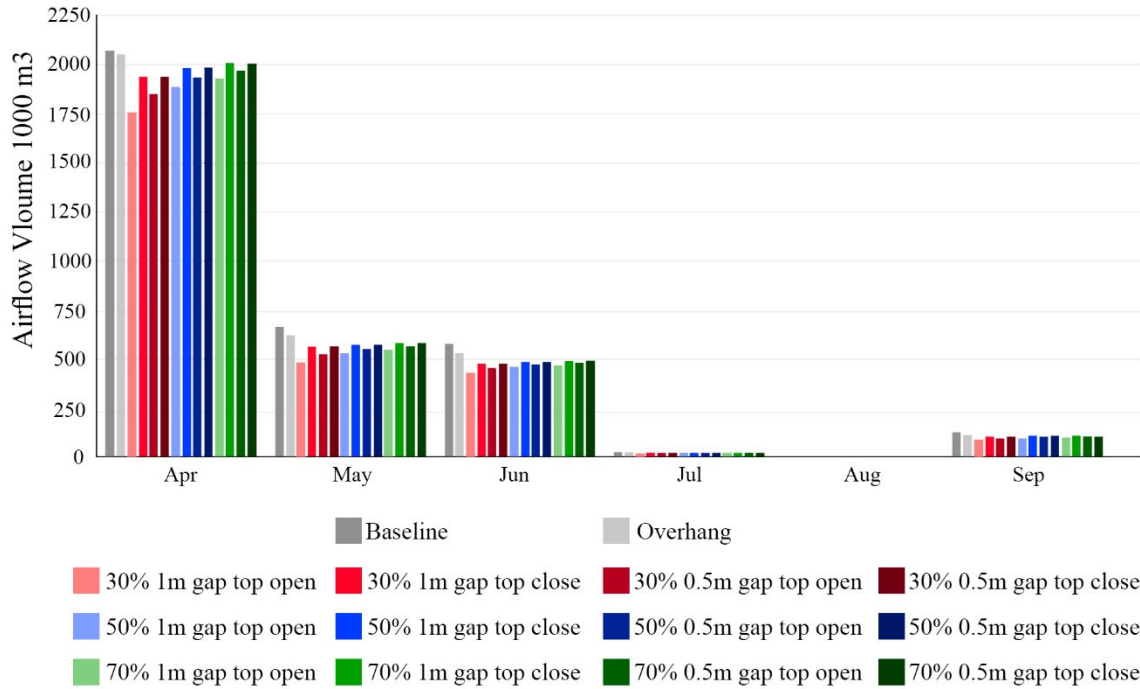


Figure 24: Airflow volume bar chart for cooling season months in Phoenix (with opening profile)

4.1.4.2- MacroFlo without opening profile

Since, based on the defined opening profile, most of the time, the windows are closed during the cooling season months in Phoenix, it is worthwhile to simulate this period without any profile in order to see a better picture of the impact of different solar screen configurations. Figure 25 depicts the MacroFlo external vent when the windows are open from 9 AM to 5 PM. Based on this chart, June and July have the highest potential for taking advantage of natural ventilation, and it is because of the wind speed average, which is higher than the rest of the months. The wind speed average for these two months is 3.43 m/s and 3.57, respectively. Furthermore, as discussed previously, in order to have a better evaluation of the impact of the solar screen on natural ventilation, the eastern and western windows of the building are closed, and the wind direction is mainly from the south for these two months. This bar chart also shows that the screen with a 30% perforation ratio has the lowest potential to take advantage of natural ventilation. Among four different variations of a solar screen with a 30% perforation ratio, the MacroFlo external vent

increases when the attached area's top is closed. When the top of the attached area is open, the stack effect happens, and consequently, some portion of wind, instead of moving into the building, goes upward (this happening could be observed clearly in CFD analysis). In addition, the results show that the MacroFlo external vent is higher when the solar screen is closer to the building. The solar screen with a 50% and 70% perforation ratio shows a similar result to 30%; however, the amount of MacroFlo external vent is higher.

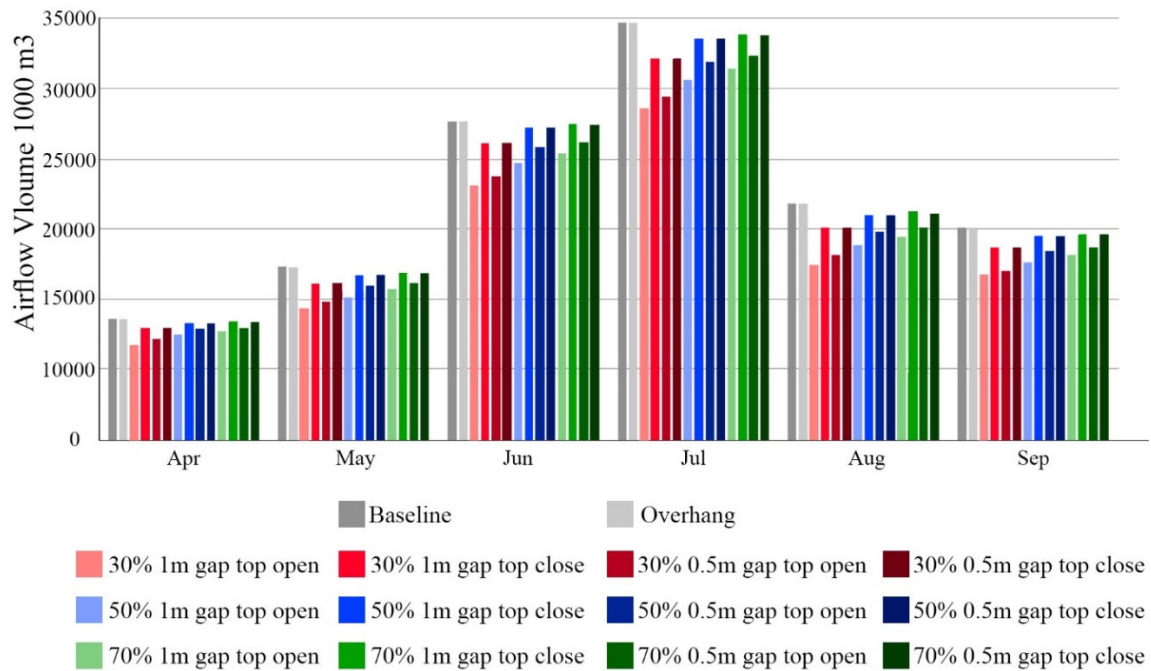


Figure 25: Airflow volume bar chart for cooling season months in Phoenix (without opening profile)

The MacroFlo external vent for the week of July in Phoenix have been plotted in figure 26. Similar to the bar chart results, these graphs show that the screen with a 70% perforation ratio has the best potential to take advantage of natural ventilation, and in some cases, the MacroFlo external vent amount is similar to the baseline condition. Moreover, these graphs show that a solar screen with a 30% perforation ratio has the lowest MacroFlo external vent amount once it is located 1m from the building and the attached area's top is open.

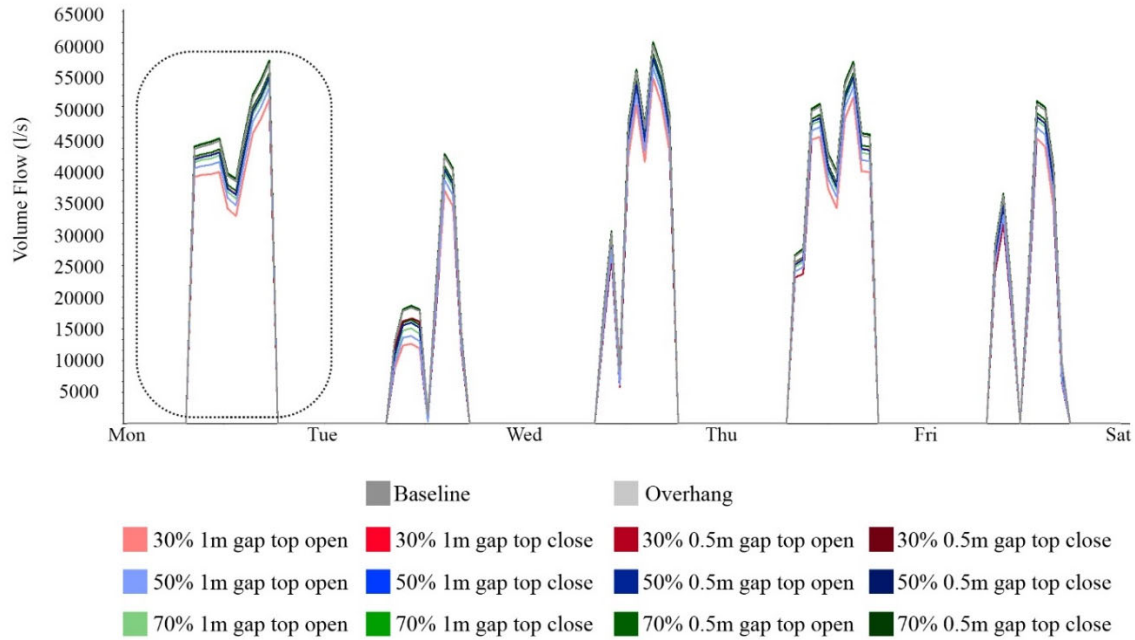


Figure 26: Airflow volume for a week of July in Phoenix without opening profile

In order to have a better understanding of the exact impact of these different configurations, figure 28 focuses on a day of July, which has been marked as a dashed line in figure 27. In this picture, wind speed has also been plotted due to the direct relationship between airflow volume and wind speed. Since the opening profile has been removed, once the office hours start, the airflow volume increases by opening the windows. For this specific day, since the wind speed is low at 1:00 PM, the air volume flow is at its minimum amount; on the other hand, the air volume flow reaches its highest amount at 5:00 PM. This pattern is the same for all different solar screen configurations. This picture also depicts that the screen with a 30% perforation ratio due to the minimum open area gets the lowest air volume flow, specifically if it is located 1m from the building and the top of the attached area is open. Conversely, the solar screen with a 70% perforation ratio can get the highest air volume flow if it is located 0.5 from the building and the top of the attached area is closed.

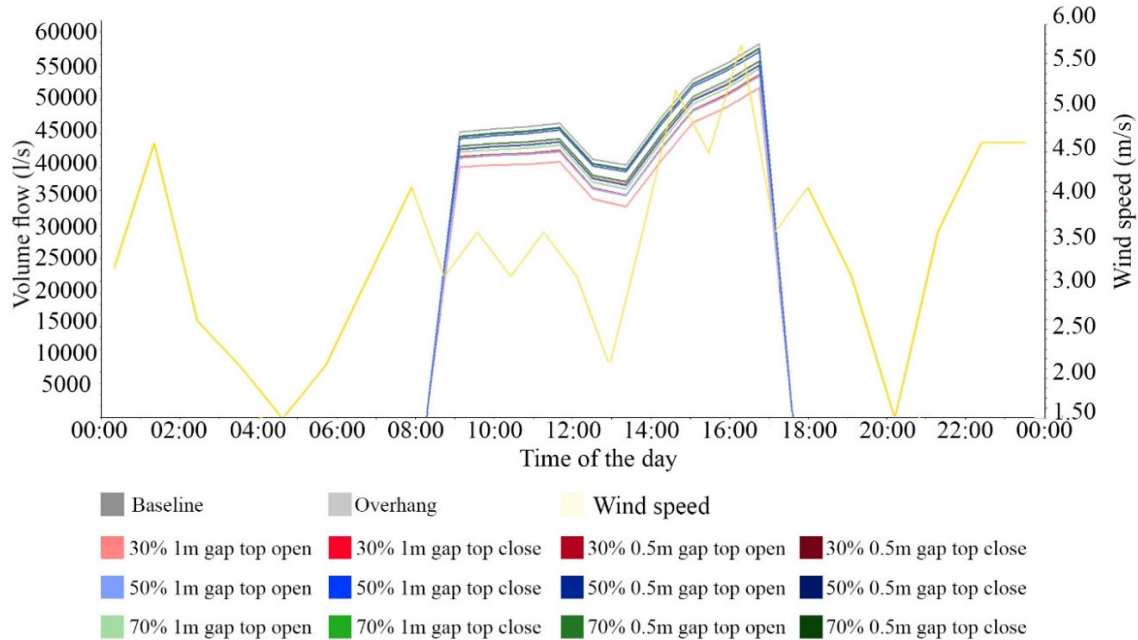


Figure 27: Airflow volume for a day of July in Phoenix without opening profile

4.1.5- Room Air Temperature

Figure 28 shows the impact of solar screens on room temperature for the week of April in phoenix. The room air temperature based on the building HVAC system setting is in the range of 19 °C and 24 °C, which means that the cooling system gets activated once the temperature rises more than 24° C. Since this graph is for a week of April, the room is able to take advantage of natural ventilation based on the set profiles which discussed previously. As plotted in the graph, the room air temperature during the night hours is different based on the different solar screen configurations. The graph demonstrates that the screen with a 30% perforation ratio has the best performance in terms of reducing the indoor air temperature, which is able to reduce up to 1°C in some cases. The highest reduction happens when the attached area's top is closed. Furthermore, being closer to the building can reduce room air temperature by about 0.1°C. The screen with a 50% perforation ratio is also able to reduce air temperature up to 0.5 °C. Conversely, the results show that the screen with a 70% perforation ratio increases air temperature up to 0.3°C. When the attached area's top is closed, this increase could be 0.1° C.

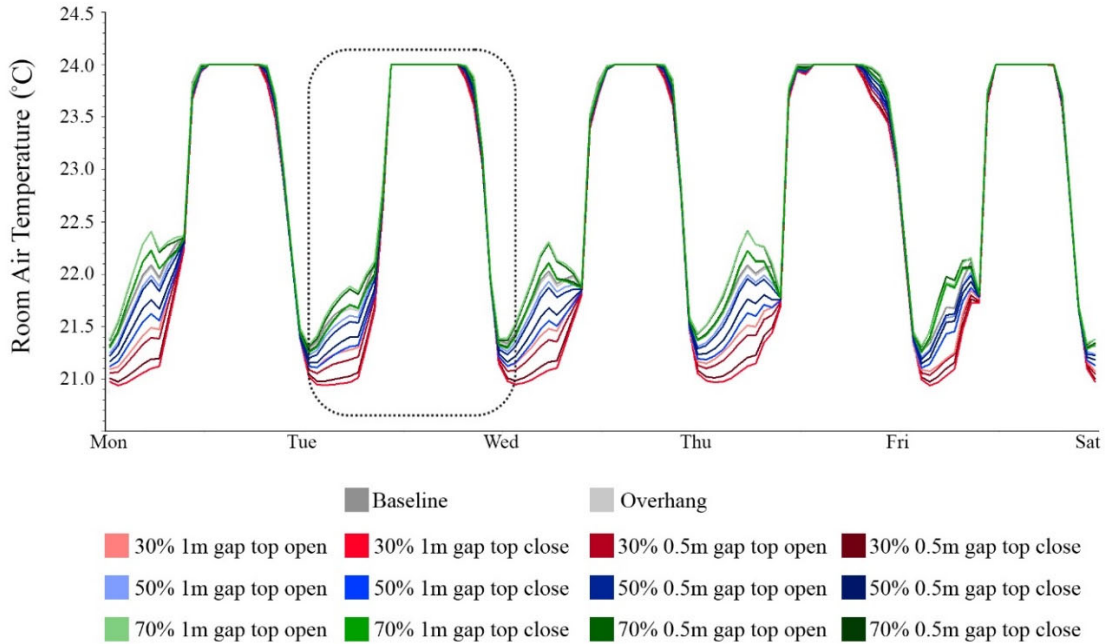


Figure 28: The room air temperature for a week of April as a result of various configurations in Phoenix.

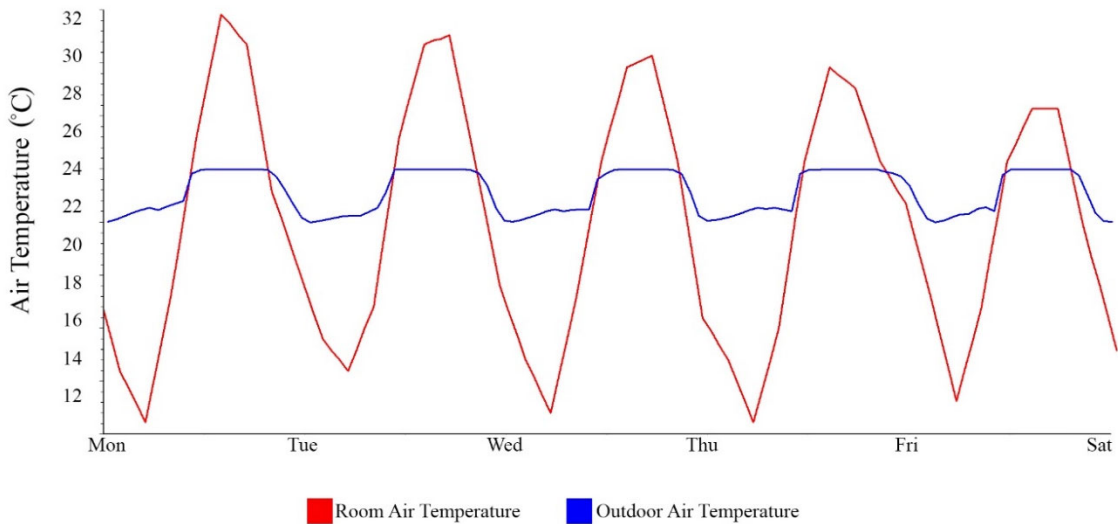


Figure 29: Room air temperature and outdoor air temperature for a week of August in Phoenix

Figure 30 demonstrates the room air temperature for the day of April in Phoenix, which is marked with a dashed line in figure 27. By starting the office hours, the room air temperature starts rising due to the internal gain sources like computers, lighting, and people. Besides internal gain sources, increasing the outdoor air temperature, which is

shown in figure 29, is another reason for increasing the indoor air temperature. However, due to HVAC system settings, the room air temperature does not go more than 24. Therefore, for this specific day, the room air temperature is 24°C during most office hours. After hours, the room air temperature starts decreasing from 24°C to 21°C. As plotted in the graph, the screens with 30% and 50% perforation ratios are able to reduce room air temperature during the night hours up to 0.5 °C in comparison with baseline.

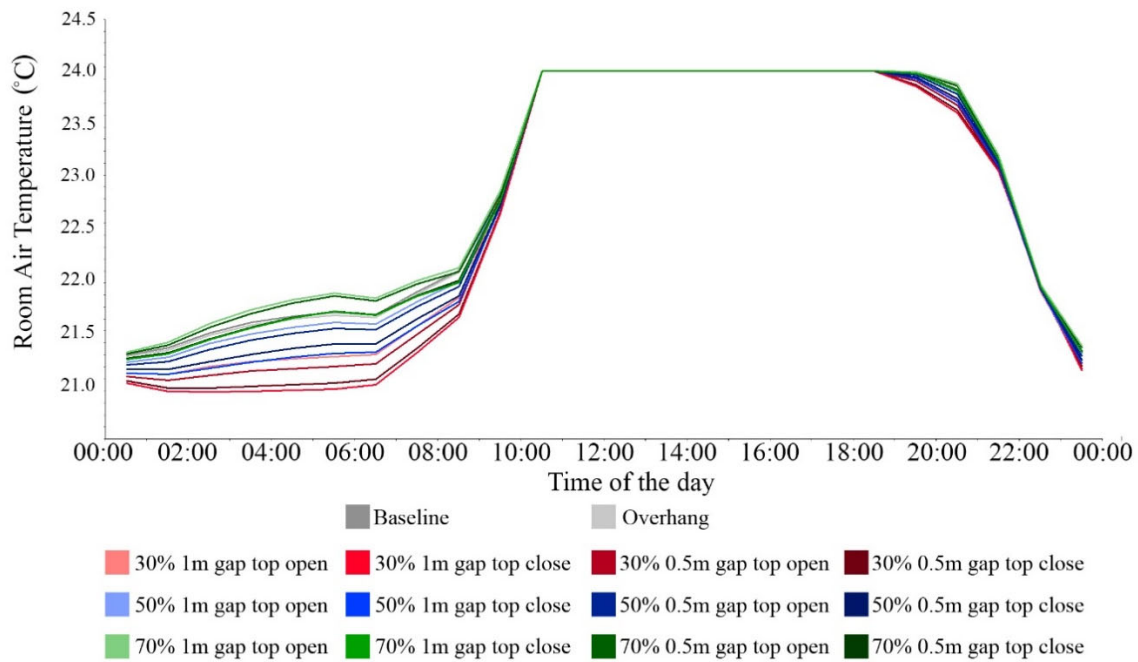


Figure 30: The room air temperature for a day of April as a result of various configurations in Phoenix.

4.1.6- Room CO2 Concentration

One of the goals of this study is the evaluation of indoor air quality, which directly impacts occupants' health and performance during office hours. Figure 31 shows the impact of different screen types on CO2 Concentration in a week of July in Phoenix. As discussed in the MacroFlo section, solar screens are able to impact natural ventilation in this building. Since there is a direct relationship between room ventilation and CO2 Concentration, as it is plotted below, different solar screens have a different impact on CO2 Concentration.

However, this impact is not significant, and it could be enhanced by using mechanical equipment. Based on this graph, the room CO2 concentration is ranged from 400 ppm to 450 ppm, which is within the acceptable range of ASHRAE standards (below 800 ppm for office buildings).

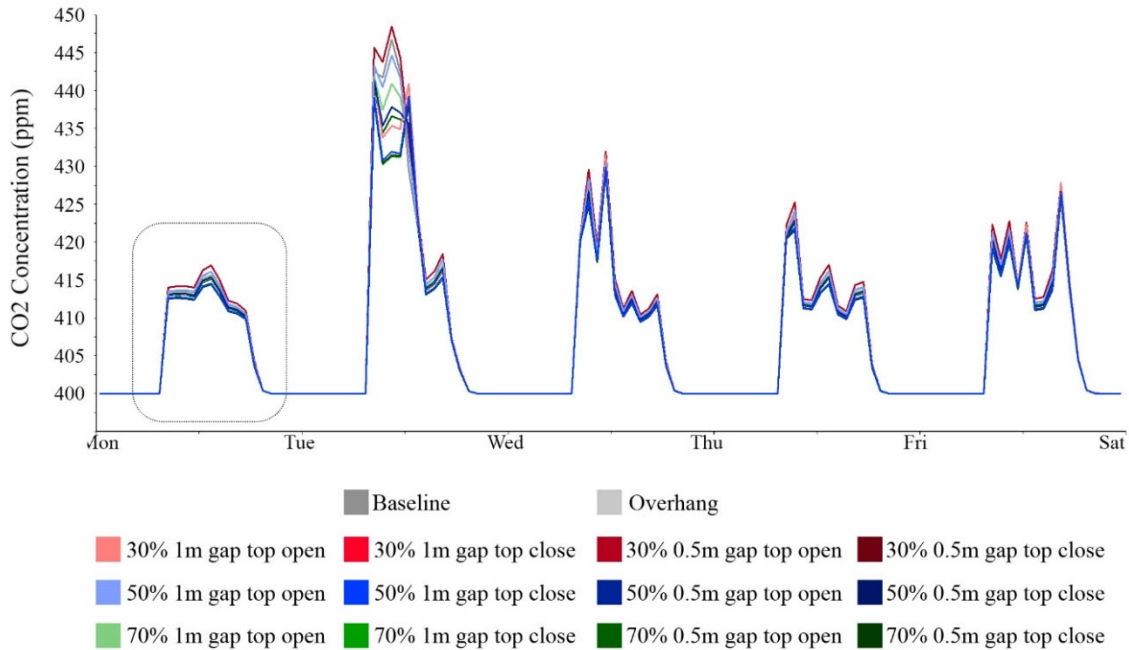


Figure 31: The room CO2 concentration for a week of July in Phoenix.

Figure 32 focuses on a CO2 concentration for the day of July to better understand the impact of these screens. In addition, airflow volume has been plotted in this graph which helps to understand the fluctuation of room CO2 level at different times of the day (the volume flow lines have been faded). This graph demonstrates that room CO2 levels because of occupancy increase during office hours, and as it is shown, the CO2 level is not the same during different times of the day. For this specific day, the highest CO2 concentration happens between noon and 3:00 PM, and it is due to the lowest volume airflow. Moreover, based on this graph, the solar screen with a 30% perforation ratio has the lowest airflow volume, leading to the highest CO2 concentration, specifically, if it is located 0.5 m from the building and the top of the attached area is closed. Conversely, from

3:00 PM until 5:00 PM, the room CO2 concentration starts decreasing due to increased airflow volume.

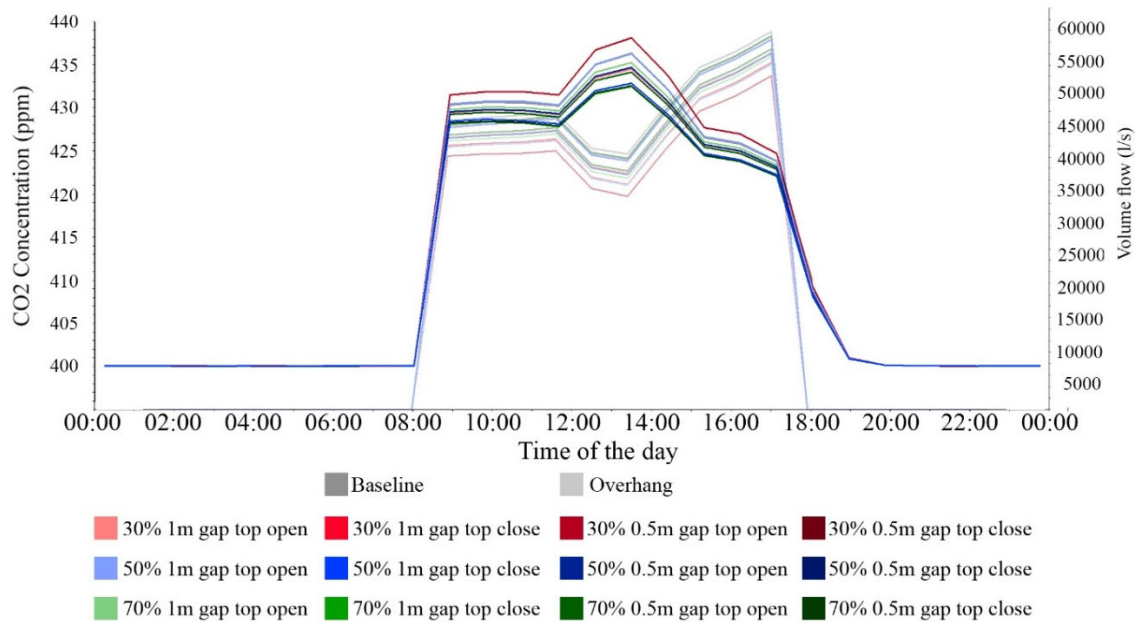


Figure 32: The room CO2 concentration and airflow volume for a day of July in Phoenix

4.1.7- CFD Analysis for Phoenix

The pictures below belong to the results of the CFD analysis for a specific day and time. In IES-VE, once the ApacheSim is done, the results are shown in VistaPro, and in this section, the thermal information of a target day could be exported as a boundary condition to the MicroFlo section. The solar screen for this study is located on the southern side of the building. Since this study aims to investigate the impact of the solar screen on airflow patterns for the indoor spaces, the target date has been set for a day the wind direction is from the south. Based on the wind rose chart, April 18th is one of the days the wind direction is from the south. Furthermore, based on the MacroFlo external vent graph, 11 am has the highest potential for natural ventilation on this specific day; therefore, the boundary condition is set for April 18th at 11 am, and the thermal information of this day is exported to MicroFlo for CFD analysis. Once the boundary condition is imported in

MicroFlo, the CFD grid needs to be defined and, for this study, has been set as 20 cm by 20 cm.

4.1.7.1- CFD Analysis for a screen with 30% perforation ratio

Figure 33 is the results of the CFD analysis for air velocity on the third floor of the office building in Phoenix. In order to have a clear comparison, the air velocity for all of these variations is ranged between 0.01 and 1 m/s. In the baseline condition, air enters the room, and its velocity is about 1 m/s and penetrates directly to one-third of the room while its velocity drops to near 0.5 m/s. Once the solar screen with a 30% perforation ratio is added, based on the position of the screen and the state of the top of the attached area the airflow changes.

One of the significant impacts of adding a solar screen happens when the top of the attached area's state changes. When the top of the attached area is open, due to the stack effect, the air moves upward inside the room, which has a better circulation in the room. Moreover, the airspeed is slightly higher in the room when the distance between the building and the solar screen is 1m. In general, as discussed in MacroFlo results, a solar screen with a 30% perforation ratio due to the minimum opening area reduces the chance of taking advantage of an external vent which can be seen in this figure. In the baseline condition, the entire room has a higher air velocity in comparison with other variations, although the difference is not significant. The air velocity in the baseline condition is about 0.3 m/s in the most part of the room, while the air velocity gets lower after adding the solar screen with a 30% perforation ratio and in some parts of the room the air velocity drops to less than 0.1 m/s. Therefore, based on the results of the CFD analysis the main impact of adding the solar screen is changing the airflow inside the room, specifically, the time when the top of the attached area is open.

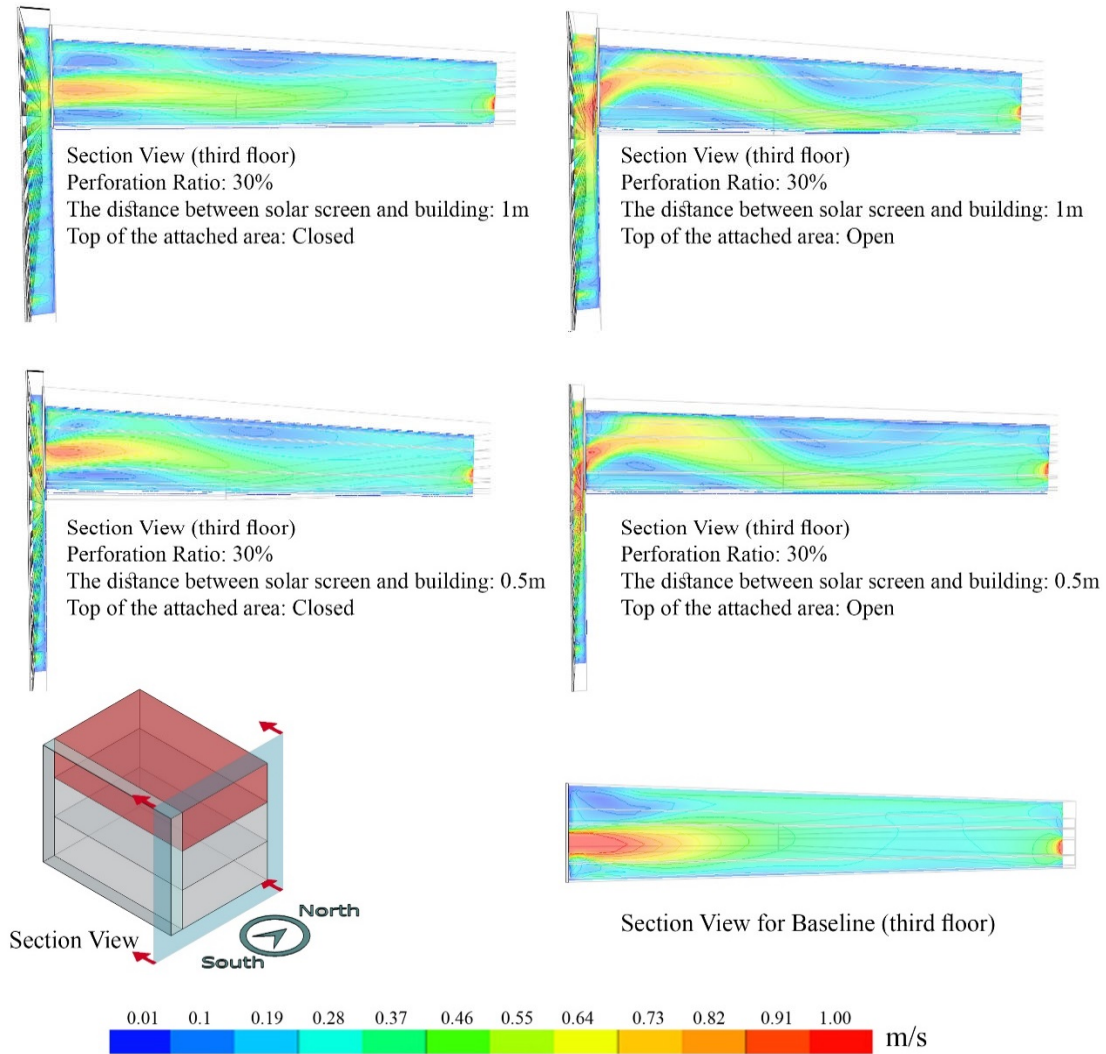


Figure 33: Air velocity pattern for the screen with 30% perforation ratio

4.1.7.2- CFD Analysis for a screen with 50% perforation ratio

Figure 34 is the results of the CFD analysis for air velocity on the third floor. In order to have a clear comparison, the air velocity for all of these variations is ranged between 0.01 and 1 m/s. Similar to the previous perforation ratio, in the baseline condition, air enters the room with a speed of near 1 m/s and penetrates directly to one-third of the room while its velocity drops to near 0.5 m/s. Once the solar screen with a 50% perforation ratio is added, the airflow changes based on the position of the screen and the state of the top of the attached area. The most significant impact of adding a solar screen happens when the top

of the attached area is changed. When the top of the attached area is open, due to the stack effect, the air moves upward inside the room, which leads a better circulation in the room. The results show a small increase in air velocity in comparison with a screen with a 30% perforation ratio, and this is due to the bigger opening area in this screen which could get more external vent. Besides the stated issues, when the top of the attached area is closed, the air moves directly towards the middle of the room, and it is similar to the baseline condition. In the previous section (screen with 30% perforation ratio), in all four types, the air goes up at first, which means that the stack effect is more powerful than in a screen with lower perforation ratios.

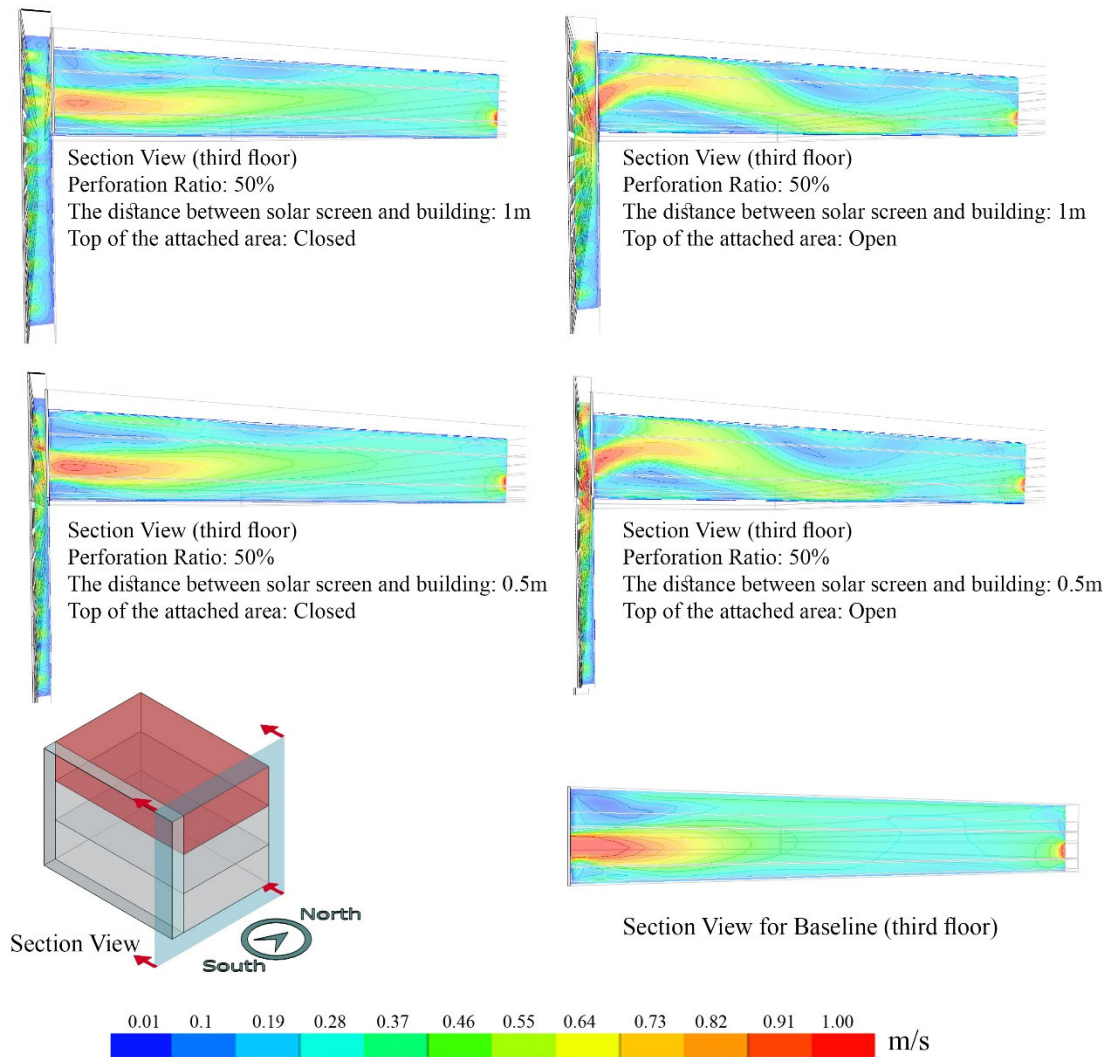


Figure 34: Air velocity pattern for the screen with 50% perforation ratio

4.1.7.3- CFD Analysis for a screen with 70% perforation ratio

Figure 35 is the results of the CFD analysis for air velocity on the third floor. In order to have a clear comparison, the air velocity for all of these variations is ranged between 0.01 and 1 m/s. Similar to the previous perforation ratio, in the baseline condition, air enters the room with a speed of near 1 m/s and penetrates directly to one-third of the room while its velocity drops to near 0.5 m/s. Once the solar screen with a 70% perforation ratio is added, the airflow changes based on the position of the screen and the state of the top of the attached area. The most significant impact of adding a solar screen is similar to previous types and happens when the top of the attached area is changed. When the top of the attached area is open, due to the stack effect, the air moves upward inside the room, which leads a better circulation in the room.

The results show a slight increase in air velocity in comparison with a screen with a 30% perforation ratio, and this is due to the bigger opening area in this screen which could get more external vent. In terms of airspeed, when the top of the attached area is closed, the air with a higher velocity goes down, which is the opposite direction of a screen with a 30% perforation ratio. When the top of the attached area is open like the previous types stack effect happens, and it moves toward the ceiling at first and then goes downward in the middle of the room. However, the stack effect is weaker than the previous types and it is due to the larger opening area.

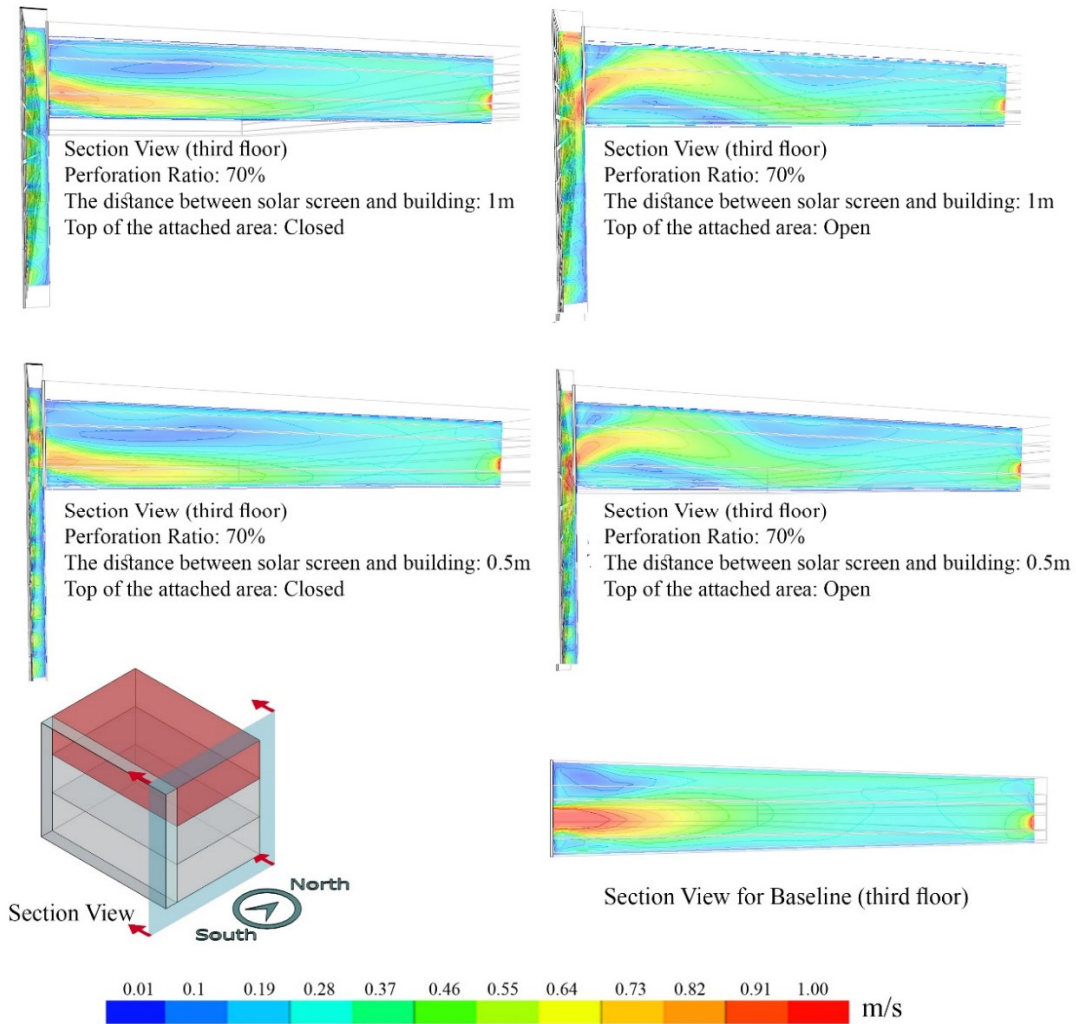


Figure 35; Air velocity for the screen with 70% perforation ratio

4.2- Boston Massachusetts, ASHRAE climate zone 5

4.2.1- SunCast

Figure 36 below shows the result of running SunCast for the city of Boston based on the six different solar screen types. Similar to Phoenix, these results are based on the impact of the solar screen on the southern side of the building. As it is plotted on the buildings' facade, even changing the distance between the building and the solar screen has an impact on the solar absorbing energy (kWh/m²); the closer the screen to the building, the lower the solar energy could be absorbed. Moreover, the results show that increasing the

perforation ratio corresponds to increasing the amount of absorbed energy because the solar screen has a more open area, and solar energy could pass through the openings and be absorbed by the building façade.

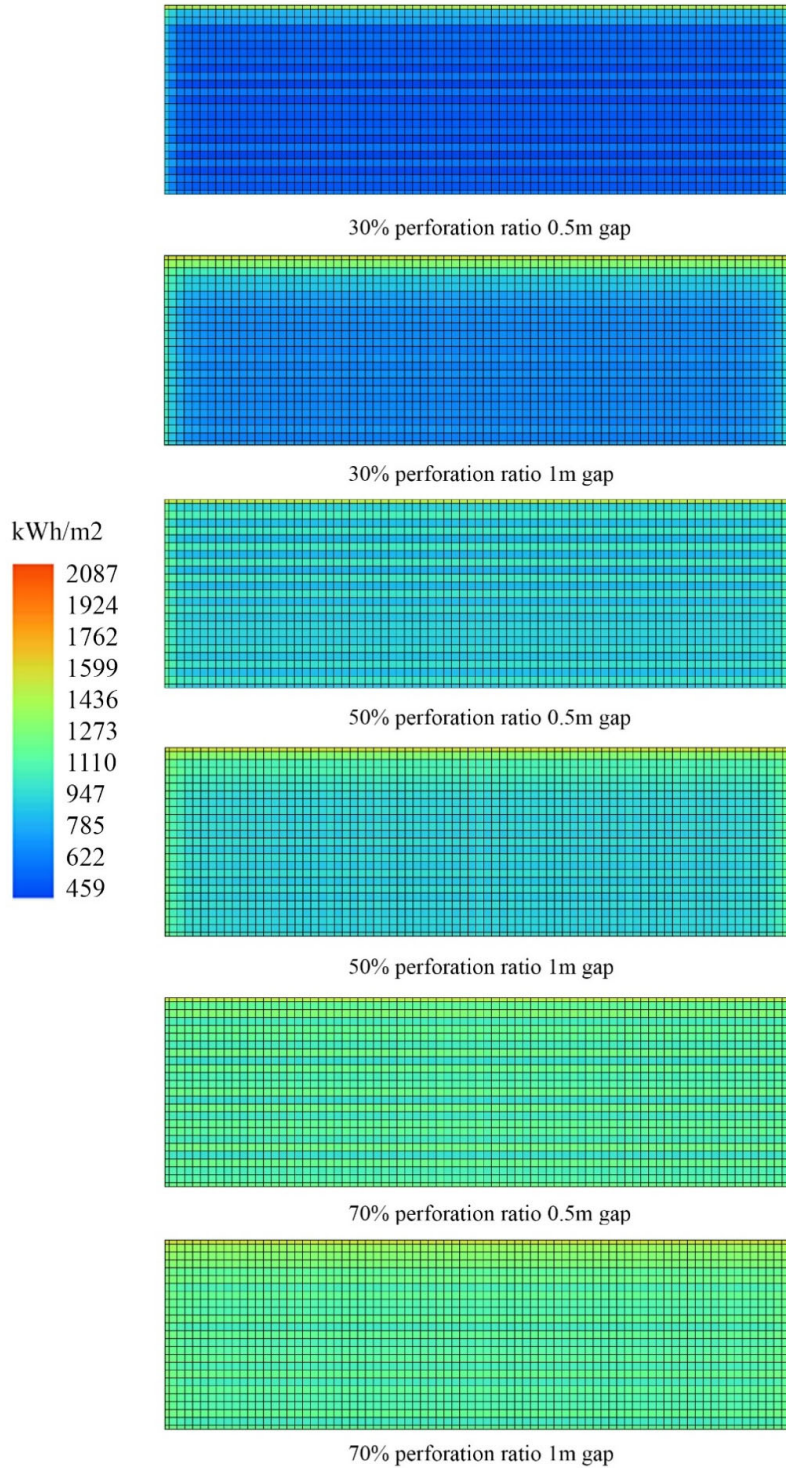


Figure 36: SunCast analysis for the city of Boston during the cooling season months

4.2.2- Energy Performance

Like Phoenix, Energy Utilization Index (EUI) was used in various studies to show the energy benchmarking of building and design strategies. The mean EUI of commercial buildings in the US was calculated from the Zero Tool website and used to compare the base case with the building with different solar screen configurations. Based on the result of the Zero tool website as shown in figure 37, the energy usage intensity for an office building with a dimension of 50m (164 ft) by 33m (108 ft) is 263 (kWh/m²/yr) for Boston, and the target EUI based on 30% reduction is 184 (kWh/m²/yr).

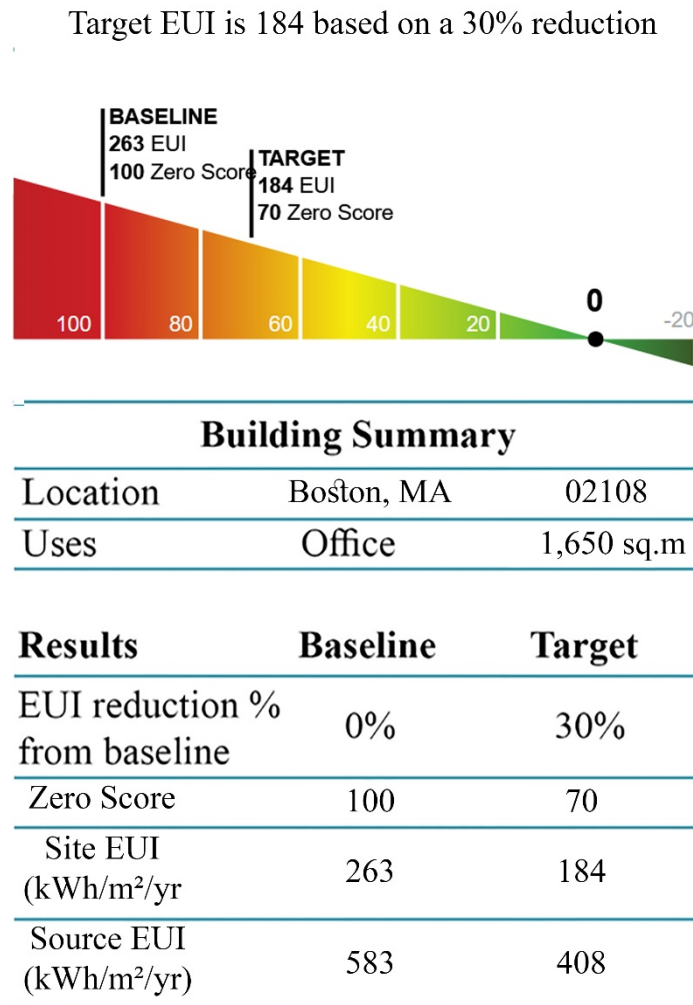


Figure 37: Baseline EUI for an office building in the city of Boston

4.2.3- Whole Building Energy

The city of Boston, which is in ASHRAE climate five, has been studied, and the energy consumption of building with different solar screen configurations has been analyzed mainly in the hot period, i.e., between June and September. Figure 38 shows the total energy consumption for Boston during the cooling season months. Similar to Phoenix, for Boston, 14 different variations have been defined to delineate the effect of important designs and constructions, including solar screens with different levels of perforation. This seems to be an essential parameter that directly affects the energy consumption while keeping the indoor environment like air velocity, air temperature, and relative humidity at an acceptable level. The results show that among all of these configurations, the building which has a solar screen with a 30% perforation ratio has the best performance in terms of energy consumption. Since each of these perforation ratios represent of different state of the dynamic façade, it can be concluded that once the dynamic façade is in a closed state, it has the best performance in terms of energy consumption. As is plotted in the bar chart, the performance of this screen is different based on its position on the building and the state of the attached area's top. The bar chart shows that the best performance happens when the top of the attached area is closed. Furthermore, when the solar screen is closer to the building, its performance can increase. Moreover, the results show that the solar screen does not have the same performance in these four months. As it is plotted, the highest reduction can be seen in June and September, which is more than a 60% reduction in some cases. Once the state of the dynamic façade is changed from closed (30% perforation ratio) to semi-open (50% perforation ratio), the performance of the screen in terms of energy-saving is decreased. However, in some cases, the screen with a 50% perforation ratio is able to reduce energy consumption up to 40%. Similar to the screen with a 30% perforation ratio, once the top of the attached area is closed, the screen has a better performance for energy consumption. In addition, the graph shows that if the screen is located closer to the building, its performance will increase. Once the state of the dynamic façade changes from semi-open (50% perforation ratio) to open (70% perforation ratio), as is shown in the bar chart, the performance of the screen is at its lowest. In other words, increasing the perforation ratio corresponds to the reduction of performance for energy consumption.

However, this screen with a 70% perforation ratio is still effective in reducing energy consumption and, in some case, is able to reduce the energy consumption up to 25%. As discussed earlier, the impact of these screens on energy consumption is not the same during the cooling season months. The bar chart shows that in July and August, the performance of the screen with a 70% perforation ratio is lower than in June and September, and in some cases, like the one that is located 1m from the building and the top of the attached area is open, does not have a tangible impact on energy consumption.

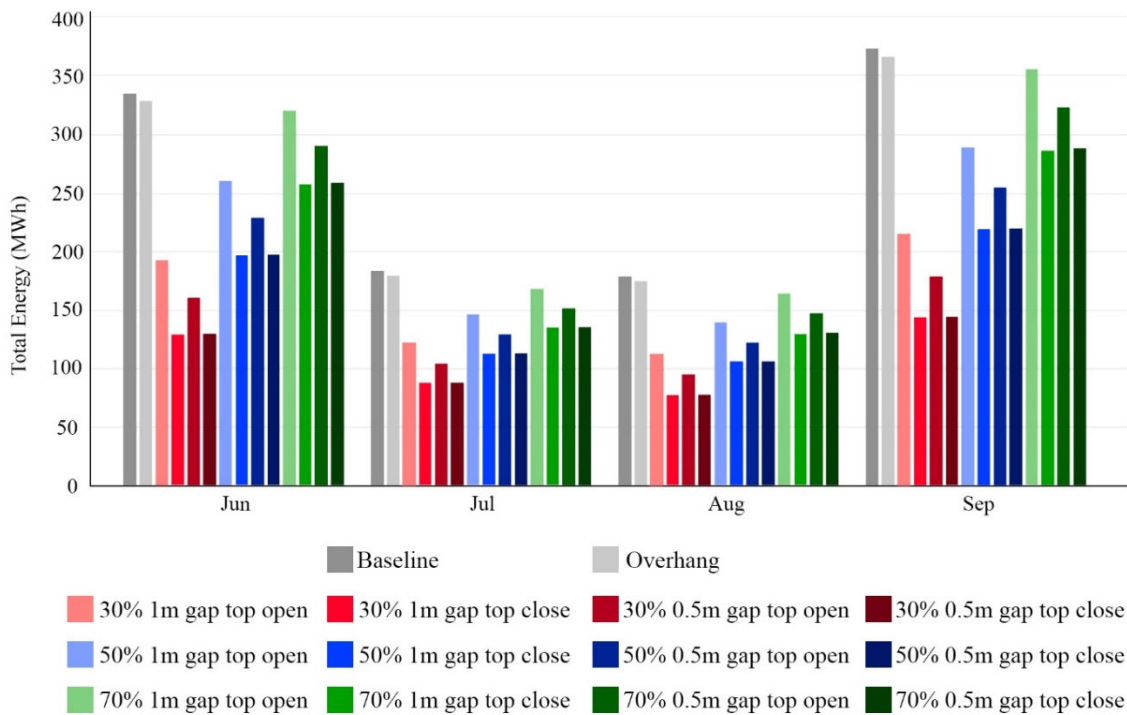


Figure 38: The impact of different solar screen configurations on energy consumption for the cooling season months in Boston.

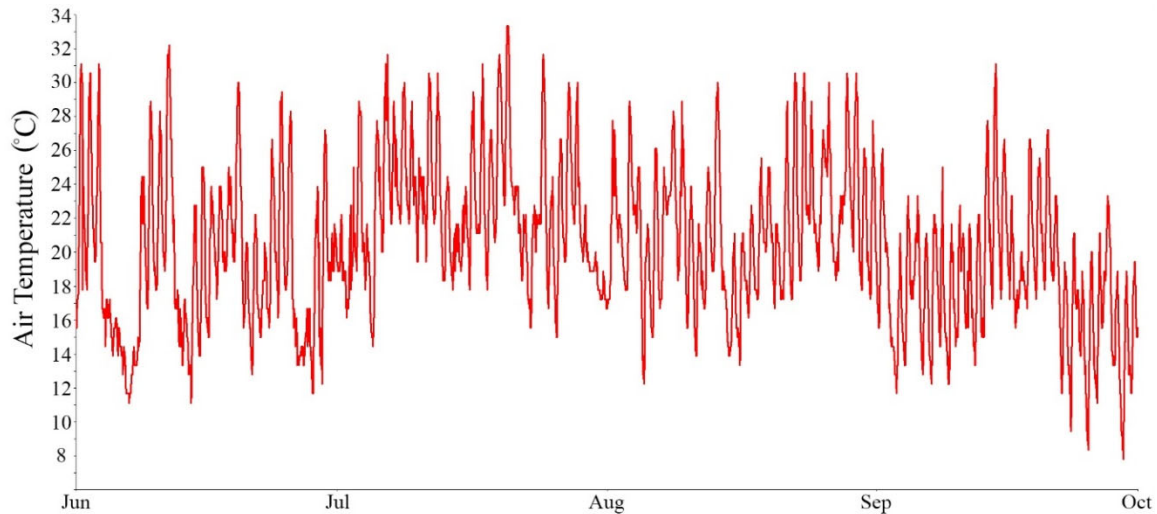


Figure 39 Boston outdoor air temperature

To better observe the superior effect of solar screens on the energy consumption of buildings, a more detailed graph has been provided in the Figure 40. In this graph, the energy consumption for a shorter period of one week in the month of July has been plotted and demonstrates the amount of energy consumption for this given week in Boston. In addition, the outdoor air temperature has been plotted, which shows that by increasing the outdoor air temperature during the day, the energy consumption increases, and during the cooler days, the energy consumption is lower. It should be borne in mind that the data presented in this graph belong to an office where the cooling devices are mainly used during office hours, i.e., between 9 am and 5 pm. By referring to this Figure, one can see how the solar screening is efficient in reducing the energy from a high value of 1000 KW to less than 400 KW in some hours, 60% reduction in energy consumption. It is worth mentioning that the total system energy contains various energy constituents such as boilers energy, air-conditioning, lighting, and ventilation. Since this simulation has been carried out for the cooling season, the major impact of solar screens has been to reduce the cooling energy consumption. This graph clearly shows that even a small change in the position of the screen could change the energy consumption of the whole building effectively. The graph also shows that, these screens are more efficient during the day with higher temperatures.

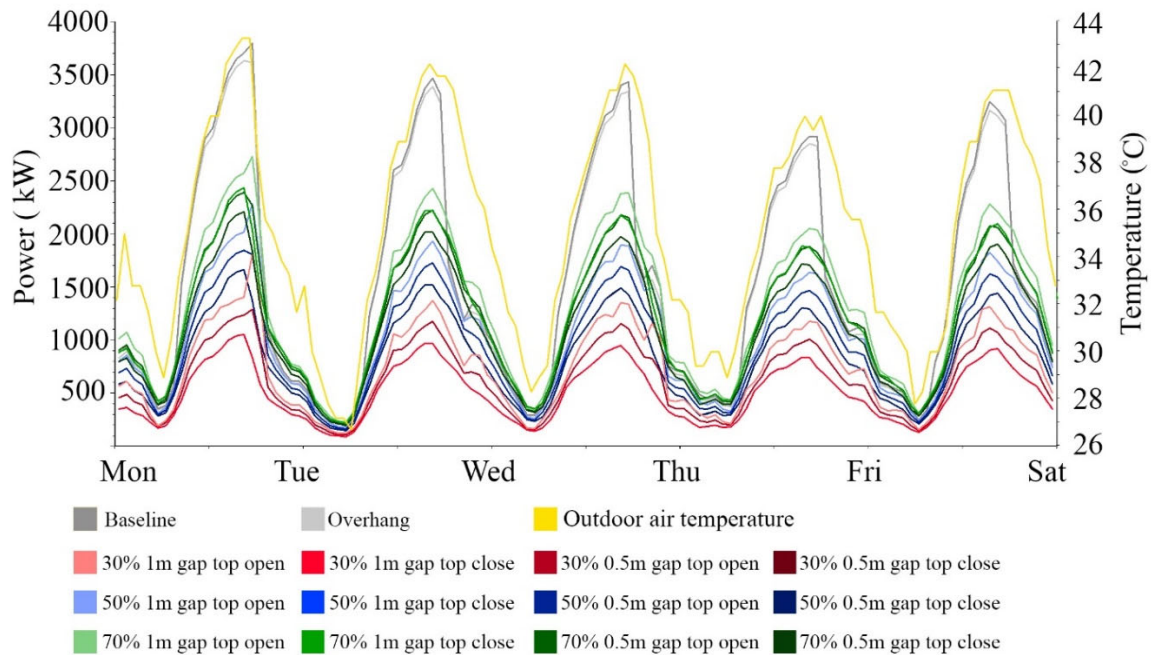


Figure 40: The impact of different solar screen configurations on energy consumption in a week of July in Boston.

4.2.4- MacroFlo

4.2.4.1- MacroFlo with opening profile

Figure 41 collects the MacroFlo external vent (airflow volume) for the third floor of this office building during the cooling season months (June to September). As previously discussed in the methodology, the result of this section is directly related to the opening profiles and their opening degree. For this study, it has been assumed that windows will not open unless the indoor air temperature goes upper than 21 C, and at the same time, the outdoor temperature is lower than 27 C. In addition, since this is an office building, the windows are closed during the weekends or night hours. All different configurations would lead to similar venting values, a rather surprising result which does not show any direct impact of solar-screening on the ventilation of the building. These results are unlike the MacroFlo external vent result for Phoenix. Since Boston has a lower outdoor air

temperature in the cooling season months, the building is able to take advantage of natural ventilation in all these four months specifically the range between July and September.

Figure 40 demonstrates that the building without any solar screen has better potential for taking advantage of the outdoor wind. Furthermore, a solar screen with 70% perforation ratios shows good potential for natural ventilation and taking advantage of the outdoor wind. On the other hand, a solar screen with a 30% perforation ratio has the lowest potential for natural ventilation, and it is due to the minimum opening area. Although air ventilation is more effective for the baseline or solar screens with high perforation ratios (higher openings), the difference is not quite significant for all different configurations. For instance, by looking at the graph, one can observe that for July, the MacroFlo External Vent has a value of 8.9 million cubic meters (8900 times 1000 m³) for a baseline configuration. By digging up the data for the screen with a 30% perforation ratio in this figure and for the very same month, one can realize that the level of MacroFlo External Vent is around 7.8 million cubic meters (7800 times 1000m³), which is about 12% lower in terms of ventilation potential. Although ventilation is more powerful for the baseline or overhang structures, the amount of energy saving is about two times for configurations with solar screening with proper perforation. Furthermore, based on this chart, the room has a higher MacroFlo external vent once the top of the attached area is closed. In terms of the position of the screen, it is depicted that the distance of the screen does not have an impact on MacroFlo external vent once the top of the attached area is closed. Conversely, once the top gets opened, the amount of MacroFlo external vent is changed in different positions, and it shows the closer screen is able to improve MacroFlo external vent.

It is worth mentioning that this chart is the total amount of entered air for the third floor and does not show the exact behavior of the air inside the room. In order to have a better picture of the impact of these screens on natural ventilation and airflow, it is essential to run a CFD simulation.

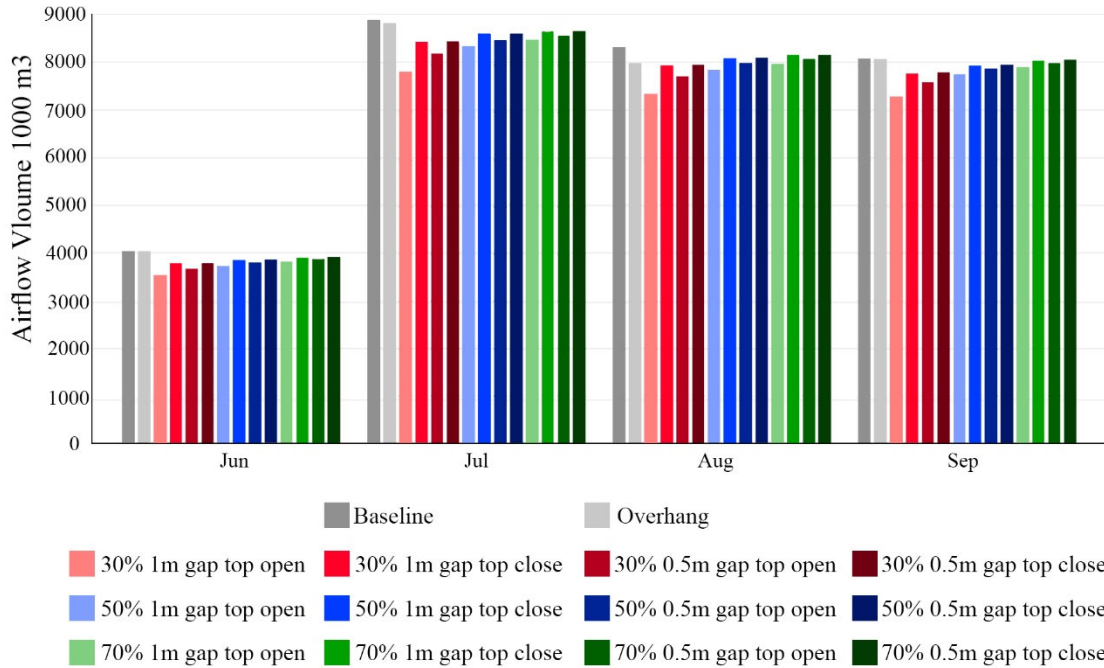


Figure 41: Airflow volume bar chart for cooling season months in Boston (with opening profile)

4.2.4.2- MacroFlo without opening profile

Similar to Phoenix, it is worthwhile to simulate this period without any profile in order to see a better picture of the impact of different solar screen configurations. Figure 42 depicts the MacroFlo external vent when the windows are open from 9 AM to 5 PM. For this city (Boston) the bar chart is similar to previous chart. Based on this chart, July, August and September have the highest potential for taking advantage of natural ventilation, and it is because of the wind speed average. The wind speed average for these three months is 4.87 m/s, 4.51 and 4.58 m/s. respectively. Furthermore, as discussed previously, in order to have a better evaluation of the impact of the solar screen on natural ventilation, the eastern and western windows of the building are closed, and the wind direction is mainly from the south for these two months. This bar chart also shows that the screen with a 30% perforation ratio has the lowest potential to take advantage of natural ventilation. Among four different variations of a solar screen with a 30% perforation ratio, the MacroFlo external vent increases when the attached area's top is closed. When the top of the attached

area is open, the stack effect happens, and consequently, some portion of wind, instead of moving into the building, goes upward (this happening could be observed clearly in CFD analysis). In addition, the results show that the MacroFlo external vent is higher when the solar screen is closer to the building. The solar screen with a 50% and 70% perforation ratio shows a similar result to 30%; however, the amount of MacroFlo external vent is higher.

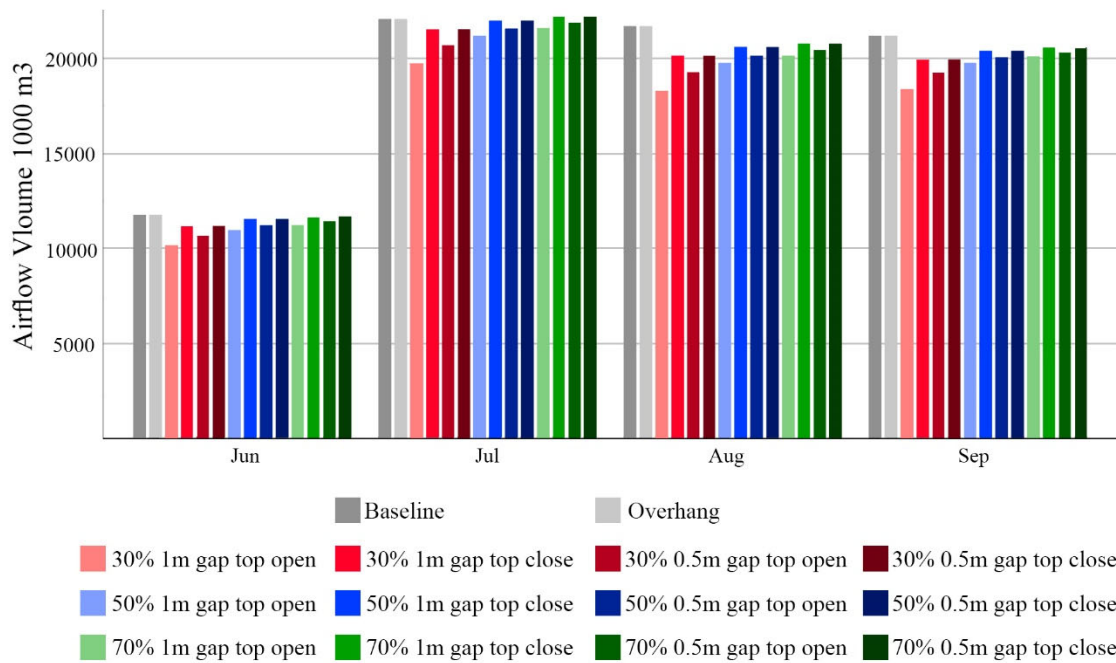


Figure 42: Airflow volume bar chart for cooling season months in Boston (without opening profile)

The MacroFlo external vent for the week of July in Boston has been plotted in figure 43. Similar to the bar chart results, these graphs show that the screen with a 70% perforation ratio has the best potential to take advantage of natural ventilation, and in some cases, the MacroFlo external vent amount is similar to the baseline condition. Moreover, these graphs show that a solar screen with a 30% perforation ratio has the lowest MacroFlo external vent amount once it is located 1m from the building and the attached area's top is open.

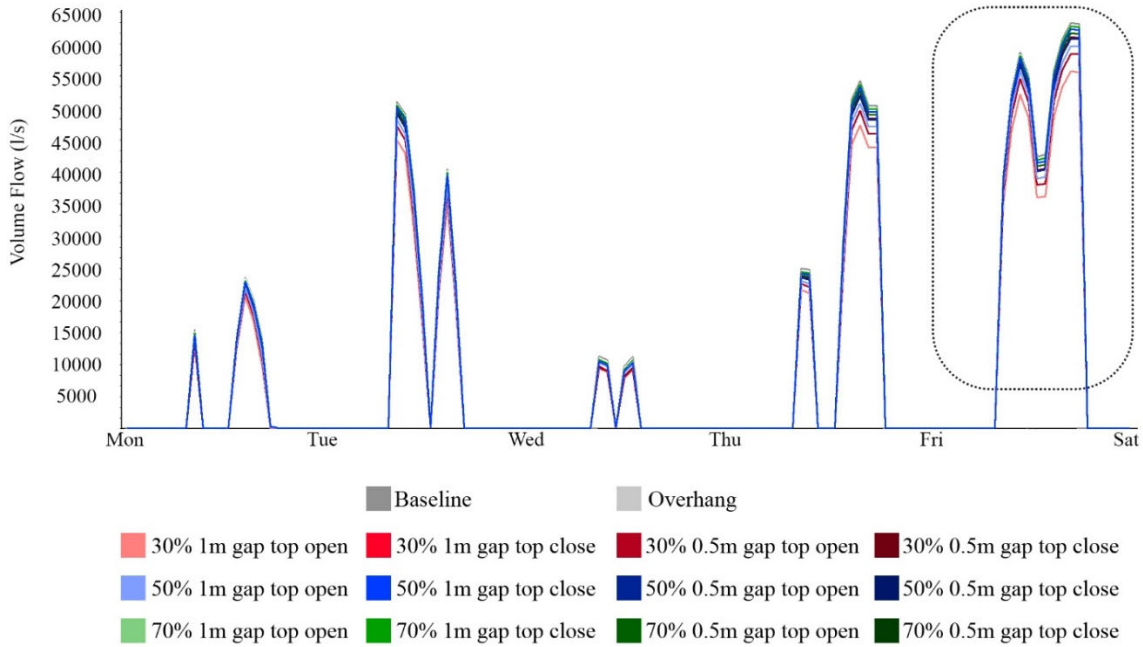


Figure 43: MacroFlo external vent without opening profile for a week of August in Boston

In order to have a better understanding of the exact impact of these different configurations, figure 44 focuses on a day of July, which has been marked as a dashed line in figure 43. In this picture, wind speed has also been plotted due to the direct relationship between airflow volume and wind speed. Since the opening profile has been removed, once the office hours start, the airflow volume increases by opening the windows. For this specific day, since the wind speed decreases from noon to 2:00 PM, the air volume flow is at its minimum amount; on the other hand, the air volume flow starts raising after 2:00 PM and reaches to its highest at 5:00 PM. This picture also depicts that the screen with a 30% perforation ratio due to the minimum open area gets the lowest air volume flow, specifically if it is located 1m from the building and the top of the attached area is open. Conversely, the solar screen with a 70% perforation ratio can get the highest air volume flow if it is located 0.5 from the building and the top of the attached area is closed.

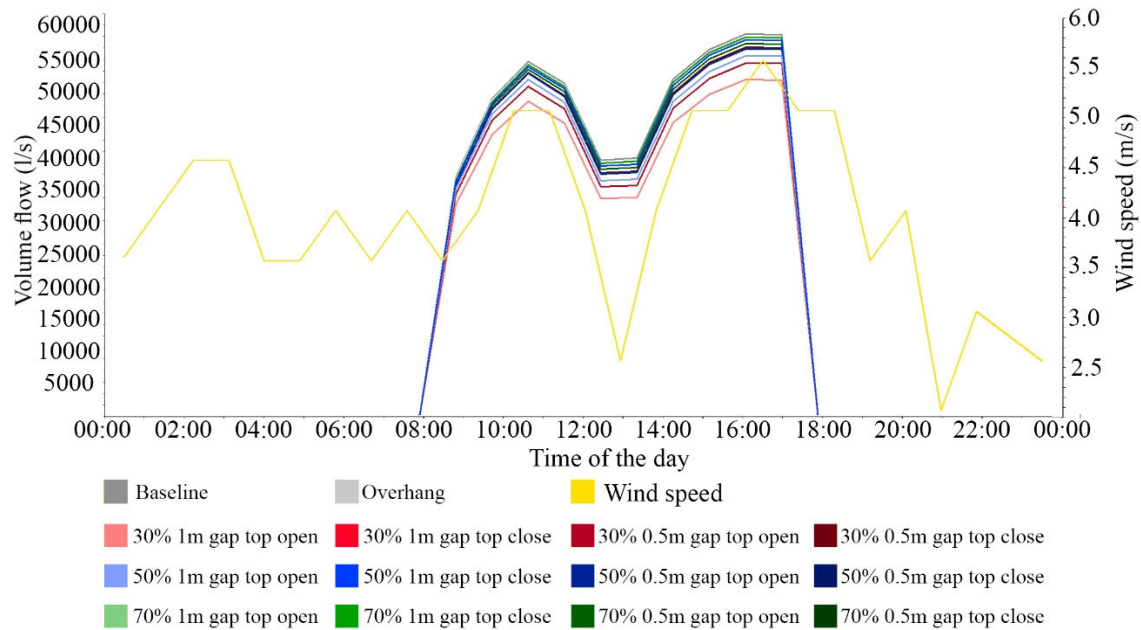


Figure 44: MacroFlo external vent without opening profile for a day of August in Boston

4.2.5- Room Air Temperature

Figure 45 shows the impact of solar screens on room temperature for a week of August in Boston. The room air temperature based on the building HVAC system setting is in the range of 21 °C and 24 °C, which means that the cooling system gets activated once the temperature rises more than 24° C. As plotted in the graph, the room air temperature during the night hours is different based on the different solar screen configurations. Similar to Phoenix, the graph demonstrates that the screen with a 30% perforation ratio has the best performance in terms of reducing the indoor air temperature, which is able to reduce up to 1°C in some cases. The highest reduction happens when the attached area’s top is closed. Furthermore, being closer to the building can reduce room air temperature by about 0.1°C. The screen with a 50% perforation ratio is also able to reduce air temperature up to 0.5 °C. The results of the screen with a 70% perforation ratio is similar to the previous perforations and it is unlike phoenix. Based on the graph, the screen with 70% perforation ratios is still able to reduce room air temperature up to 0.2 °C in some cases.

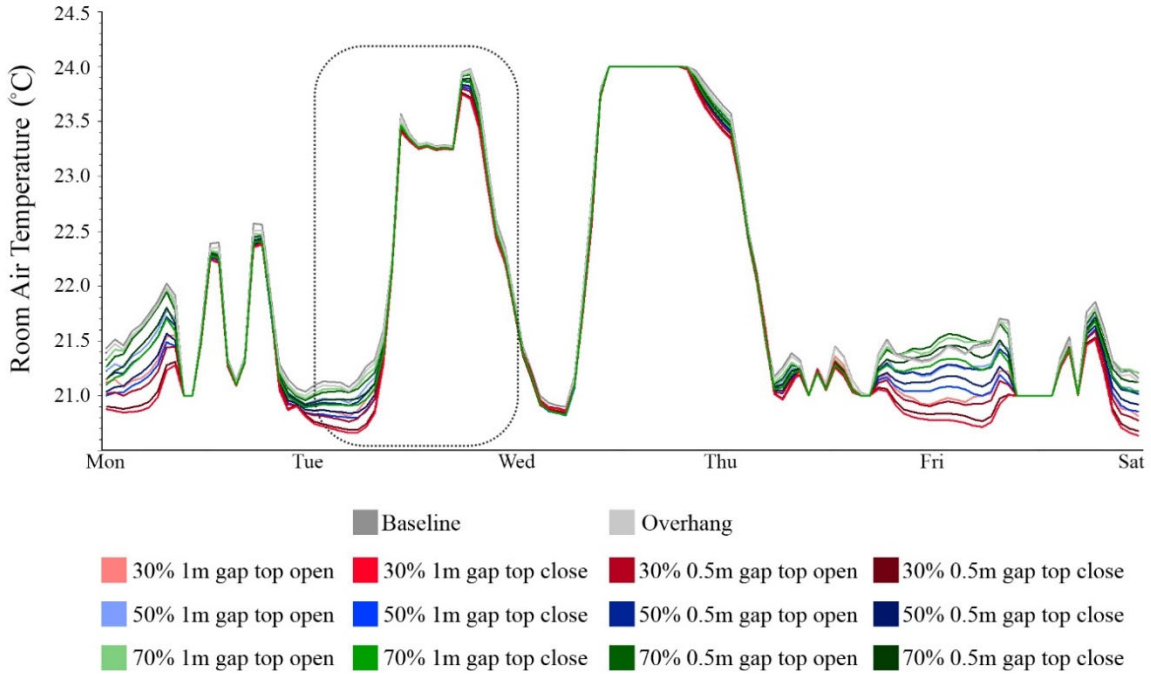


Figure 45: The room air temperature for a week of August as a result of various configurations in Boston.

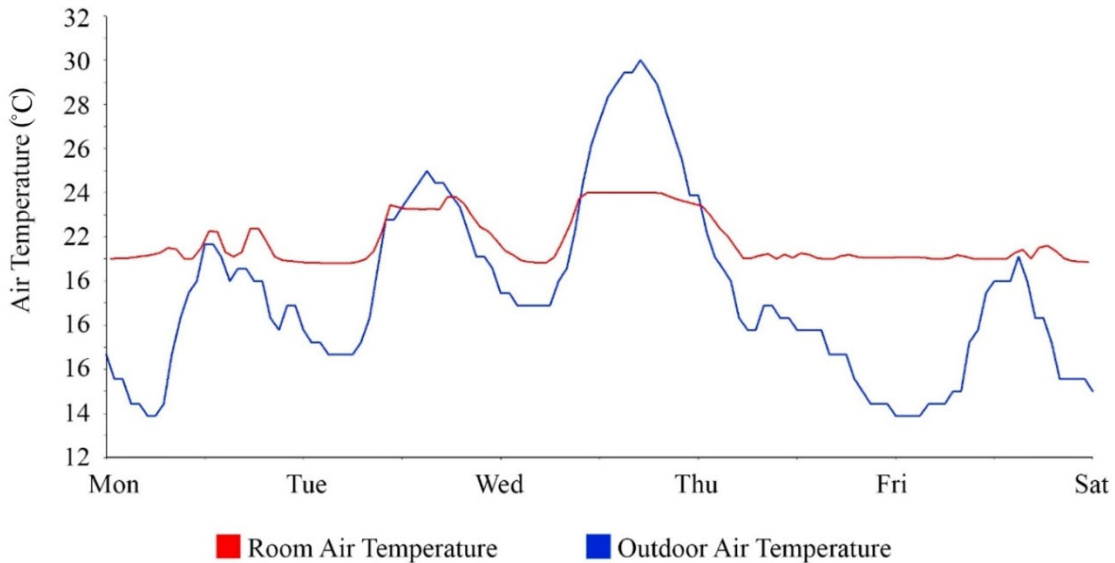


Figure 46: Room air temperature and outdoor air temperature for a week of August in Boston.

Figure 47 demonstrates the room air temperature for the day of August in Boston, which is marked with a dashed line in figure 44. By starting the office hours, the room air temperature starts rising due to the internal gain sources like computers, lighting, and people. Besides internal gain sources, increasing the outdoor air temperature, which is

shown in figure 46, is another reason for increasing the indoor air temperature. However, since the outdoor air temperature for this specific day does not increase a lot, the HVAC system does not need to get activated to control the room air temperature, and the room air temperature is less than 24°C. As plotted in the graph, the screens with 30% and 50% perforation ratios are able to reduce room air temperature during the night hours up to 0.5 °C in comparison with baseline.

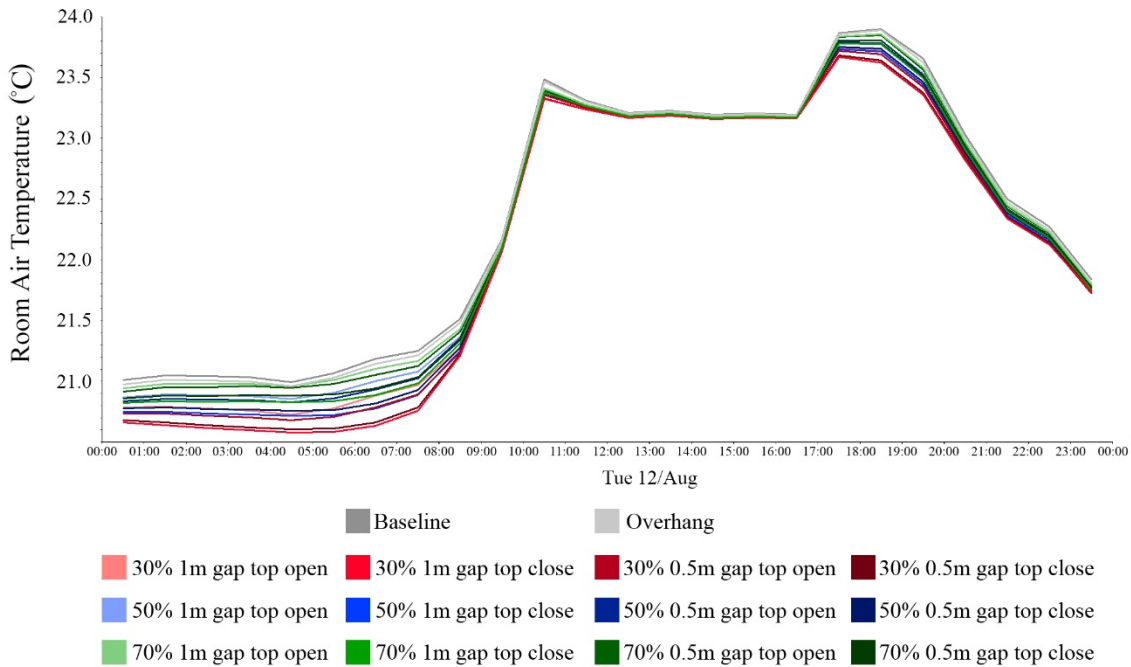


Figure 47: The room air temperature for a day of August as a result of various configurations in Boston.

4.2.6- Room CO2 Concentration

Figure 48 shows the impact of different screen types on CO2 Concentration in a week of August in Boston. As discussed in the MacroFlo section, solar screens are able to impact natural ventilation in this building. Since there is a direct relationship between room ventilation and CO2 Concentration, as it is plotted below, different solar screens have a different impact on CO2 Concentration. However, this impact is not significant, and it could be enhanced by using mechanical equipment. Based on this graph, the room CO2 concentration is ranged from 400 ppm to 450 ppm, which is within the acceptable range of

ASHRAE standards (below 800 ppm for office buildings). As it is clear, during the weekends, this amount is 400 ppm, and during the office hours, due to the usage of equipment and also occupancy increases up to 470 ppm. In comparison with Phoenix, the room CO2 concentration is lower in Boston and it is due to the higher MacroFlo external vent amount for Boston which helps the room to have a better ventilation.

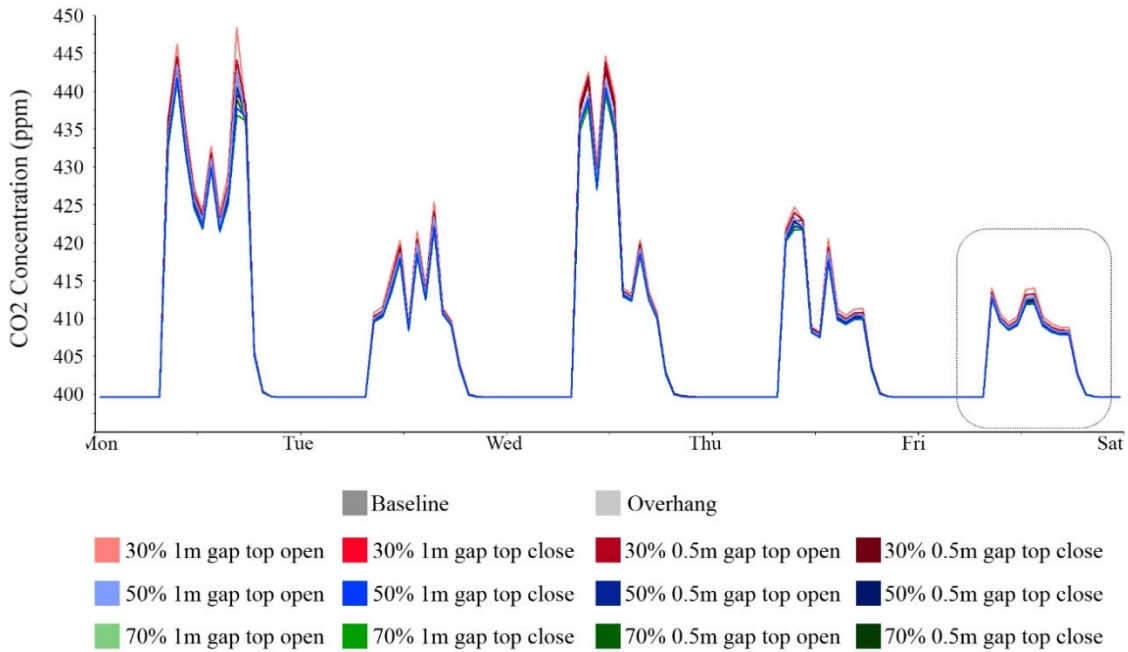


Figure 48: The room CO2 concentration for a week of August in Boston

Figure 49 focuses on a CO2 concentration for the day of August to better understand the impact of these screens. In addition, airflow volume has been plotted in this graph which helps to understand the fluctuation of room CO2 level at different times of the day (the volume flow lines have been faded). This graph demonstrates that room CO2 levels because of occupancy increase during office hours, and as it is shown, the CO2 level is not the same during different times of the day. For this specific day, the room CO2 concentration is at its highest at 9:00 AM, but once the airflow volume increases, the room CO2 concentration decreases. This graph shows that at 11:00 AM CO2 level is less than 410 ppm. Furthermore, from noon to 2:00 PM, due to airflow volume reduction, the CO2 level starts rising again. From 2:00 PM until the end of the day, since airflow volume increases again, CO2 level drops. This graph also shows that the solar screen with a 30%

perforation ratio has the lowest airflow volume, which leads to the highest CO2 concentration, specifically if it is located 0.5 m from the building and the top of the attached area is closed.

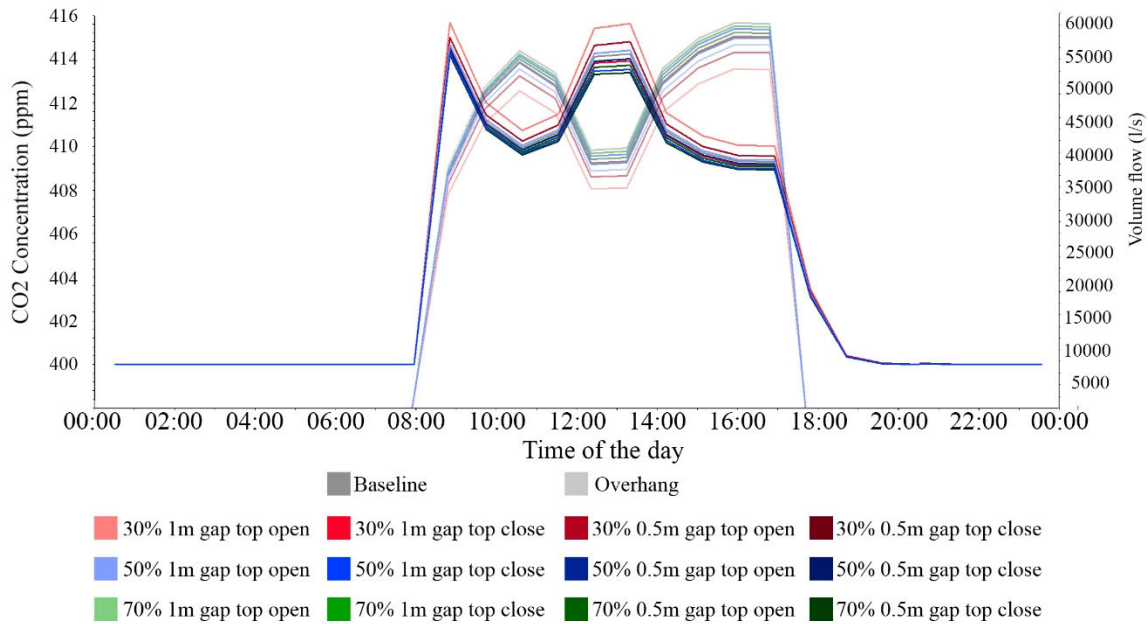


Figure 49: The room CO2 concentration and airflow volume for a day of August in Boston

4.2.7- CFD Analysis for Boston

The pictures below belong to the results of the CFD analysis for a specific day and time. In IES-VE, once the ApacheSim is done, the results are shown in VistaPro, and in this section, the thermal information of a target day could be exported as a boundary condition to the MicroFlo section. The solar screen for this study is located on the southern side of the building. Since this study aims to investigate the impact of the solar screen on airflow patterns for the indoor spaces, the target date has been set for a day the wind direction is from the south. Based on the wind rose chart, April 18th is one of the days the wind direction is from the south. Furthermore, based on the MacroFlo external vent graph, 11 am has the highest potential for natural ventilation on this specific day; therefore, the boundary condition is set for April 18th at 11 am, and the thermal information of this day is exported to MicroFlo for CFD analysis. Once the boundary condition is imported in

MicroFlo, the CFD grid needs to be defined and, for this study, has been set as 20 cm by 20 cm. Moreover, in order to have a clear picture of the CFD analysis, this office is located in a place without any adjacent buildings.

4.2.7.1- CFD Analysis for a screen with 30% perforation ratio

Figure 50 is the results of the CFD analysis for the air velocity when the screen is in the closed state. The air velocity is ranged between 0.01 and 1 m/s. As shown, there is a significant difference between the left and right pictures. Based on the results, once the top of the attached area is open due to the stack effect, the air tends to go upward, and as a result, the air pattern is different from the closed one. In terms of air velocity, there is a reduction in airspeed that can be seen in comparison with the baseline condition. In the baseline, the air velocity near the opening is around 1m/s. On the other hand, the airspeed near the opening after adding the solar screen with a 30% perforation ratio drops to around 0.8 m/s. There is also a difference that can be seen between the screens with a different positions. Once the screen is located 0.5 m from the building, the mainstream of airflow moves to the lower level of the room, which is the opposite side of the time when the screen is located 1m from the building. The air velocity in the baseline condition is about 0.35 m/w in the most part of the room, while the air velocity gets lower after adding the solar screen with a 70% perforation ratio and in some parts of the room the air velocity drops to less than 0.1 m/s. Therefore, based on the results of the CFD analysis the main impact of adding the solar screen is changing the airflow inside the room, specifically, the time when the top of the attached area is open.

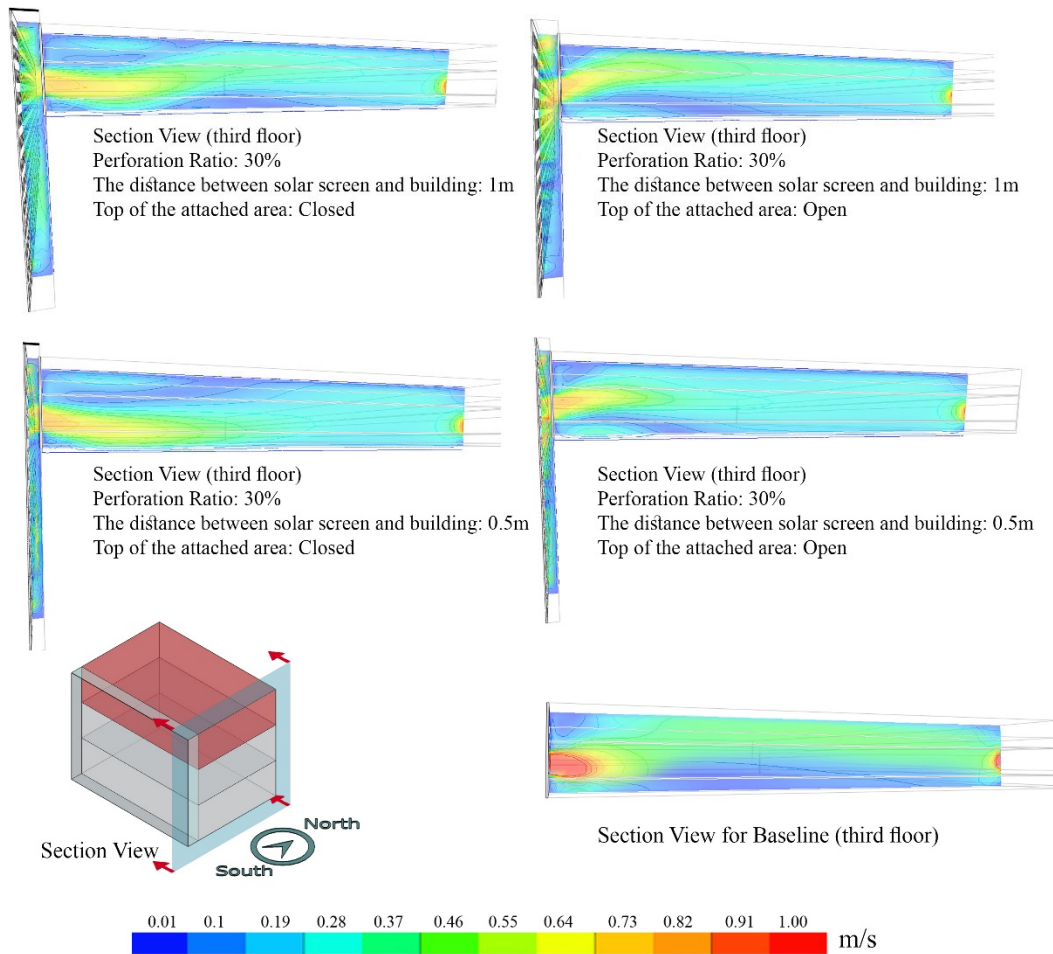


Figure 50: Air velocity pattern for the screen with 30% perforation ratio

4.2.7.2- CFD Analysis for a screen with 50% perforation ratio

Figure 51 is the results of the CFD analysis when the screen is in a semi-open state. The air velocity is ranged between 0.01 and 1 m/s. Based on the results, once the top of the attached area is open due to the stack effect, the air tends to go upward, and as a result, the air pattern is different from the closed one. However, since a higher perforation ratio corresponds to the more open area, the stack effect in this state is weaker than the previous one, and as it is shown, the mainstream of the air with higher velocity is in the middle levels of the room. In the closed state, the mainstream of the air with higher air velocity is in the

higher level of the room. In addition, when the attached area's top is closed, the mainstream of the air with higher air velocity is in the lower levels of the room.

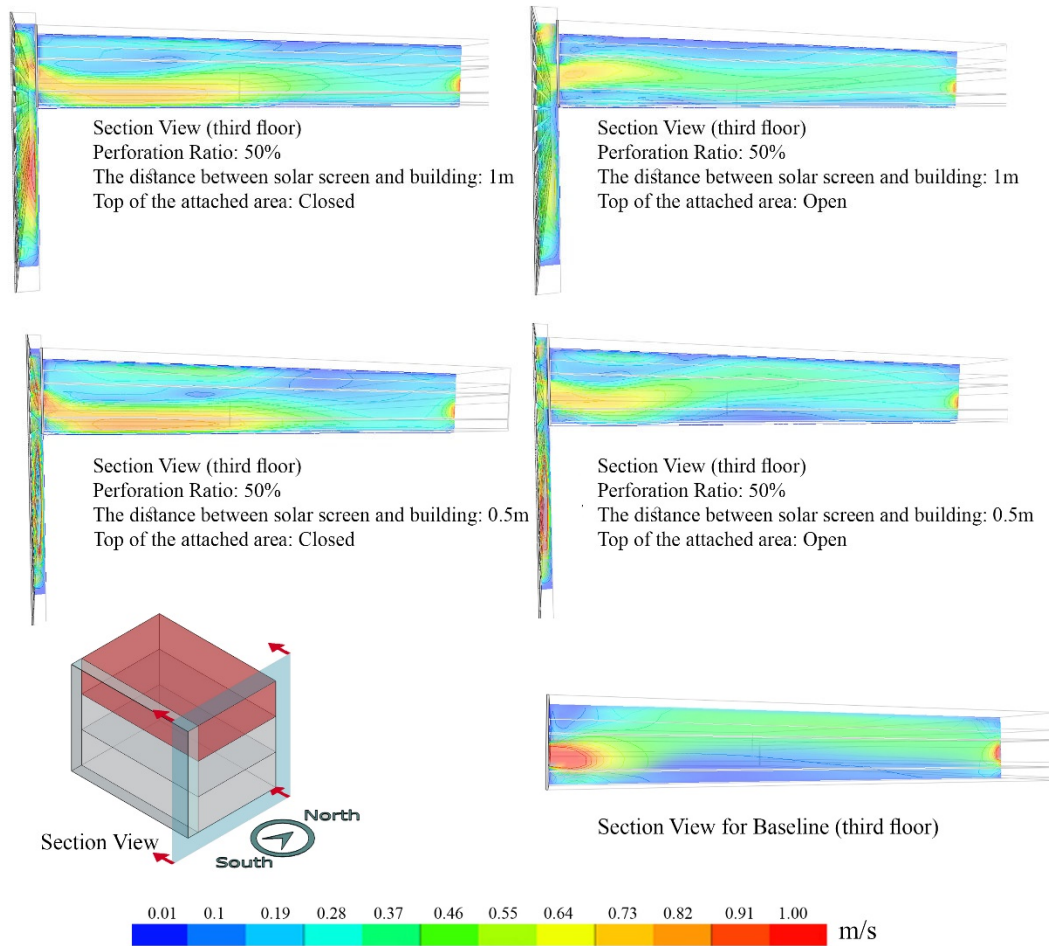


Figure 51: Air velocity pattern for the screen with 50% perforation ratio

4.2.7.3- CFD Analysis for a screen with 70% perforation ratio

Figure 52 is the results of the CFD analysis when the screen is in an open state. The air velocity is ranged between 0.01 and 1 m/s. Based on the results, once the top of the attached area is open due to the stack effect, the air tends to go upward, and as a result, the air pattern is different from the closed one. However, in this state, the stack effect is even weaker than the previous ones, and as it is shown, the mainstream of the air with higher velocity is in the lower levels of the room. When the attached area's top is closed, the mainstream of the

air with higher air velocity is in the lower levels of the room with higher air velocity. In the open state, the air velocity in some parts of the room is near 1 m/s, but once the attached area's top get open, the air velocity drops to 0.5 m/s.

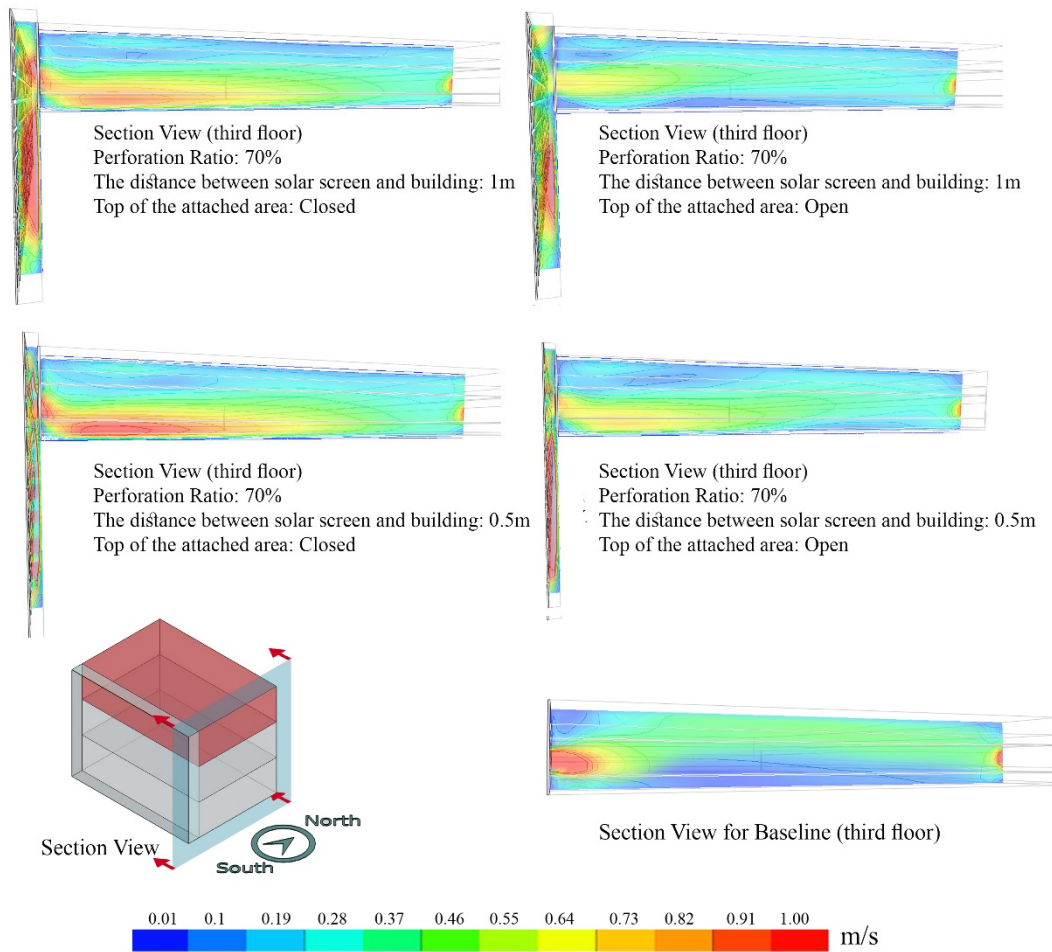


Figure 52: Air velocity pattern for the screen with 70% perforation ratio

CHAPTER V: CONCLUSION

This thesis examined the effect of dynamic solar Screen façades on energy performance, natural ventilation, and indoor air quality (air temperature and CO₂ level in particular) in two different ASHRAE climate zones (2B and 5A). The conclusion is focused on the impact of different solar screen configurations like screens with different perforation ratios, different positions of the screen, and different states of the attached area's top (open and closed).

5.1- Energy Performance and natural ventilation

This study showed that dynamic solar screens are able to reduce energy consumption during the cooling season months in the city of Phoenix (ASHRAE climate 2B). The results of this study showed that once the dynamic solar screen is in the closed state (30% perforation ratio) due to its shading effect, it reduces building energy consumption by more than 50% percent in comparison with the base case, specifically during the hottest months of the year (June, July, and August). Moreover, it depicts that if the dynamic solar screen is closer to the building and at the same time, the top of the attached area is closed, this reduction can increase up to 60%. Once the dynamic solar screen's state changes from closed to open (70% perforation ratio), the building starts absorbing more heat. This happens because of increasing the open area, which leads to a reduction in the shading effect on the building and thereby consuming more energy required to cool the building. However, the results still show that the dynamic solar screen is able to reduce energy consumption even in the open state. By investigating other parameters like airflow volume, it can be observed that when the dynamic solar screen is in the open state, it has a higher airflow volume in comparison with the closed state. Thus, improvement in energy consumption can be seen even in the open state, and this is because of natural ventilation. In other words, when the dynamic solar screen is closed, shading plays a more significant role in building energy consumption performance, and once the dynamic façade is open natural ventilation is more significant than shading.

The same pattern can be observed for Boston (ASHRAE climate zone 5A). When the dynamic solar screen is closed (30% perforation ratio), the shading effect causes a reduction in energy consumption. Furthermore, similar to Phoenix, Once the dynamic solar screen's state changes from closed to open (70% perforation ratio), the building starts absorbing more heat, and the performance for energy consumption reduces. However, it is still effective for energy consumption, specifically, if the solar screen is located closer to the building and at the same time, the top of the attached areas is closed. Overall, when the results of these two cities are compared with each other, the dynamic solar screen shows a better performance in terms of energy consumption in Phoenix.

5.2- Room CO2 Concentration

Besides energy consumption and airflow, this study investigated the impact of dynamic solar screen facades on room CO2 concentration. Both cities showed that once the dynamic solar screen is closed (30% perforation ratio), the room has a higher CO2 concentration. Since there is an opposite relationship between room CO2 level and airflow volume when the dynamic solar screen is in a closed state, it has lower airflow volume in both cities, and as a result, the room CO2 level is higher. On the other hand, once the dynamic solar screen's state changes from closed to open (70% perforation ratio), the room CO2 concentration starts decreasing.

5.3- Room air temperature

This study also examined the impact of dynamic solar screen facades on indoor air temperature. This study showed that by adding a dynamic solar screen on the southern side of the building, the indoor air temperature could be reduced up to 1 degree Celsius. The results showed that once the solar screen is in the closed state (30% perforation ratio), the room air temperature can be decreased up to 1°C, specifically if the solar screen is located closer to the building and at the same time, the top of the attached area is open. As discussed in the previous chapter, stack ventilation happens in the interval between the building and

the solar screen when the top of the attached area is open. Therefore, the dynamic solar screen reduces room air temperature by its shading effect and natural ventilation.

5.4- Room Airflow

The results of this study demonstrate that the solar screens are capable of changing the airflow pattern inside the building. Figure 53 and 54 show the impact of screens with different perforation ratio once they are located 1m far from the building and the attached area's top is open. As it is observed, the stack ventilation happens in all of these three configurations and the screen with a 30% perforation ratio demonstrate a stronger stack effect.

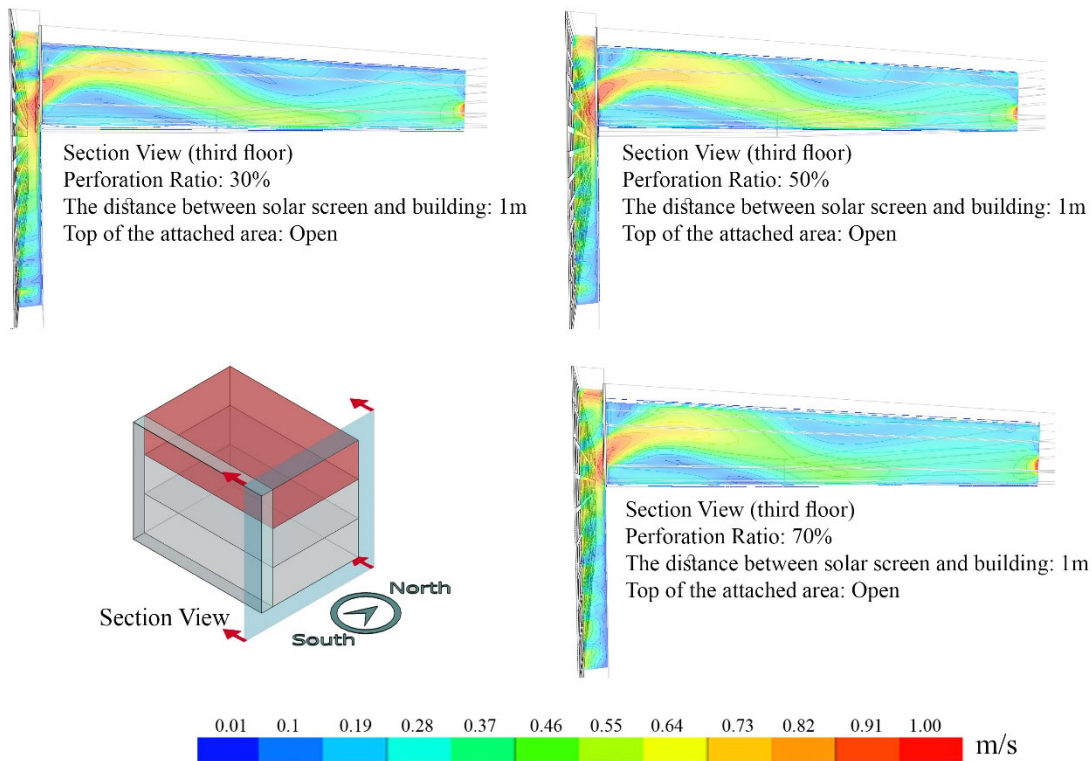


Figure 53: Air velocity pattern based on the different perforation ratios in Phoenix.

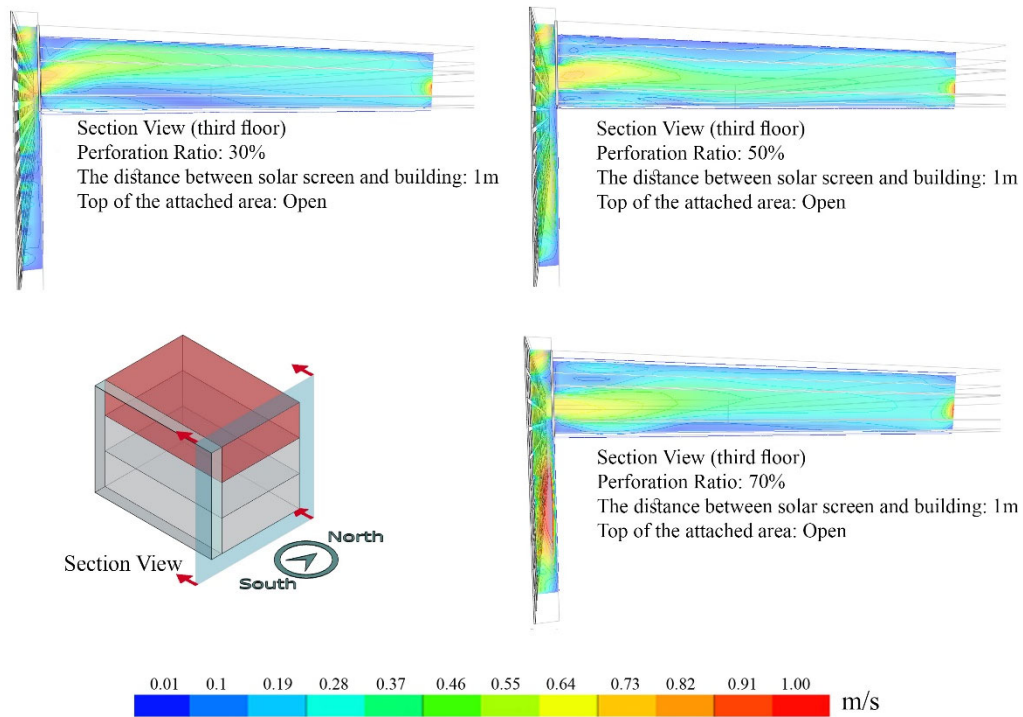


Figure 54: Air velocity pattern based on the different perforation ratios in Boston.

5.5- Limitation and Future Research

Although the research framework illustrated in Chapter 1 laid out most of the aspects of research in dynamic solar screen façades, this research was limited to variation in perforation ratio, the distance between the building and the solar screen, and the state of the attached areas' top. Other aspects of dynamic solar screen design that are recommended for future research are as follows:

- 1- Materiality of solar screen facades.
- 2- Depth of the solar screen facades.
- 3- Analyzing the impact of the solar screen in taller buildings

APPENDIX A

SENSITIVITY STUDY RESULTS FOR DIFFERENT SCREEN THICKNESS AND MATERIAL

Figures 55 and 56 show the results of solar screens with a 50% perforation ratio with 10 cm and 20 cm thickness. These results are for building total energy consumption and MacroFlo external vent (airflow volume). As it is shown, there is no difference between the screen with 10cm thickness and 20 cm. Therefore, it can be concluded that the software is not sensitive to different solar screen thicknesses.

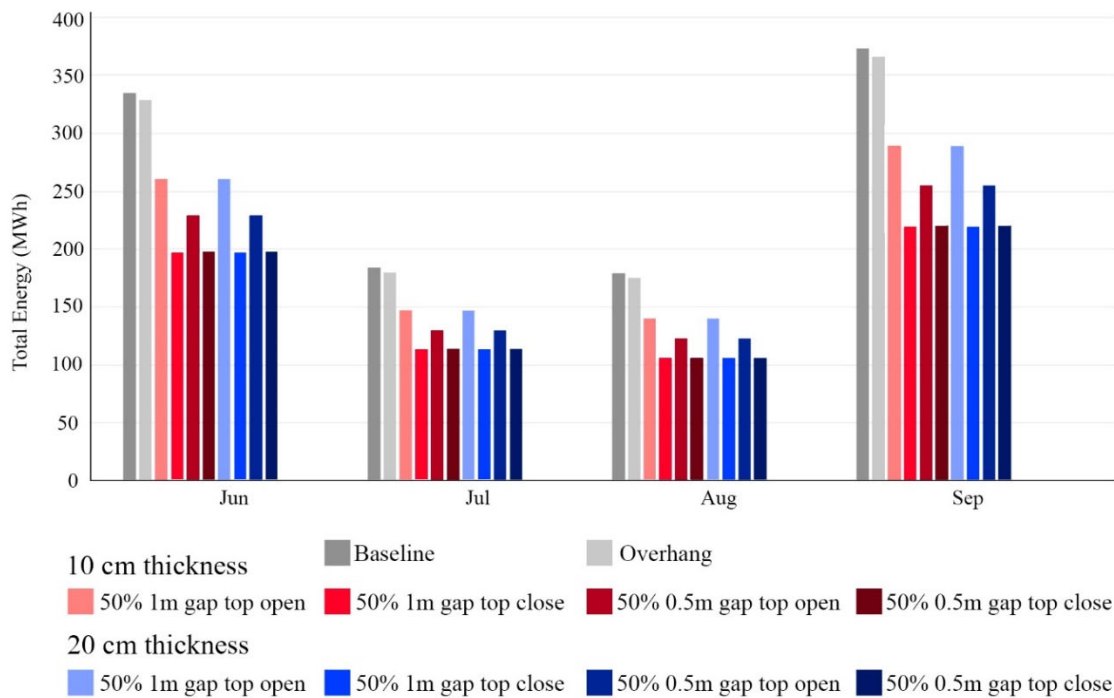


Figure 55: Total energy consumption for a solar screen with a 50 % perforation ratio and two different thickness in Boston

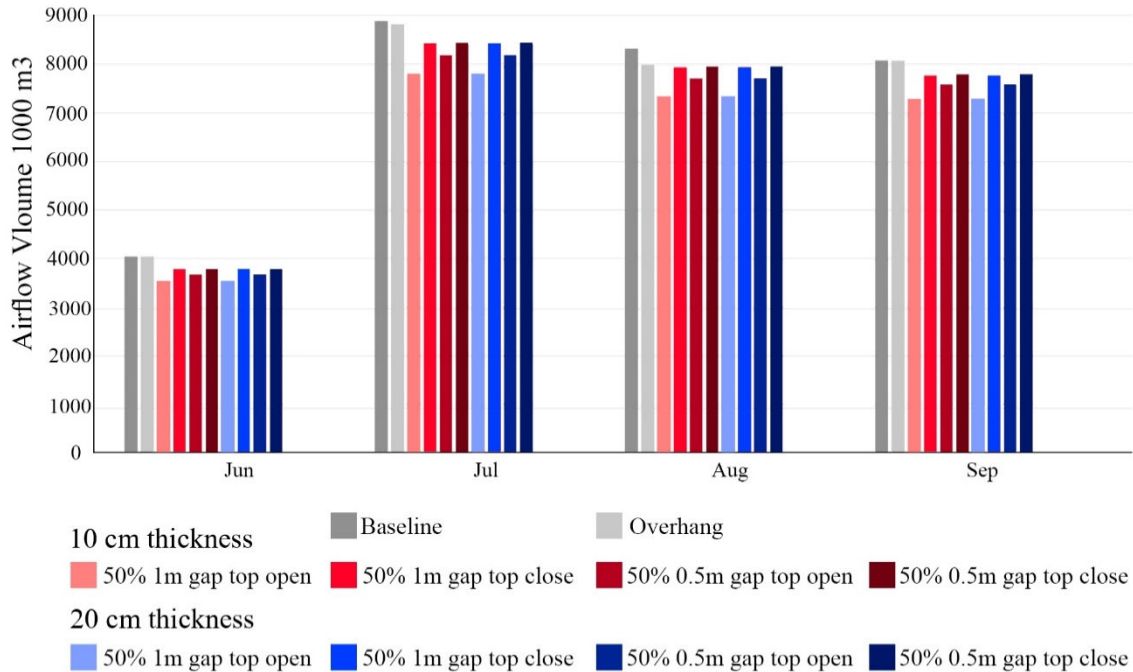


Figure 56: Airflow volume for a solar screen with a 50 % perforation ratio and two different thickness in Boston

Figures 57 and 58 show the results of solar screens with a 50% perforation ratio with two different materials, one with concrete and the other with aluminum. These results are for building total energy consumption and MacroFlo external vent (airflow volume). As it is shown, there is no difference between the screen with 10cm thickness and 20 cm. Therefore, it can be concluded that the software is not sensitive to different solar screen materials. In addition, it is worth mentioning that the sensitivity study has been done for the solar screen with 30% and 70% perforation ratios and the results are the same.

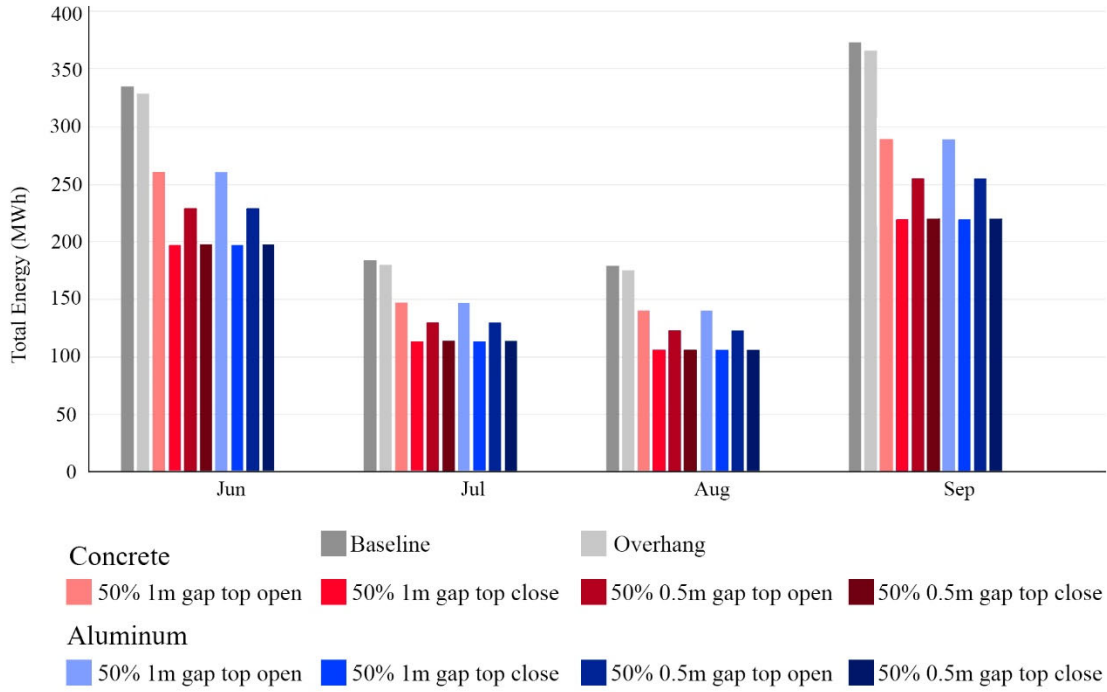


Figure 57: Total energy consumption for a solar screen with a 50 % perforation ratio and two different materials in Boston

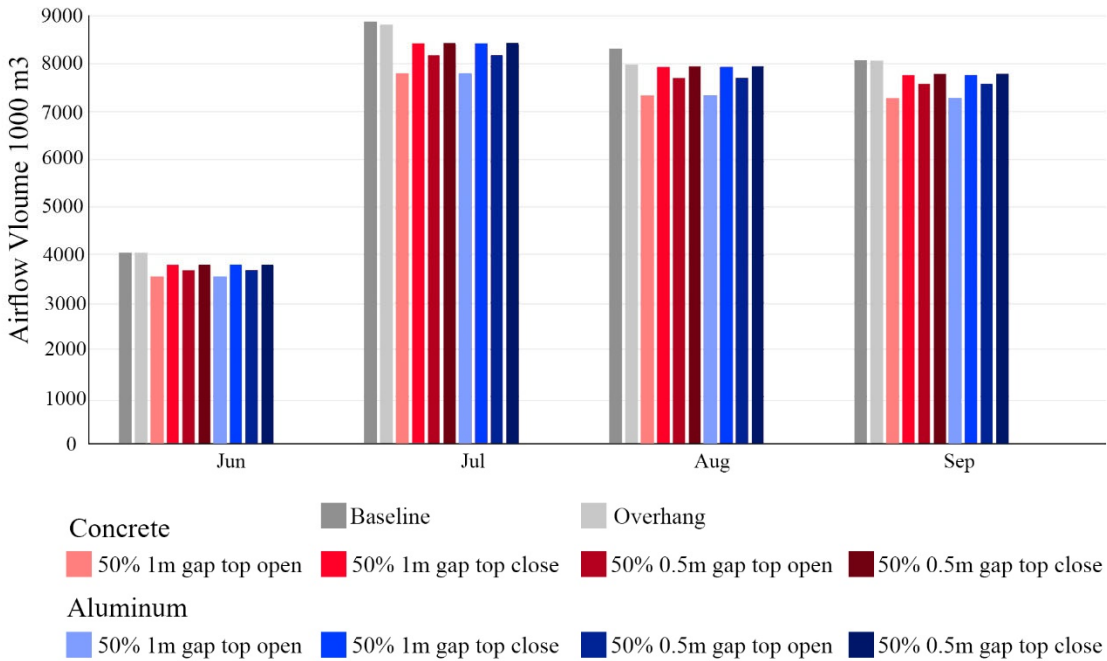


Figure 58: Airflow volume for a solar screen with a 50 % perforation ratio and two different materials in Boston

APPENDIX B

ADDITIONAL SIMULATION RESULTS

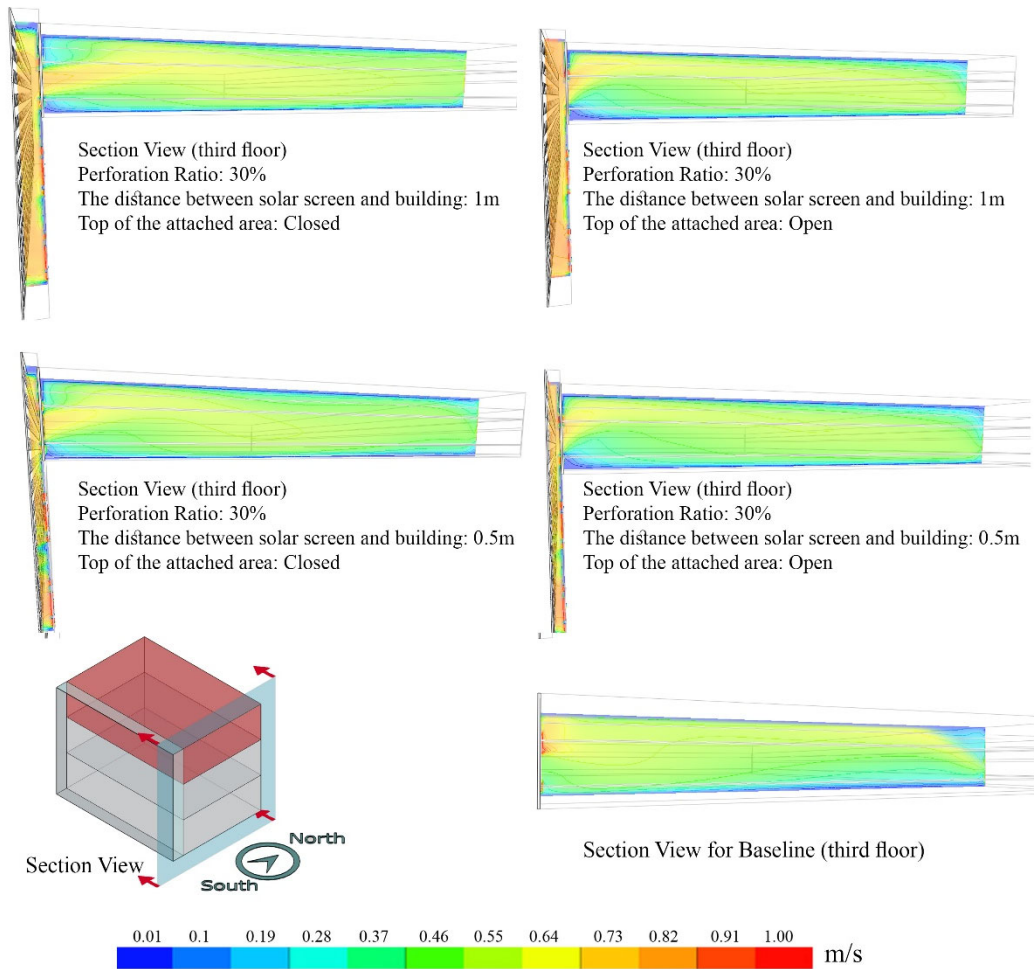


Figure 59: Air temperature for the screen with 30% perforation ratio in Phoenix

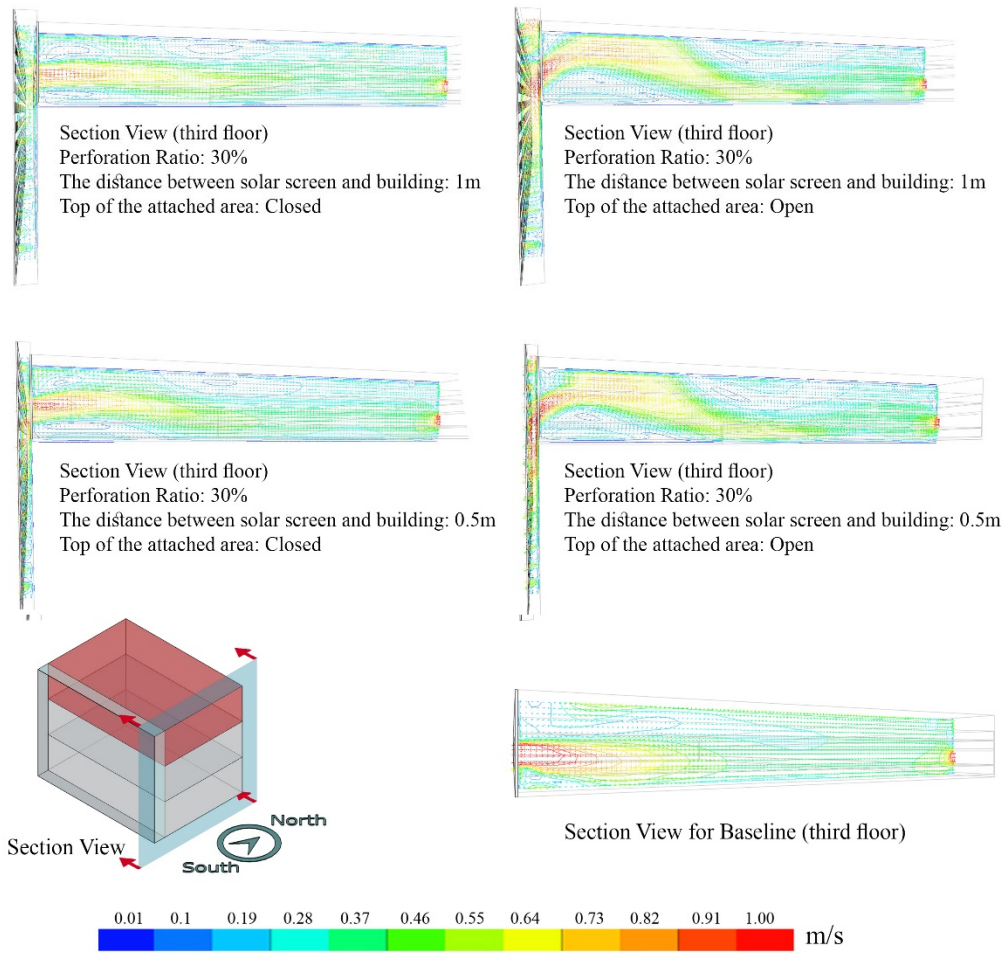


Figure 60: Air velocity vector for the screen with 30% perforation ratio in Phoenix

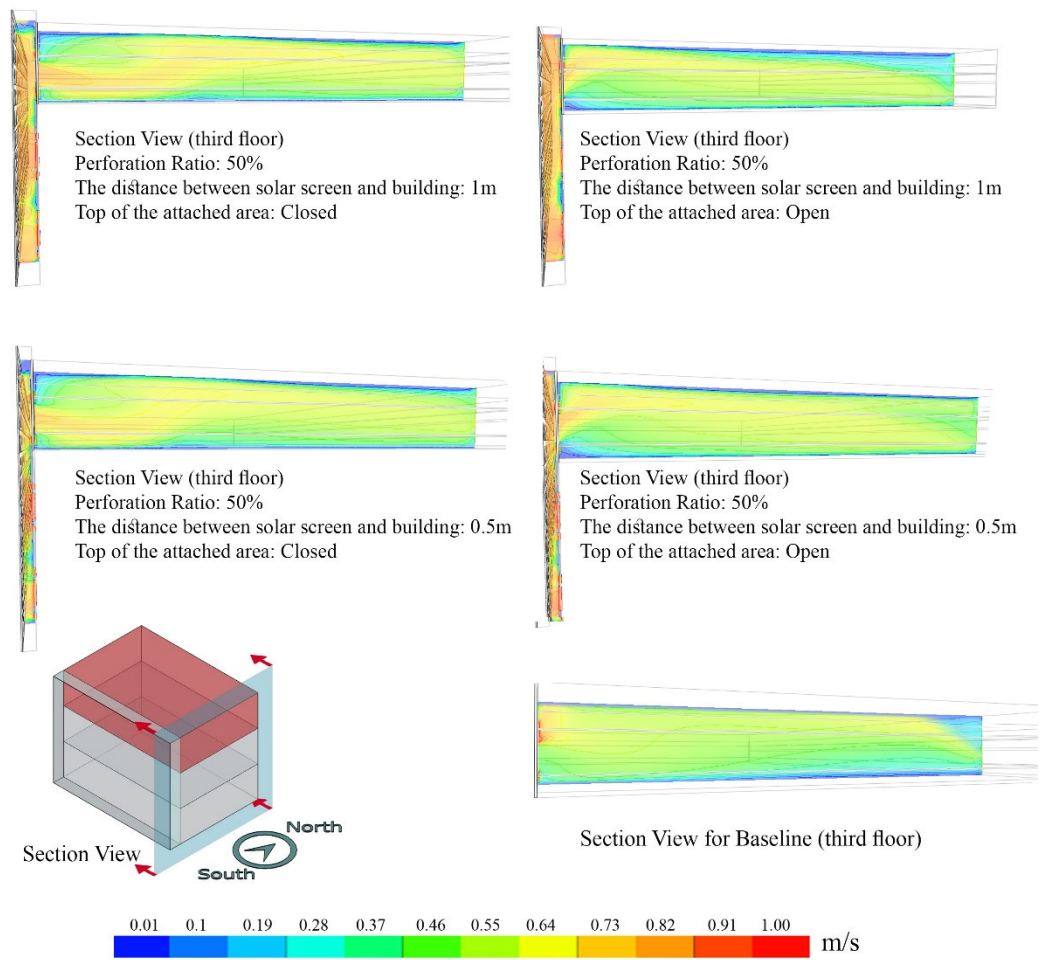


Figure 61: Air temperature pattern for the screen with 50% perforation ratio in Phoenix

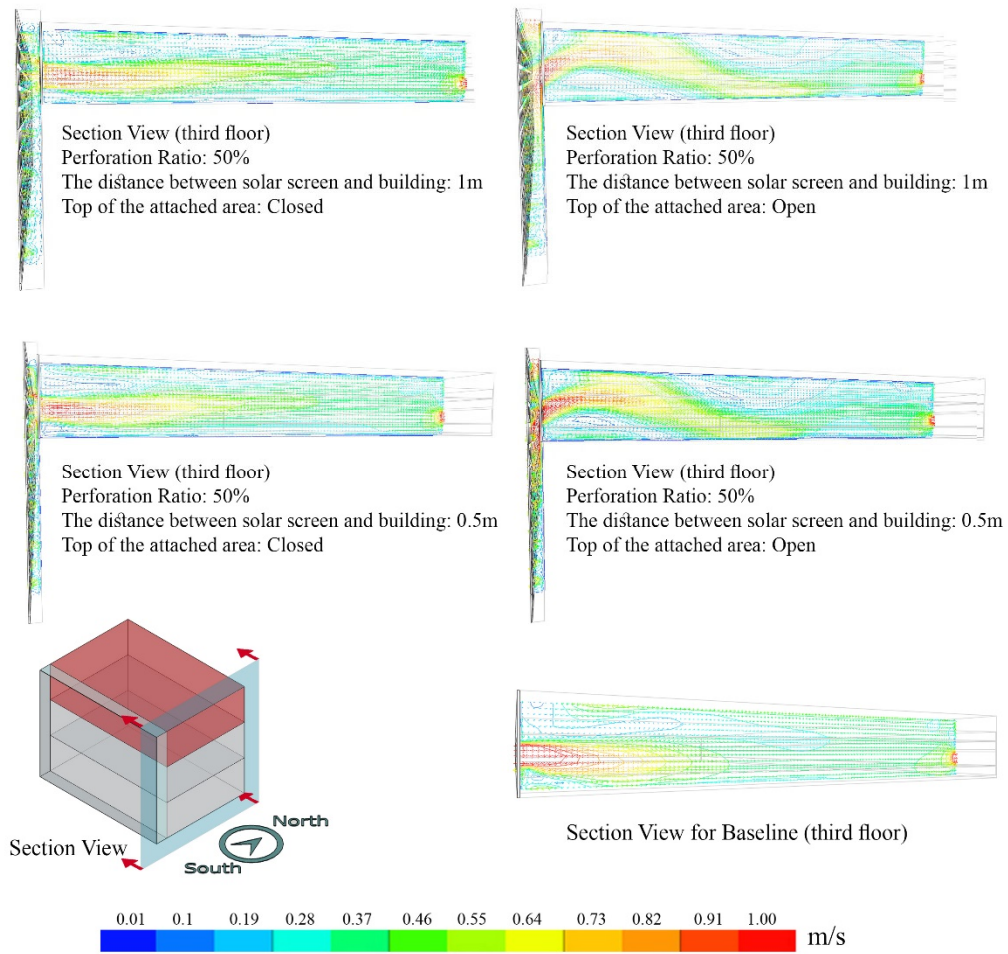


Figure 62: Air velocity vector for the screen with 50% perforation ratio in Phoenix

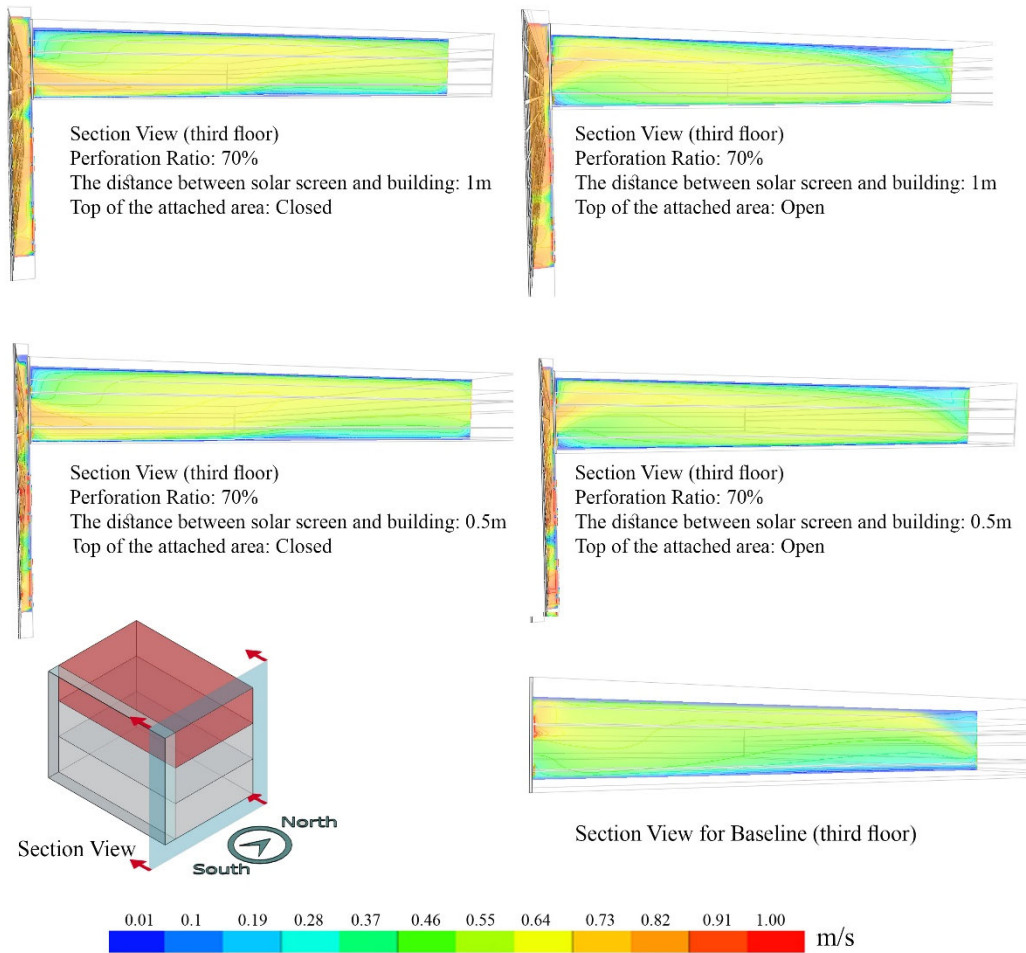


Figure 63: Air temperature pattern for the screen with 70% perforation ratio in Phoenix

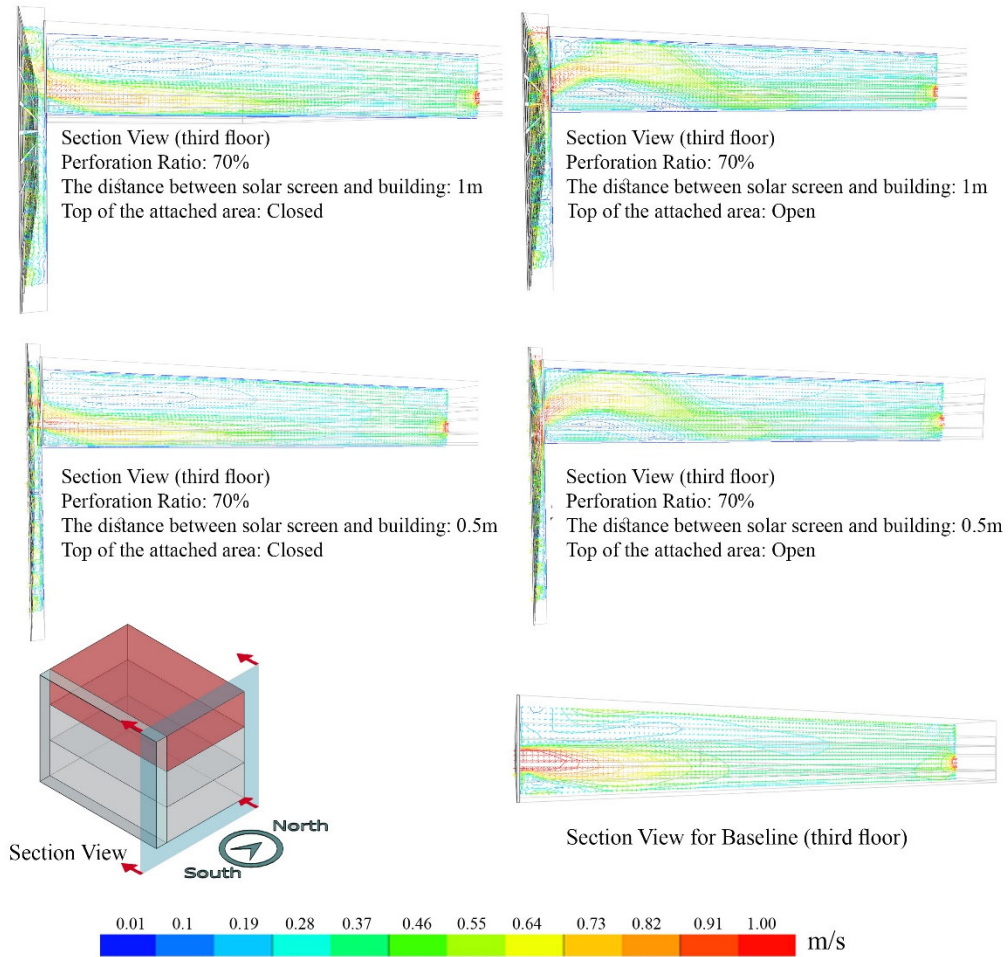


Figure 64: Air velocity vector for the screen with 70% perforation ratio in Phoenix

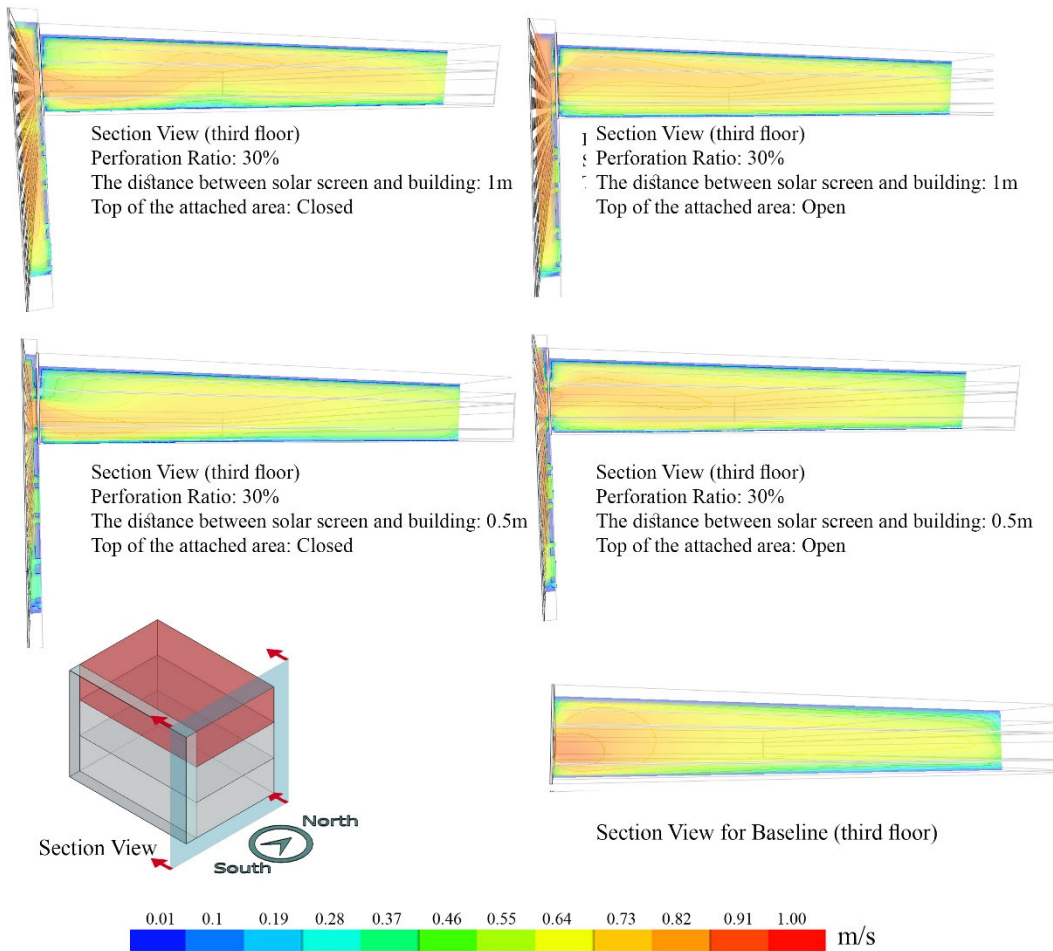


Figure 65: Air temperature pattern for the screen with 30% perforation ratio in Boston

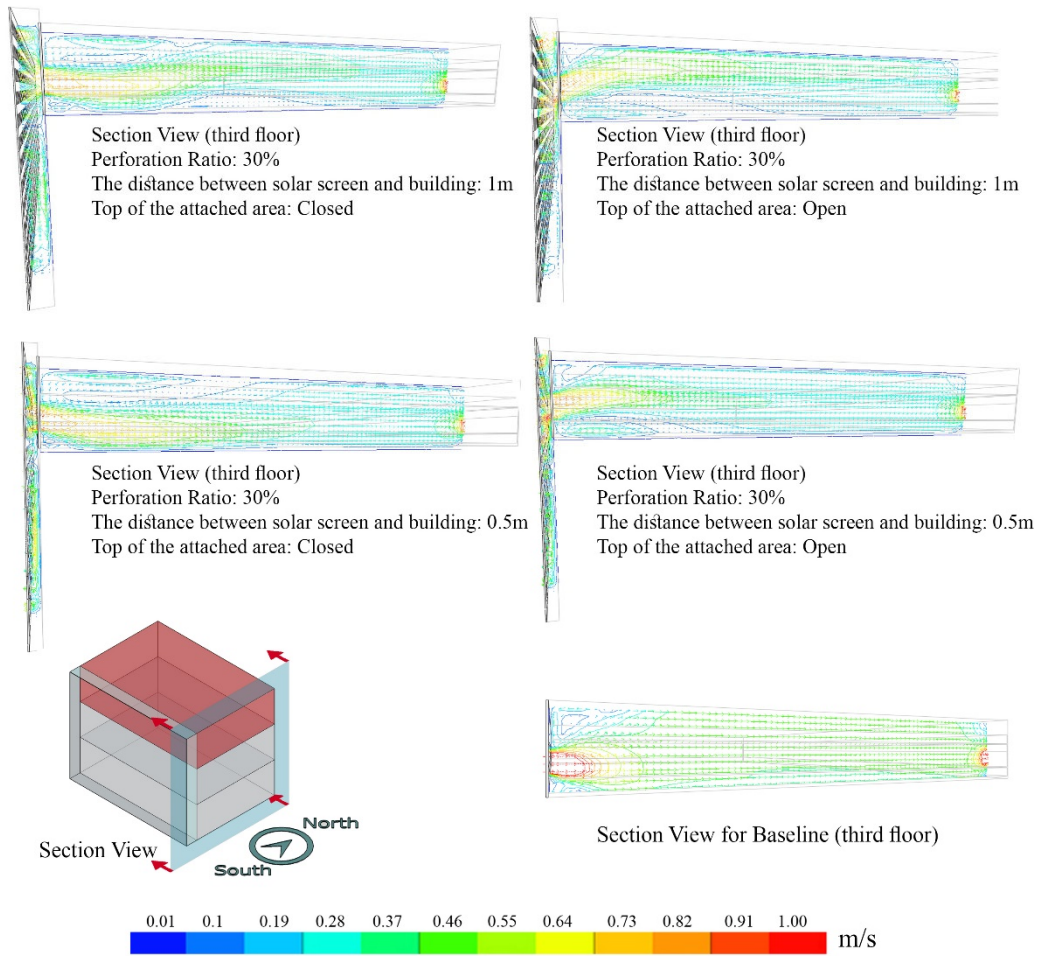


Figure 66: Air velocity vector for the screen with 30% perforation ratio in Boston

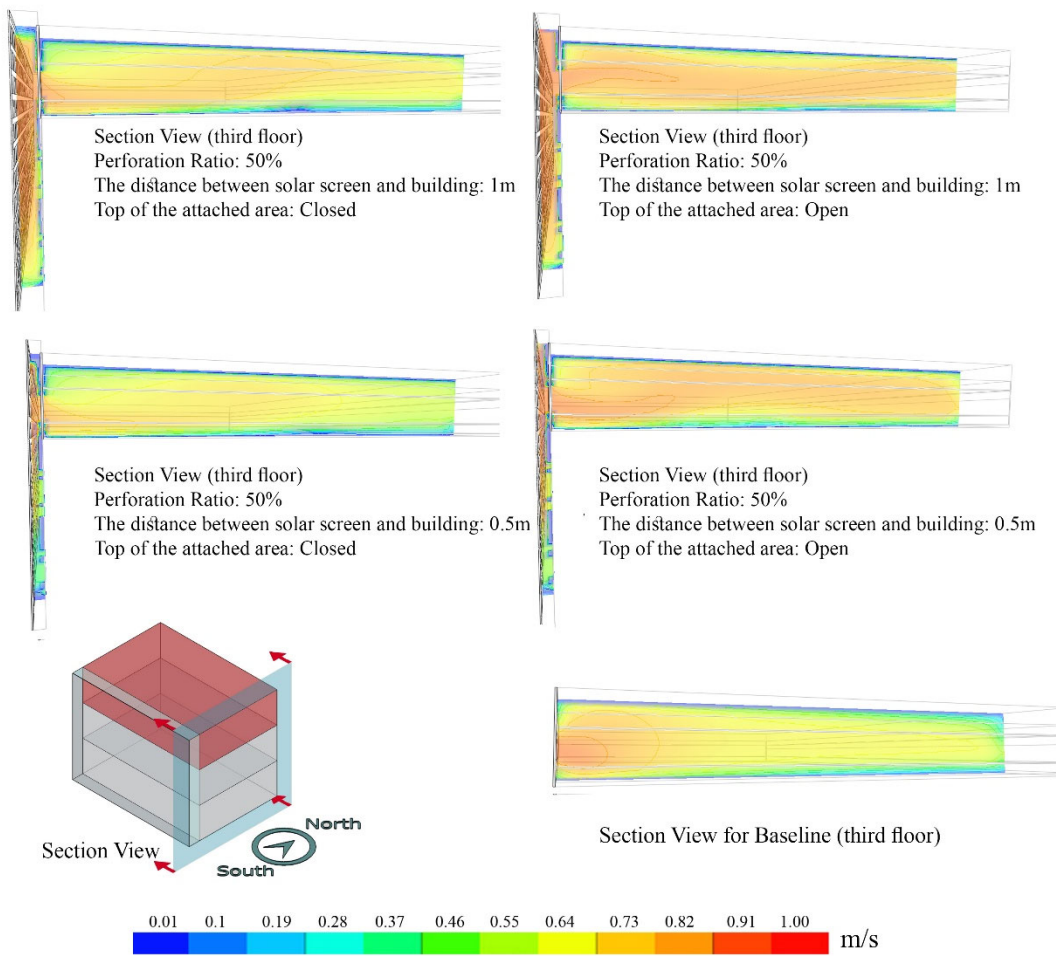


Figure 67: Air temperature pattern for the screen with 50% perforation ratio in Boston

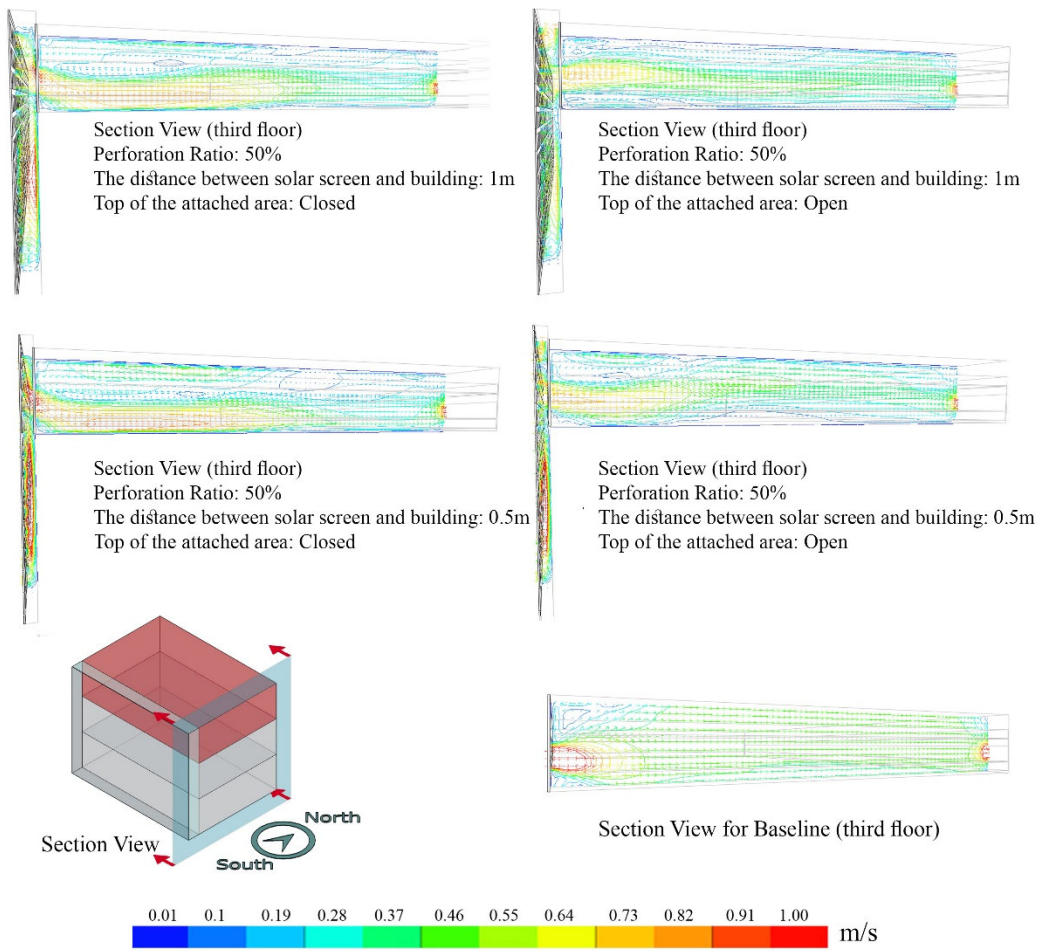


Figure 68: Air velocity vector for the screen with 50% perforation ratio in Boston

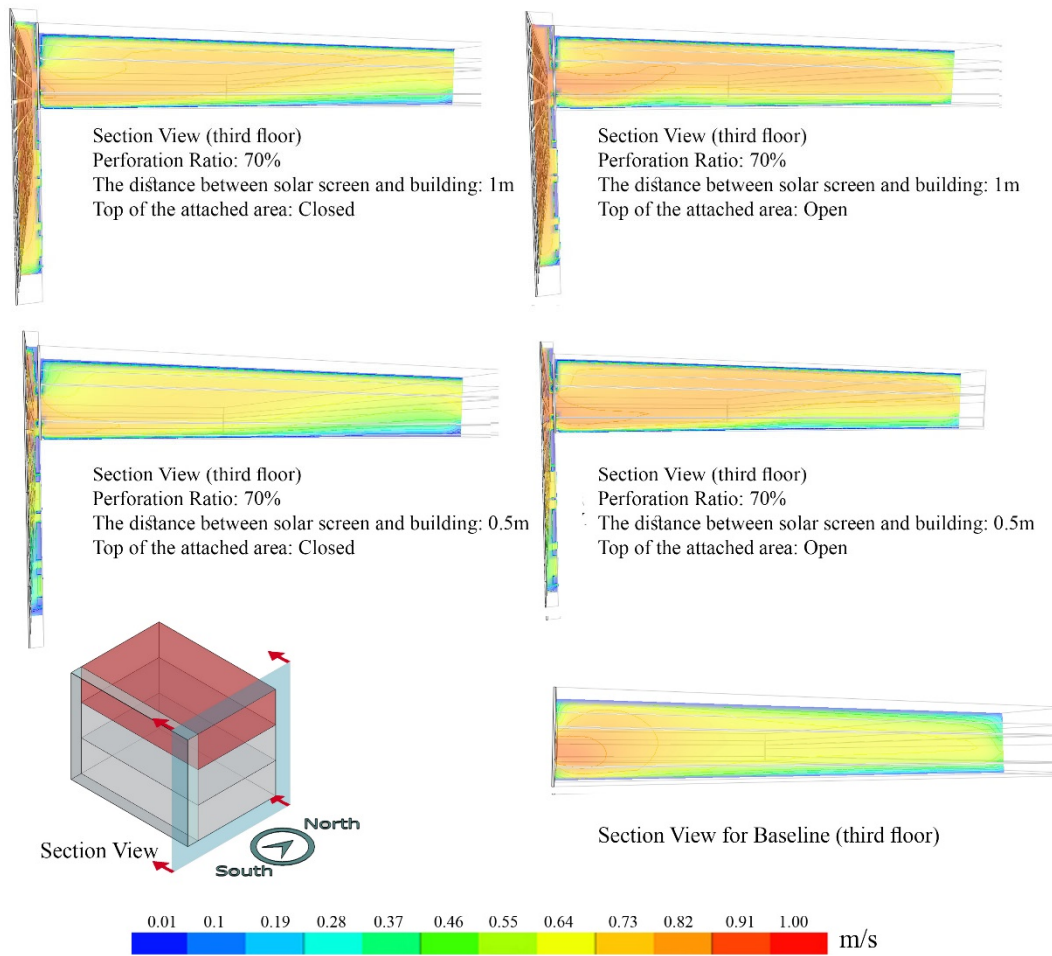


Figure 69: Air temperature pattern for the screen with 70% perforation ratio in Boston

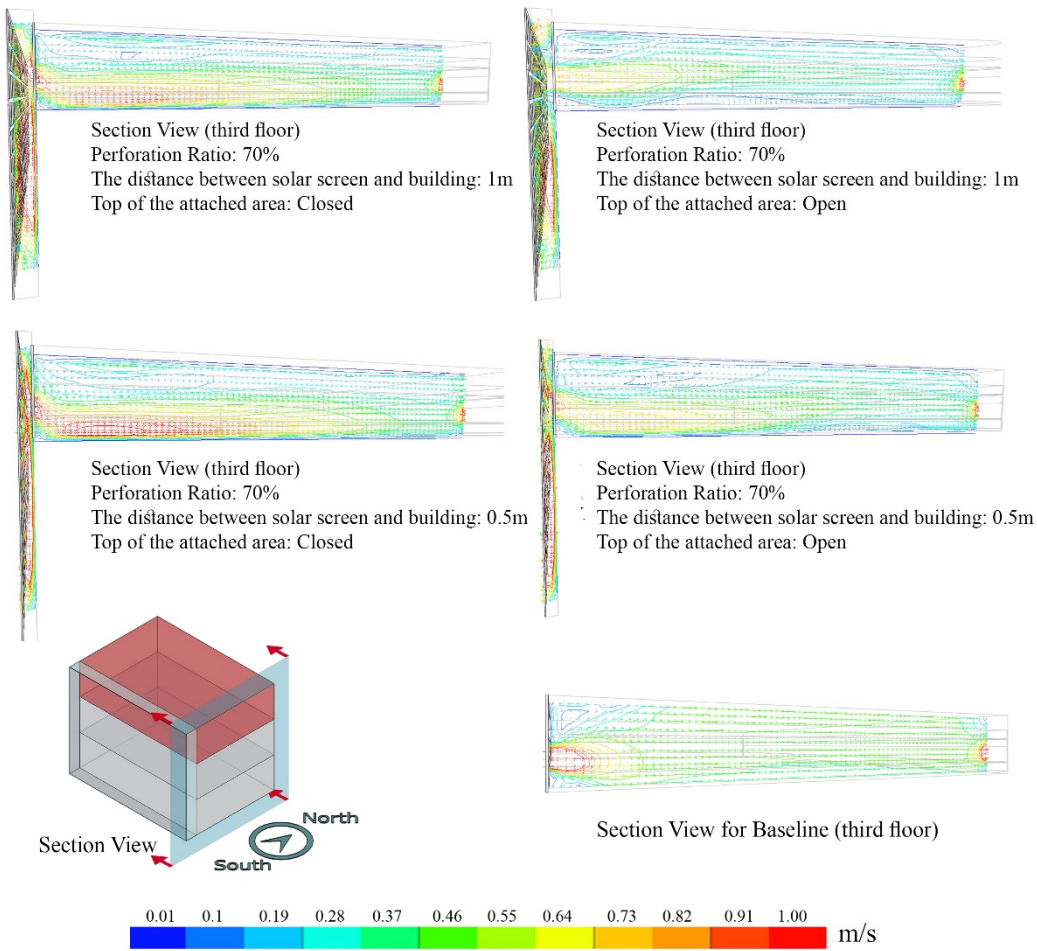


Figure 70: Air velocity vector for the screen with 70% perforation ratio in Boston

REFERENCES CITED

- Aflaki, A., Mahyuddin, N., Al-Cheikh Mahmoud, Z., & Baharum, M. R. 2015. "A review on natural ventilation applications through building façade components and ventilation openings in tropical climates." *Energy and Buildings* 101: 153–162. <https://doi.org/10.1016/j.enbuild.2015.04.033>.
- Aflaki, A., Mahyuddin, N., & Baharum, M. R. 2016. "The influence of single-sided ventilation towards the indoor thermal performance of high-rise residential building: A field study." *Energy and Buildings* 126: 146–158. <https://doi.org/10.1016/j.enbuild.2016.05.017>.
- Al-Masrani, S. M., & Al-Obaidi, K. M. 2019. "Dynamic shading systems: A review of design parameters, platforms and evaluation strategies." *Automation in Construction* 102: 195–216. <https://doi.org/10.1016/j.autcon.2019.01.014>.
- Baxevanou, C., Fidaros, D., & Tsangrassoulis, A. 2017. "Management of Natural Ventilation in High-Rise Building – a CFD Study." *Procedia Environmental Sciences* 38: 428–435. <https://doi.org/10.1016/j.proenv.2017.03.128>.
- Cao, B., Ouyang, Q., Zhu, Y., Huang, L., Hu, H., & Deng, G. 2012. "Development of a multivariate regression model for overall satisfaction in public buildings based on field studies in Beijing and Shanghai." *Building and Environment* 47: 394–399. <https://doi.org/10.1016/j.buildenv.2011.06.022>.
- de Dear, R. J., & Brager, G. S. 2002. "Thermal comfort in naturally ventilated buildings: revisions to ASHRAE Standard 55." *Energy and Buildings* 34(6): 549–561. [https://doi.org/10.1016/s0378-7788\(02\)00005-1](https://doi.org/10.1016/s0378-7788(02)00005-1).
- Carrer, P., & Wolkoff, P. 2018. "Assessment of Indoor Air Quality Problems in Office-Like Environments: Role of Occupational Health Services." *International Journal of Environmental Research and Public Health* 15(4): 741. <https://doi.org/10.3390/ijerph15040741>.
- Chen, Y., Tong, Z., & Malkawi, A. 2017. "Investigating natural ventilation potentials across the globe: Regional and climatic variations." *Building and Environment* 122: 386–396. <https://doi.org/10.1016/j.buildenv.2017.06.026>.
- Chenari, B., Dias Carrilho, J., & Gameiro Da Silva, M. 2016. "Towards sustainable, energy-efficient and healthy ventilation strategies in buildings: A review." *Renewable and Sustainable Energy Reviews* 59: 1426–1447. <https://doi.org/10.1016/j.rser.2016.01.074>.

- Cheung, J. O., & Liu, C. H. 2011. "CFD simulations of natural ventilation behavior in high-rise buildings in regular and staggered arrangements at various spacings." *Energy and Buildings* 43(5): 1149–1158. <https://doi.org/10.1016/j.enbuild.2010.11.024>.
- Carrilho Da Graça, G., & Linden, P. 2016. "Ten questions about natural ventilation of non-domestic buildings." *Building and Environment* 107: 263–273. <https://doi.org/10.1016/j.buildenv.2016.08.007>.
- Elzeyadi, I. 2017. "The impacts of dynamic façade shading typologies on building energy performance and occupant's multi-comfort." *Architectural Science Review* 60(4): 316–324. <https://doi.org/10.1080/00038628.2017.1337558>.
- Elzeyadi, I. M. K., and A. Batool. 2017. "Veiled Facades: Impacts of Patterned-Mass Shades on Building Energy Savings, Daylighting Autonomy, and Glare Management in Three Different Climate Zones." Paper presented at the Conference International Building Performance Simulation Association (IBPSA), San Francisco, CA, August 7–9.
- Elzeyadi, I. M. K., and A. Batool. 2018. "Learning from the Vernacular: The Impacts of Massive Perforated Screen Shades on Building Energy Savings and Thermal Comfort in Two Different Hot Climate Zones." Paper presented at ASHRAE Winter Conference Proceedings, Chicago, IL, January 20-24.
- Guo, F., Zhu, P., Wang, S., Duan, D., & Jin, Y. 2017. "Improving Natural Ventilation Performance in a High-Density Urban District: A Building Morphology Method." *Procedia Eng.* 205: 952–958. <https://doi.org/10.1016/j.proeng.2017.10.149>.
- Hosseini, S. M., Mohammadi, M., Rosemann, A., Schröder, T., & Lichtenberg, J. 2019. "A morphological approach for kinetic façade design process to improve visual and thermal comfort: Review." *Building and Environment* 153: 186–204. <https://doi.org/10.1016/j.buildenv.2019.02.040>.
- Khatami, N., & Hashemi, A. 2017. "Improving Thermal Comfort and Indoor Air Quality through Minimal Interventions in Office Buildings." *Energy Procedia* 111: 171–180. <https://doi.org/10.1016/j.egypro.2017.03.019>.
- Kim, Y. M., Lee, J. H., Kim, S. M., & Kim, S. 2011. "Effects of double skin envelopes on natural ventilation and heating loads in office buildings." *Energy and Building* 43(9): 2118–2126. <https://doi.org/10.1016/j.enbuild.2011.04.012>.
- Lai, K., Wang, W., & Giles, H. 2017. "Solar shading performance of window with constant and dynamic shading function in different climate zones." *Solar Energy*, 147: 113–125. <https://doi.org/10.1016/j.solener.2016.10.015>.
- Liping, Hien. 2007. "Applying Natural Ventilation for Thermal Comfort in Residential Buildings in Singapore." *Architectural Science Review* 50 (3): 224-233.

- Pérez-Lombard, L., Ortiz, J., & Pout, C. 2008. "A review on buildings energy consumption information." *Energy and Buildings* 40(3): 394–398. <https://doi.org/10.1016/j.enbuild.2007.03.007>.
- Luther, M. B. 2000. "Dynamic and Responsive Building Envelopes." *SAE Technical Paper Series*. <https://doi.org/10.4271/2000-01-2463>.
- Ma, N., Aviv, D., Guo, H., & Braham, W. W. 2021. "Measuring the right factors: A review of variables and models for thermal comfort and indoor air quality." *Renewable and Sustainable Energy Reviews* 135: 110436. <https://doi.org/10.1016/j.rser.2020.110436>.
- Meek, Breshears. 2010. "Dynamic Solar Shading and Glare Control for Human Comfort and Energy Efficiency at UCSD: Integrated Design and Simulation Strategies."
- Okochi, G. S., & Yao, Y. 2016. "A review of recent developments and technological advancements of variable-air-volume (VAV) air-conditioning systems." *Renewable and Sustainable Energy Reviews* 59: 784–817. <https://doi.org/10.1016/j.rser.2015.12.328>.
- Omrani, S., Garcia-Hansen, V., Capra, B. R., & Drogemuller, R. 2017. "Effect of natural ventilation mode on thermal comfort and ventilation performance: Full-scale measurement." *Energy and Buildings* 156: 1–16. <https://doi.org/10.1016/j.enbuild.2017.09.061>.
- Pasquay, T. 2004. "Natural ventilation in high-rise buildings with double facades, saving or waste of energy." *Energy and Buildings* 36(4): 381–389. <https://doi.org/10.1016/j.enbuild.2004.01.018>.
- Passe, U., & Battaglia, F. 2015. "Designing Spaces for Natural Ventilation" *An Architect's Guide* (1st ed.). Routledge.
- Priyadarsini, R., Cheong, K., & Wong, N. 2004. "Enhancement of natural ventilation in high-rise residential buildings using stack system." *Energy and Buildings* 36(1): 61–71. [https://doi.org/10.1016/s0378-7788\(03\)00076-8](https://doi.org/10.1016/s0378-7788(03)00076-8).
- Ramponi, R., Gaetani, I., & Angelotti, A. 2014. "Influence of the urban environment on the effectiveness of natural night-ventilation of an office building." *Energy and Buildings* 78: 25–34. <https://doi.org/10.1016/j.enbuild.2014.04.001>.
- Ren, J., Liu, J., Cao, X., & Hou, Y. 2017. "Influencing factors and energy-saving control strategies for indoor fine particles in commercial office buildings in six Chinese cities." *Energy and Buildings* 149: 171–179. <https://doi.org/10.1016/j.enbuild.2017.05.061>.

- Santamouris, M., Papanikolaou, N., Livada, I., Koronakis, I., Georgakis, C., Argiriou, A., & Assimakopoulos, D. 2001. "On the impact of urban climate on the energy consumption of buildings." *Solar Energy* 70(3): 201–216. [https://doi.org/10.1016/s0038-092x\(00\)00095-5](https://doi.org/10.1016/s0038-092x(00)00095-5).
- Schulze, T., & Eicker, U. 2013. Controlled natural ventilation for energy efficient buildings. *Energy and Buildings* 56: 221–232. <https://doi.org/10.1016/j.enbuild.2012.07.044>.
- Sherif, A., El-Zafarany, A., & Arafa, R. 2012. "External perforated window Solar Screens: The effect of screen depth and perforation ratio on energy performance in extreme desert environments." *Energy and Buildings* 52: 1–10. <https://doi.org/10.1016/j.enbuild.2012.05.025>.
- Shi, X., Abel, T., & Wang, L. 2020. "Influence of two motion types on solar transmittance and daylight performance of dynamic façades." *Solar Energy*, 201: 561–580. <https://doi.org/10.1016/j.solener.2020.03.017>.
- Srisamranrungruang, T., & Hiyama, K. 2020. "Balancing of natural ventilation, daylight, thermal effect for a building with double-skin perforated facade (DSPF)." *Energy and Buildings* 210: 109765. <https://doi.org/10.1016/j.enbuild.2020.109765>.
- Stoakes, P., Passe, U., & Battaglia, F. 2011. "Predicting natural ventilation flows in whole buildings. Part 1: The Viipuri Library." *Building Simulation* 4(3): 263–276. <https://doi.org/10.1007/s12273-011-0045-4>.
- Tong, Z., Chen, Y., & Malkawi, A. 2017. "Estimating natural ventilation potential for high-rise buildings considering boundary layer meteorology." *Applied Energy* 193: 276–286. <https://doi.org/10.1016/j.apenergy.2017.02.041>.
- Zhou, C., Wang, Z., Chen, Q., Jiang, Y., & Pei, J. (2014). "Design optimization and field demonstration of natural ventilation for high-rise residential buildings." *Energy and Buildings* 82: 457–465. <https://doi.org/10.1016/j.enbuild.2014.06.036>.